The Role of Paraoxonase-1 in Retinal Physiology and Age-Related Macular Degeneration

DISSERTATION

zur Erlangung der naturwissenschaftlichen Doktorwürde
(Dr. sc. nat.)

vorgelegt
der Mathematisch-naturwisssenschaftlichen Fakultät
der Universität Zürich
von

Jadwiga Patrycja Oczoś

aus Polen

Promotionskomitee:

Prof. Dr. Wolfgang Berger (Vorsitz)
Prof. Dr. Christian Grimm (Leitung)
Dr. Barbara Kloeckener-Gruissem
Prof. Dr. med. Arnold von Eckardstein
PD Dr. rer. nat. Volker Enzmann

Zürich, 2014

SUMMARY

Paraxonase-1 (PON1) is a hydrolase expressed mainly in liver and secreted into the blood, where it associates with high-density lipoprotein (HDL). Thanks to its anti-oxidant and anti-inflammatory properties PON1 contributes to protective, anti-atherogenic function of HDL. Decreased levels of serum PON1 activity have been found in several pathological conditions such as type 1 and type 2 diabetes, metabolic syndrome, coronary artery disease and age-related macular degeneration (AMD). The *PON1* gene contains a number of functional single nucleotide polymorphisms (SNPs) in both the coding and upstream regulatory regions, which affect either the level or the substrate specificity of PON1. These SNPs have been found to be associated with several diseases.

To expand the knowledge on effects of *PON1* gene on AMD, we studied association of SNPs and haplotypes within the upstream regulatory region of *PON1* with neovascular AMD in the Swiss population. Four SNPs (rs705379, rs705381, rs854573, rs757158) and two haplotypes (TGGCCTC and CGATGCT) were significantly associated with the disease. Protective and risk haplotypes within the 5' untranslated region of *PON1* differently affected luciferase reporter activity *in vitro*, suggesting that their regulatory function might play a role in AMD.

Genetic and biochemical analyses indicate involvement of PON1 in the pathophysiology of AMD. However, the function of PON1 in the eye and how it might affect eye pathology had not been addressed up to now. In the present study we used *Pon1*$^{-/-}$ mice to investigate the role of PON1 in the retina and retinal pigment epithelium (RPE). We demonstrated that PON1 is not essential for normal development, function, defense against light damage and aging of the mouse retina. Reduced levels of lysophosphatidylcholines in eyes of *Pon1*$^{-/-}$ mice implicate a phospholipase A2 (PLA2)-like enzymatic activity of PON1 to be involved in the modulation of the phospholipid content of retina and RPE.

Studies presented in this thesis together with previous reports on the role of PON1 in atherosclerosis suggest that PON1 may be involved in AMD as a modulatory protein. The interplay with additional genetic and environmental factors could influence its contribution to disease development and/or progression.

ZUSAMMENFASSUNG

Paraoxonase-1 (PON1) ist eine vornehmlich von Leberzellen produzierte Hydrolase, die sekretiert wird und mit HDL (Lipoprotein hoher Dichte) im Blut assoziiert. Dank seiner anti-oxidativen und anti-inflammatorischen Aktivität trägt PON1 zur protektiven Wirkung von HDL gegen Arteriosklerose bei. In mehreren Krankheiten, wie zum Beispiel Diabetes (Typ 1 und Typ 2), dem metabolischen Syndrom, der koronaren Herzkrankheit und der altersabhängigen Makula-degeneration (AMD), wurde eine reduzierte Aktivität von PON1 im Serum von Patienten festgestellt. Sowohl in der kodierenden Sequenz als auch in den 5' regulatorischen Regionen des *PON1* Gens entdeckte man eine Reihe von funktionellen Einzelnukleotid-Polymorphismen (SNPs), die entweder die Menge von PON1 oder dessen Substratspezifität beeinflussen. Es wurde gezeigt, dass diese SNPs mit verschiedenen Krankheiten assoziiert sind.

Um die Verbindung von *PON1* mit AMD besser zu verstehen, haben wir den Einfluss von SNPs und Haplotypen in der 5' regulatorischen Region von *PON1* auf die neovaskuläre Form von AMD in der Schweizer Bevölkerung untersucht. Wir konnten zeigen, dass vier SNPs (rs705379, rs705381, rs854573, rs757158) und zwei Haplotypen (TGGCCTC und CGATGCT) signifikant mit der Krankheit assoziiert sind. Protektions- und Risiko-Haplotypen beeinflussten die Luziferase Reporter-aktivität in *in vitro* Versuchen unterschiedlich. Dies deutet darauf hin, dass diese regulatorischen Sequenzen eine Rolle bei der Pathogenese von AMD spielen könnten.

Obwohl genetische und biochemische Analysen auf eine Rolle von PON1 in AMD hindeuten, wurde die physiologische Funktion von PON1 im Auge noch nicht erforscht. Auch ist bislang nicht bekannt, wie PON1 Augenpathologien beeinflussen könnte. Mit Hilfe von *Pon1* knockout Mäusen haben wir deshalb die Rolle von PON1 in der Netzhaut und im retinalen Pigmentepithel (RPE) untersucht. Wir konnten zeigen, dass PON1 weder für die normale Netzhautentwicklung, noch für die Netzhautfunktion, den Schutz gegen Lichtschäden oder das normale Altern essentiell ist. Jedoch deuten die reduzierten Mengen von Lysophosphatidylcholinen in den Augen von *Pon1*$^{-/-}$ Mäusen auf eine Phospholipase A2 (PLA2)-ähnliche Aktivität von PON1 hin. Diese könnte den Gehalt von Phospholipiden in der Netzhaut und dem RPE beeinflussen.

Zusammen mit bereits publizierten Daten lassen die Resultate dieser Doktorarbeit vermuten, dass PON1 als modulatorisches Protein bei der Pathogenese von AMD eine Rolle spielt. Ausserdem könnte das Zusammenspiel von genetischen und umweltbedingten Faktoren die Wirkung von PON1 auf die Krankheitsentwicklung und/oder Progression zusätzlich beeinflussen.

CONTENTS

I. INTRODUCTION

1.1 The role of retina and retinal pigment epithelium in vision

The visual system is the part of the nervous system allowing organisms to see, meaning to detect and interpret the information from visible light to build a representation of the surrounding environment. Visual perception involves not only the eye but also various brain structures. The eye is the primary sensory organ for vision, responsible for collecting the light, focusing it and generating first neural signals of the visual pathway. Light must pass through the transparent media and structures of the eye: the tear film, the cornea, the anterior chamber, the lens, and the posterior chamber-vitreous, to be finally projected upside-down and backwards on to the retina (Prasad and Galetta, 2011) (Fig. 1). In the retina the light is converted by photoreceptors into an electrochemical signal that is further relayed by neurons to the cerebral cortex of the brain. The cortex combines received signals. Ultimately, these initial pieces of information are being integrated and serve to define the borders of objects and create an image (Masland and Martin, 2007).

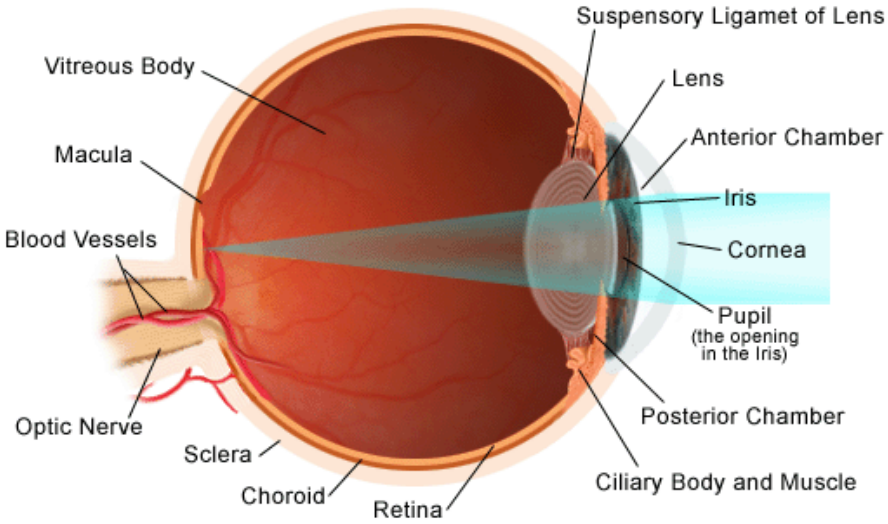

Figure 1. Sagittal section of the adult human eye.
Adapted from http://smsm2a2012.weebly.com/reading-site.html

1.1.1 Retina

The neurosensory retina consists of three major cell layers through which the signal in response to light is transduced vertically: photoreceptors connected to bipolar cells, further interacting with the ganglion cells. Additionally, horizontal and amacrine cells form lateral connections at the photoreceptor-bipolar cell synapses, and at the bipolar cell-ganglion cell synapses respectively (Fig. 2).

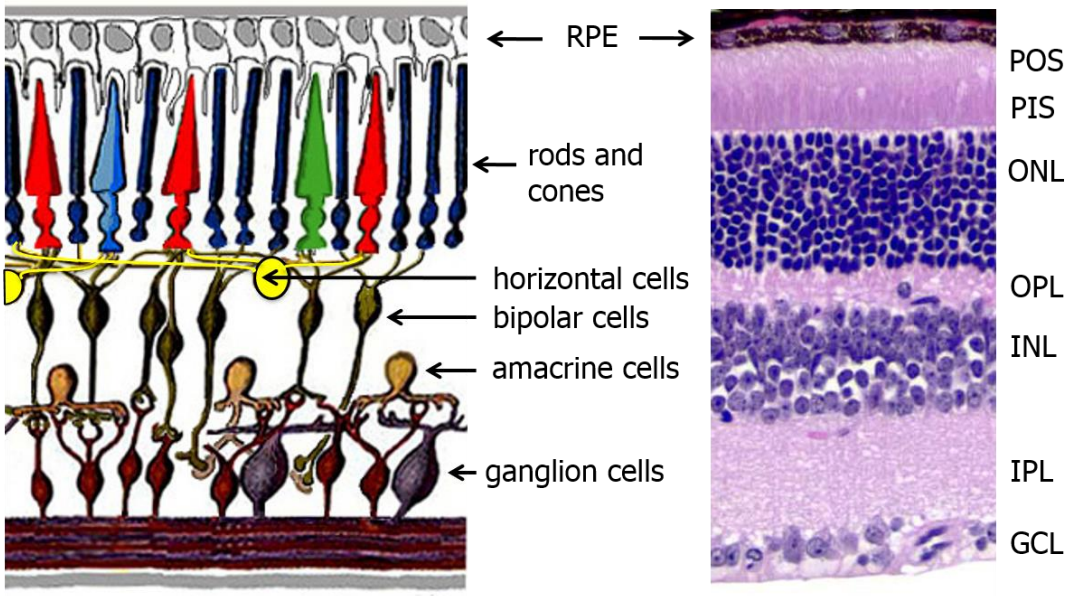

Figure 2. Human retinal architecture.
Left panel: schematic diagram of the retina with an emphasis on the sensory photoreceptors (rods and cones), the ganglion cells and the interneurons (horizontal, bipolar and amacrine cells) connecting photoreceptors with ganglion cells. Right panel: light microphotograph of a vertical section through the central human retina. Three layers of nerve cell bodies: outer nuclear layer (ONL) containing cell bodies of rods and cones, inner nuclear layer (INL) containing cell bodies of the bipolar, horizontal and amacrine cells, and the ganglion cell layer (GCL) are separated by the outer and the inner plexiform layers (OPL and INL), where synaptic contacts occur. PIS, photoreceptor inner segments; POS photoreceptor outer segments; RPE, retinal pigment epithelium.
Adapted from http://webvision.med.utah.edu/book/part-i-foundations/simple-anatomy-of-the-retina/

1.1.1.1 Phototransduction and visual pathways

Photon absorption and its conversion into an electrochemical signal (phototransduction) take place in the photoreceptor outer segments (POS). The POS are built of hundreds of membranous discs stacks. These membranous structures are rich in proteins involved in the phototransduction, most importantly the photopigment

composed of a membrane protein, opsin, and a chromophore molecule, the 11-*cis*-retinal. Absorption of the photon by the chromophore causes its conformation change from 11-*cis*-retinal to all-*trans*-retinal, and subsequent release from the protein moiety. The unbound opsin stimulates another membrane complex, transducin, by replacing guanosine diphosphate (GDP) with guanosine triphosphate (GTP). Active α-transducin-GTP interacts with phosphodiesterase (PDE), leading to hydrolysis of the cytosolic second messenger, cyclic guanosine monophosphate (cGMP) (Palczewski, 2012). A lowered cGMP level causes closing of membrane sodium channels, decreases the inward sodium current, and results in the membrane hyperpolarization, followed by the reduction in neurotransmitter (glutamate) release from the photoreceptor into the synapse. Glutamate is a signalling molecule recognized by bipolar cells. Various bipolar cells have different types of the glutamate receptors needed for tuning the response to photoreceptor input. The so-called ON bipolar cells, triggering the ON pathway, possess inhibitory glutamate receptors, preventing the cells from firing when exposed to the neurotransmitter (response to the darkness). In light, when there is glutamate shortage in the photoreceptor-bipolar cell synapses, the ON bipolar cells are no longer inhibited but instead release glutamate at their synapses in the inner plexiform layer, and thus stimulate the ON ganglion cells. This pathway enables detecting light images against a dark background. Another type of bipolar cells, the OFF bipolar cells, have excitatory glutamate receptors, activating the OFF ganglion cells upon the glutamate binding. The OFF pathway is functioning in darkness, and is shut down by the light, making visible the dark areas on light background. The electrochemical signals received by the ganglion cells travel within the axons in the nerve fiber layer (the innermost retinal layer) to the optic nerve, and further to the primary visual cortex of the brain (Kolb, 2003).

1.1.1.2 Human retinal topography

Humans, like other primates, possess a so-called duplex retina, consisting of two main photoreceptor classes: cones and rods (Fig. 3). The general mechanism of phototransduction described in the previous section applies to both types of photoreceptors, because both use photopigments composed of the 11-*cis*-retinal chromophore and an opsin protein. Nevertheless, distinct structural and biochemical characteristics of the protein moiety, as well as the specific anatomical and physiological features of the cones and rods determine their specialized tasks (Kolb, 2003). Despite the much higher proportion of rods in the adult human retina (4.6 million cones versus 92 million rods) (Curcio et al., 1990), under most conditions our vision is mediated by cones, which operate over an enormous range

of intensities and wavelengths. There are three kinds of cones in humans, each containing a different type of opsin enabling optimal response to particular wavelengths of light: S-cones (short-wavelength, absorb blue light), M-cones (middle-wavelength, absorb green light), and L-cones (long-wavelength, absorb red light). In contrast, rod photoreceptors possess only one type of the photopigment (rhodopsin, absorbs green-blue light), hence they cannot discriminate colors. More importantly, they have a sensitivity that is over a thousand times higher than the one in cones and therefore can perform well in dim light (scotopic vision).

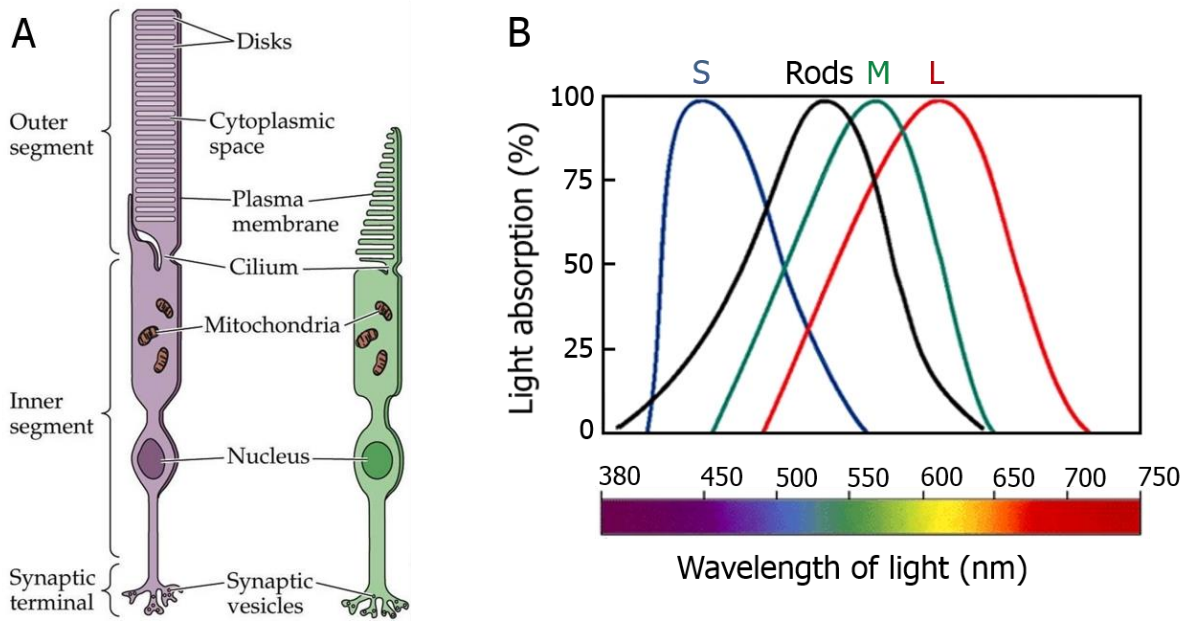

Figure 3. Photoreceptors: rods and cones.
(A) Schematic representation of the anatomy of rod (left) and cone (right) photoreceptor cells. (B) Human photoreceptor absorption spectra. Maximum absorption for each photoreceptor type was set to 100%. S, S-cones; M, M-cones; L, L-cones.
A: Adapted from http://www.studyblue.com/notes/note/n/lecture-5/deck/5665773
B: Adapted from http://askabiologist.asu.edu/rods-and-cones

The distribution of cones and rods within the human retina is highly skewed (Fig. 4A). While rods dominate in the peripheral retina in a 20:1 ratio, the central retinal region called fovea is a rod-free zone characterized by a high density of cones, nearly 15-fold higher than in the periphery (Curcio et al., 1990). The fovea lies at the center of macula, an area located temporal to the optic nerve, appearing on the fundus image as an oval-shaped highly pigmented yellow spot, histologically distinguished by having more than one layer of ganglion cell nuclei (Fig. 4B). Anatomical differences between the peripheral and the foveal region of the retina concern not only the photoreceptor layer. In contrast to the retinal periphery,

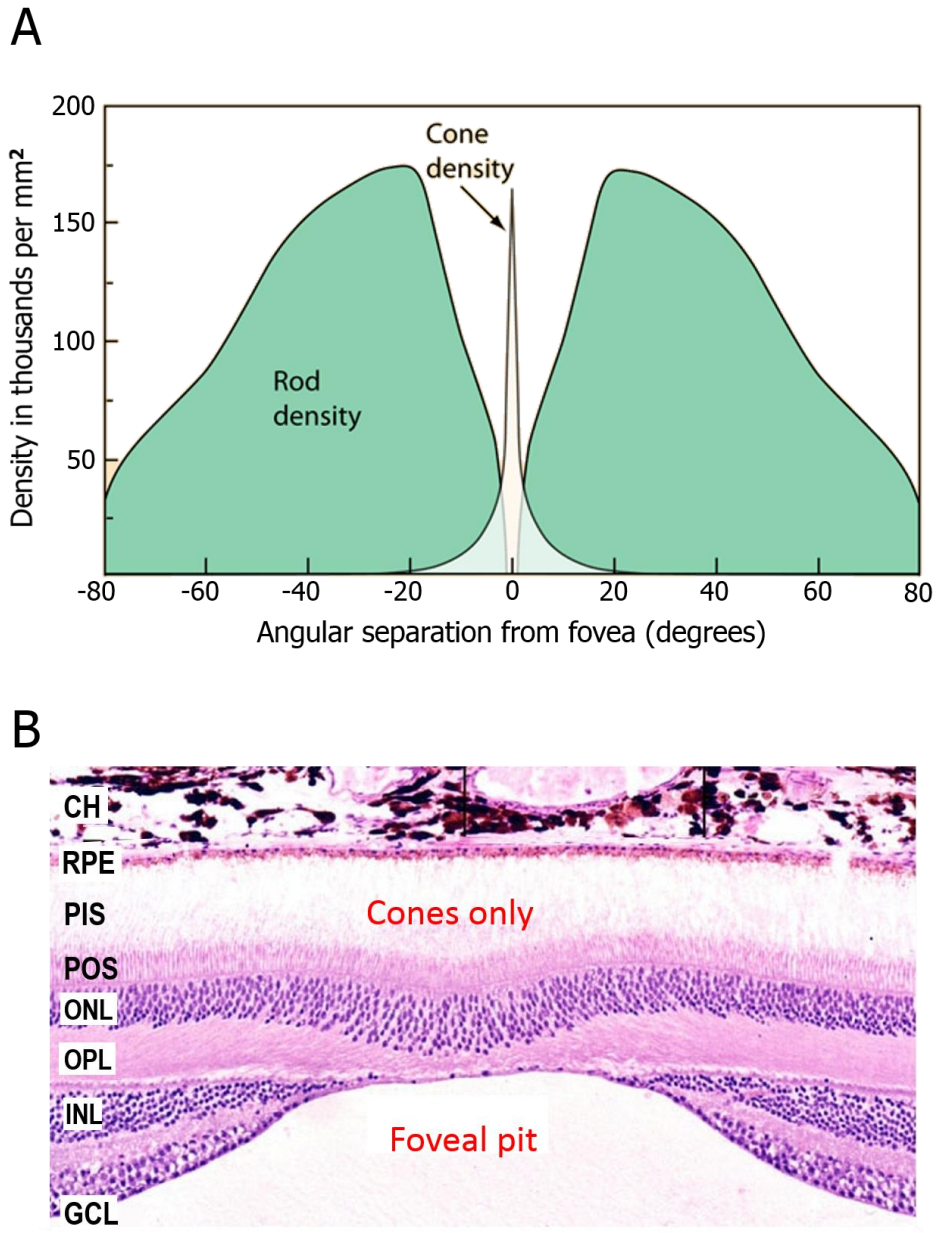

Figure 4. Characterization of the human fovea.
(A) Distribution of rods and cones in the human retina. Cones are concentrated in the fovea, which is free of rods. (B) Histology of the human retina in the foveal region. CH, choroid; RPE, retinal pigment epithelium; PIS, photoreceptor inner segments; POS, photoreceptor outer segments; ONL, outer nuclear layer; OPL, outer plexiform layer; INL, inner nuclear layer; GCL, ganglion cell layer.
A: Adapted from http://hyperphysics.phy-astr.gsu.edu/hbase/vision/rodcone.html
B: Adapted from http://webvision.med.utah.edu/book/part-xii-cell-biology-of-retinal-degenerations/age-related-macular-degeneration-amd/

where a bipolar cell summates the inputs from multiple photoreceptor cells, in the fovea each bipolar cell receives input from a single cone (Prasad and Galetta, 2011). Additionally, the fovea shows high concentration of so-called midget ganglion cells, having spectrally-opponent small receptive field, specialized for high spatial acuity, color vision, and fine stereopsis. The peripheral retina, on the contrary, has equal contribution of the midget and parasol ganglion cells. The parasol ganglion cells have a larger receptive field, spatially opponent concentric organization allowing edge detection, but they lack spectrally opponent organization, therefore are color-insensitive. In summary, the fovea is specialized for high visual acuity, color vision and depth perception, whereas the periphery of the retina accounts for low spatial resolution, motion detection and crude stereopsis (Prasad and Galetta, 2011).

1.1.2 Retinal pigment epithelium (RPE)

Retinal pigment epithelium (RPE) is the outermost retinal layer. Unlike the neuroretina described in the previous sections, RPE is composed of epithelial cells, not of neurons. RPE is not directly involved in the phototransduction, but it is vital to support the architecture and function of the adjacent photoreceptor nerve cells, therefore it is essential for vision. In the next section diverse features and tasks of RPE will be presented. Renewal of the chromophore 11-*cis*-retinal, one of the fundamental functions of RPE, will be discussed in a separate section (1.1.2.2, “Retinoid metabolism”).

1.1.2.1 Function of RPE

The RPE is a single layer of cuboidal, polygonal, post-mitotic differentiated epithelial cells, densely packed with pigmented granules (melanosomes). Thanks to its pigmentation, RPE acts as a neutral density filter that absorbs any intraocular light passing through the photoreceptor layer. This reduces backscatter of light and therefore maintains high-fidelity acuity (Boulton and Dayhaw-Barker, 2001). The RPE monolayer forms the outer blood-retinal barrier (BRB), which separates the neuroretina from the choroid, and controls the passage of molecules and cells into and from the retina. To fulfil this role the RPE cells are joined by several junctional complexes: tight, adherens and gap junctions, which interact together to regulate the apical-basal polarity and transepithelial transport, as well as the cell size, shape and proliferation (Rizzolo et al., 2011). The RPE polarity concerns both its anatomy (structure) and physiology (function). The apical RPE surface is facing the photoreceptor cells. It contains two types of microvilli: long, thin microvilli (5-7μm) that increase the surface available for transepithelial transport; and specialized

shorter microvilli that form photoreceptor sheaths responsible for phagocytosis of the photoreceptor outer segments (Fig. 5). The basolateral surface of the RPE is directed toward the choriocapillaris (CC) and stays in contact with an extracellular matrix called Bruch's membrane (BrM). This side of the RPE contains numerous invaginations which, similarly to their apical counterparts, maximise the surface for the exchange of metabolites and ions (Boulton and Dayhaw-Barker, 2001). The architectural RPE polarity is accompanied by the asymmetric distribution of the channels and transporters throughout the apical and basal membrane. As a result, RPE can control the pH and ion concentrations in the subretinal space (matrix between the POS and RPE), thus sustain the photoreceptor excitability. Additionally, the RPE polarity allows directed transport of nutrients from the choriocapillaris to the retina and of the metabolic end-products in the opposite direction (Strauss, 2005).

Figure 5. Ultrastructure of the RPE.
Electron micrograph of the retinal pigment epithelium in contact with the photoreceptor cells. RPE microvilli extending from the apical surface participate in transepithelial transport and phagocytosis of the photoreceptor outer segments. Phagosomes and elongated melanin granules are localized apically. Presence of tight junctions (black arrow) establishes polarity of RPE cells.
Adopted from http://www.oculist.net/downaton502/prof/ebook/duanes/pages/v7/v7c021.html

The above mentioned POS phagocytosis by the RPE is critical for photo-receptor survival. Both, rods and cones are extensively exposed to light and to high oxygen levels. Their outer segments are particularly susceptible to oxidative damage, as they contain highly reactive retinoids and polyunsaturated fatty acids. Importantly, the rods and cones as terminally differentiated post-mitotic cells, do

not divide. Therefore, they have developed a unique mechanism of renewing POS by shedding outer segments tips, further phagocytosed by the RPE. The phagocytosed material is being processed by a combination of over 40 lysosomal enzymes. The end-products of degradation are either recycled back to the photoreceptors or removed from the retina via the choroidal capillaries. In mammals it takes around 10 days for the rod outer segments to be fully recycled (Boulton and Dayhaw-Barker, 2001).

The posterior part of the eye displays an immune-privileged characteristic, primarily attributed to the RPE. The RPE dampens an immune response in the subretinal space by limiting lymphatic drainage into the retina (as a BRB). Furthermore, the RPE secretes various soluble immunosuppressive factors (transforming growth factor-β, somatostatin, thrombospondin, pigment epithelial derived factor (PEDF), prostaglandin E_2), and expresses cell membrane bound, anti-inflammatory molecules, such as FasL (CD95L) (Zamiri et al., 2007). The unique immunological properties of the RPE and the subretinal space have only recently been appreciated, but are gaining more interest in the context of therapeutic retinal transplantations and the indicated immunologic etiology of some forms of age-related macular degeneration (AMD).

1.1.2.2 Retinoid metabolism

The key molecule of phototransduction, the chromophore 11-*cis*-retinal, originates from its precursors vitamin A (all-*trans*-retinol, ROL) and provitamin A (β,β-carotene), which cannot be synthesised by animals, but must be delivered through the diet. Dietary carotenoids are absorbed in the intestine, metabolized to retinyl esters (REs), packed into chylomicrons (lipoprotein particles), and in this form secreted into the lymph. Most of these circulating REs (~70%) are cleared and stored by the liver. Hepatocytes can secret retinoids into the blood as a complex with serum retinol-binding protein (RBP). The ROL-RBP is taken up by the RPE cells via the retinoid transporter STRA6, ROL is estrified to the REs, and further converted to the chromophore to maintain the vision. Additionally, the all-*trans*-retinal (RAL) released from the opsin after the photon absorption needs to be recycled back to the 11-*cis*-retinal (von Lintig, 2012). The chain of metabolic changes to which retinoids are cyclically subjected in order to regenerate the chromophore is known as the retinoid cycle or the visual cycle. This process takes place in two cellular systems, photoreceptors and the RPE, and involves sets of enzymes depicted and described in figure 6. Recent studies provide evidence for an alternative cone-specific visual cycle that occurs in Müller cells (von Lintig, 2012).

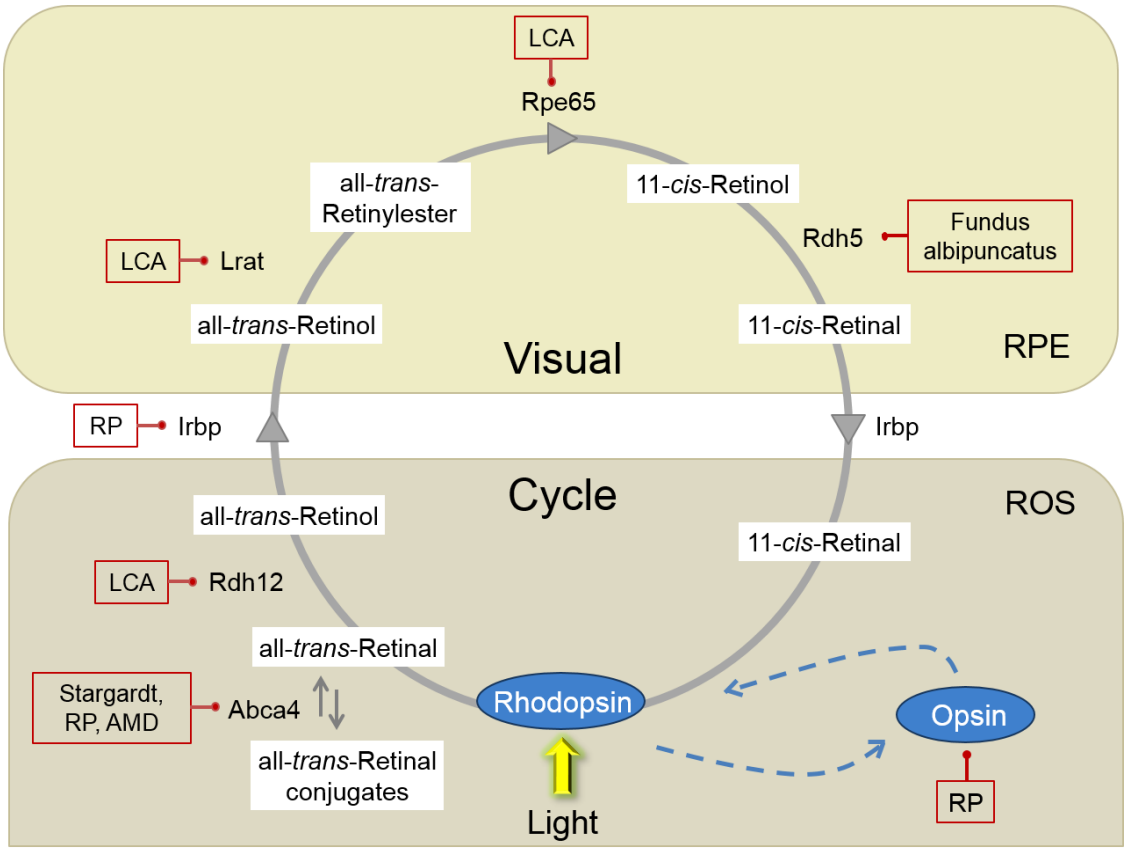

Fig.6. Visual cycle.
Phototransduction starts in the disc membranes of rod outer segments (ROS). Absorption of a photon of light by rhodopsin causes photoisomerization of 11-*cis*-retinal to all-*trans*-retinal (RAL) and its eventual release from the opsin into the disc lumen. ABCA4 (ATP-binding cassette transporter) transfers RAL to the cytosol, where it is reduced to all-*trans*-retinol (ROL) in a reaction catalyzed by retinol dehydrogenases (RDHs). ROL is then translocated to the RPE with the involvement of two retinoid-binding proteins: interphotoreceptor retinoid binding protein (IRBP), which binds retinoids in the extracellular space, and cellular retinol binding protein (CRBP), located within RPE cells. Inside the RPE the ROL is estrified to all-*trans*-retinyl esters (REs) by the lecithin:retinol acyltransferase, LRAT, which is crucial both for the clearance of ROL from ROS and for the uptake of ROL from the blood. In the next step, all-*trans*-REs undergo reaction of isomerization catalyzed by the RPE65 (retinal pigment epithelium 65kDa) protein. The product of this reaction, 11-*cis*-retinol, enters the final step of the visual cycle, in which it is oxidized to 11-*cis*-retinal, bound by cellular retinaldehyde binding protein (CRALBP) and further transported back to the ROS to be built into the photopigment molecules. In red boxes are depicted diverse retinopathies related to the defects in individual enzymes of the retinoid cycle: Stargardt disease, age-related macular degeneration (AMD), Leber congenital amaurosis (LCA), retinitis pigmentosa (RP), and fundus albipuncatus.
Adapted from Kiser et al., 2012.

Disrupting any of the enzymatic steps of chromophore regeneration severely affects visual performance and eventually leads to various forms of retinal degeneration (Kiser et al., 2012). Independently of those pathologies, under normal physiological conditions RAL present at high concentrations in the POS can form adducts with primary amino groups of cellular lipids, proteins, and ribonucleotides. An example of such by-product of the retinoid cycle is bisretinoid A2E, arisen from the reaction of two RAL molecules with the membrane lipid phosphatidylethanolamine. Ocular accumulation of A2E as a component of lipofuscin has been implicated in the pathology of AMD (Sparrow and Boulton, 2005; Sparrow et al., 2000; Zhou et al., 2006).

1.1.2.3 RPE cell cultures

In vitro cell culture is a powerful tool for studying biology and biochemistry of RPE monolayer that offers several advantages over the *in vivo* situation: examining pure RPE devoid of other retinal cells, finer control of the physical and chemical environment in which cells are cultivated, accessibility for administration of exogenous compounds, expansion of experimental material by proliferation and subculture. To be a useful *in vitro* experimental system, cultured RPE cells on the one hand have to proliferate, and on the other hand have to resemble their *in vivo* counterpart. Both these requirements can be achieved by applying specially formulated culturing media. It was observed that epithelial cells tend to lose some differentiated functions under conditions encouraging proliferations, therefore numerous groups reported usage of two distinct medium formulations in order to either stimulate proliferation or the differentiated state of RPE cells *in vitro*, where reduction of serum and calcium concentration synergistically increased proliferation rate (Hu, 2000; Pfeffer, 1991).

The fact that RPE cells lose their specialized properties after multiple passages promotes utilization of primary cultures in RPE research. Primary RPE cultures from various species have been shown to retain many normal physiological functions, including the ability to transport retinoids (Pfeffer et al., 1986), and phagocytosis of rod outer segments (Bosch et al., 1993). Despite their undeniable advantages, primary cultures may exhibit physiological differences caused by variability between the donor tissues and introduced during the isolation procedure. Therefore, each individual cell line needs to be continually monitored for the desired physiological, morphological and molecular features to verify its usefulness and to ensure controlled, reproducible experimental conditions (Pfeffer, 1991). The proper evaluation of primary RPE cultures includes examination of RPE cell morphology: polygonal shape, pigmentation, presence of apical microvilli and

junctional complexes. Additionally, it is important to test for the secretion of the components of cellular matrix, like collagen (types I, III, IV, V), laminin, fibronectin, and heparin sulphate proteoglycan, which are produced by all epithelia. Immunofluorescence can also serve to detect sub-apical actin ring, characterizing differentiated epithelia, or apical distribution of Na^+, K^+-ATPase, distinguishing RPE among other epithelia. To truly mimic the native tissue, *in vitro* RPE cultures should express enzymes metabolising visual chromophore, as RPE65, CRALBP, and RDH5 (Pfeffer, 1991).

Limited proliferation, substantial heterogeneity and related necessity for laborious, thorough characterization of primary RPE cultures caused the need for establishing RPE cell lines. ARPE19 is a commercially available, in research most widely used human RPE cell line, which arose spontaneously under selective trypsinization of a primary RPE culture derived from a 19-years old male donor (Dunn et al., 1996). When cultured to post-confluent densities, ARPE19 cells developed morphology and biochemical features of differentiated RPE, such as expression of CRALBP and RPE65 mRNA (Dunn et al., 1996), therefore they might be a useful tool to study retinoid metabolism or the regulation of RPE-specific gene expression. Importantly, original ARPE19 cultures displayed pronounced heterogeneity in any RPE-specific property that has been tested, which was reflected in a low transepithelial resistance. This feature may limit application of ARPE19 cell line in more complex studies, such as polarized secretion of proteins.

1.2 Molecular mechanisms of age-related macular degeneration

Age-related macular degeneration (AMD) is a progressive complex disease that affects the central retina (macula) in people at age of 50 years and more (Jager et al., 2008). It is the most common cause of blindness and visual disability among the elderly in the developed countries. The clinical hallmark of AMD is accumulation of focal, acellular deposits that form at the interface between the RPE and BrM, called drusen. Advanced AMD occurs in two forms: geographic atrophy, GA (non-neovascular, dry, non-exudative), and choroidal neovascularization, CNV (neovascular, wet, exudative) (Fig. 7). GA is a clinical manifestation of progressive RPE cell death. Patients with GA develop gradual central vision loss, usually over the course of months to years. CNV is characterized by the growth of abnormal blood vessels from the choroid through BrM and the RPE. This process is accompanied by increased vascular permeability and fragility. Its extension may lead to subretinal haemorrhage, exudative retinal detachment, or scar formation, and can result in sudden, profound vision loss. CNV that accounts for only 10% of all AMD cases is responsible for approximately 75% of severe central vision loss in AMD (Klein et al., 1997).

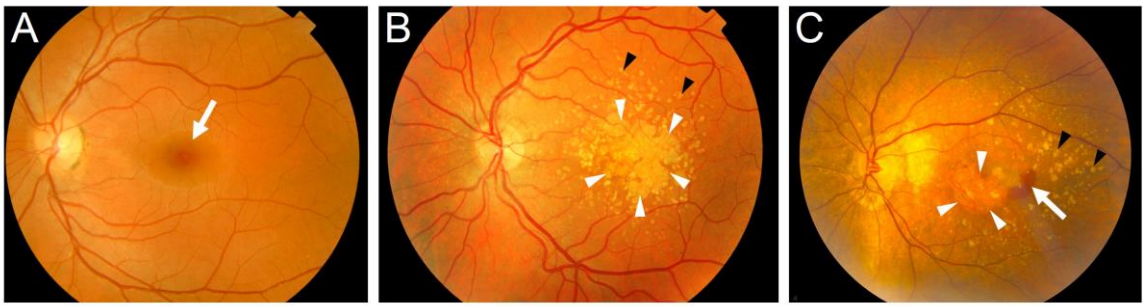

Figure 7. Fundus images.
Fundus photography presents an image of the interior surface of the eye, including the retina, optic disc, macula, and the retinal periphery. It is used in ophthalmology for diagnosis of a disease (combined with retinal angiography), and for monitoring the progression of a disease. (A) A fundus image of the normal retina. Macula is visible in the center of the retina as a highly pigmented spot (arrow). (B) A fundus image of the retina with geographic atrophy (arrowheads). Black arrowheads indicate drusen. (C) A fundus image of the retina with neovascular AMD shows subretinal haemorrhage (arrow), choroidal neovascularization (white arrowheads), and numerous drusen (black arrowheads). *Adopted from* http://www.thelondonproject.org/OurVision/TheDisease/?id=74

Age is the major risk factor for AMD. Because the population of the industrialized world is rapidly aging, the overall prevalence of advanced AMD is projected to increase more than 50% by the year 2020 (Friedman, 2004). The magnitude of this problem has driven enormous amount of studies to elucidate the

molecular mechanisms of the disease that would eventually provide prevention and therapy. How do "normal aging" processes contribute to the pathology? Which genetic, molecular and/or environmental factors shift the balance toward developing AMD? How to use this information for the early diagnosis? How to target the early-onset molecular changes to prevent AMD? Which factors accelerate progression of the disease and how to counteract them? These are the main questions that over 13'000 published studies have tried to solve to date, and the research effort is continuously growing (Fig. 8).

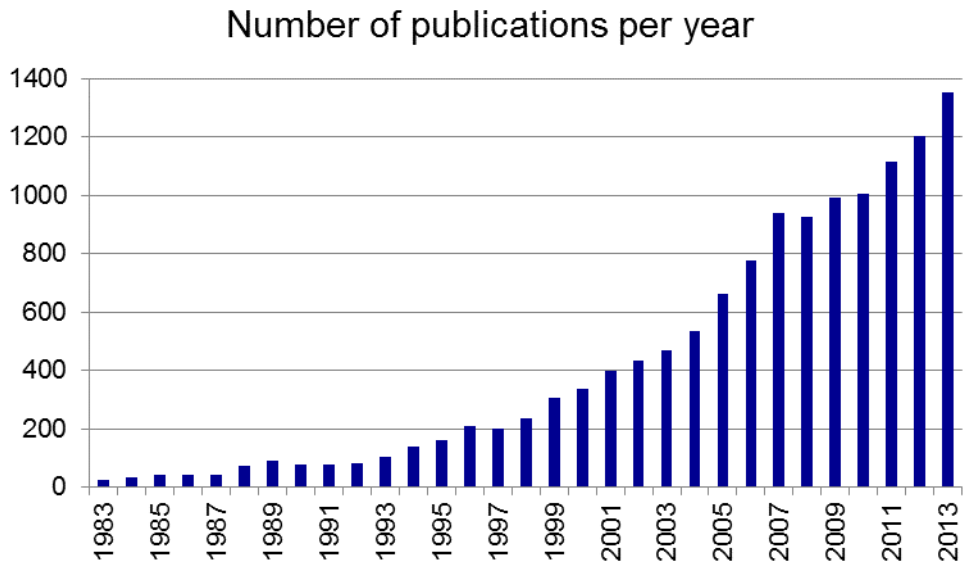

Figure 8. Number of publications on AMD available in PubMed database.
Graph was generated based on the PubMed search (http://www.ncbi.nlm.nih.gov/pubmed) using a query: (((amd[Title/Abstract]) OR age-related macular degeneration[Title/Abstract]) OR geographic atrophy[Title/Abstract]) OR choroidal neovascularization[Title/Abstract]. 13586 hits were found, February 2014.

1.2.1 Aging of RPE and Bruch's membrane

Aging is a naturally occurring process accompanied by substantial anatomical and physiological changes in the organism. It may take place without direct clinical consequences. It is clear however, that age-related, non-pathogenic changes may compromise the overall fitness of the cells and tissues, predisposing them to a pathogenic state. In the eye, progression of aging may be slow enough so that no loss of function is experienced. Nevertheless, senescence of the RPE and BrM are known to underlie the development and progression of AMD. Human RPE cells, which are a post-mitotic, non-regenerating system, undergo structural changes with increasing age that result in loss of cell shape, multilayered organization, and atrophy, hyper- and hypopigmentation (Curcio et al., 2000). Additionally, due to the

increasing metabolic insufficiency they accumulate non-degraded material originating from phagocytosed POS in form of lipid/protein aggregates (lipofuscin granules) (Wing et al., 1978). The indigestible molecules can be exported basolaterally, where they accumulate in BrM or diffuse to the bloodstream (Kinnunen et al., 2012). Otherwise, compromised lysosomal, proteasomal, and autophagosomal clearance may cause increased RPE cell damage eventually leading to cell death (Sparrow and Boulton, 2005). A2E has been long considered to be the main bisretinoid component of the RPE lipofuscin responsible for induction of the RPE apoptosis, and thus contributing to the development of AMD (Sparrow et al., 2000; Sparrow et al., 2003). Interestingly, the recent study by Ablonczy and colleagues (Ablonczy et al., 2013) that demonstrated lack of correlation between the A2E and lipofuscin distribution in the human RPE, with predominantly peripheral accumulation of A2E, has challenged the pre-existing dogma and revealed the need to revise the role of bisretinoid A2E in human retinal degeneration.

BrM, just as RPE, undergoes significant changes throughout human life. Most prominently, BrM thickness increases in a linear manner with age, being in the eighth decade of life more than twice as thick as in the first decade (Ramrattan et al., 1994). BrM thickening involves structural changes: elevated accumulation of lipids and advanced glycation end products (AGEs), collagen cross-linking, larger proteoglycans size, increased calcification, iron and zinc deposition. These age-related features of BrM impair protein turnover, decrease BrM elasticity, induce formation of a lipid wall, and as a result compromise fluid and macromolecule exchange between the choroid and RPE. Structurally and functionally altered BrM does not provide sufficient metabolic support for the RPE and promotes drusen formation, a feature of AMD (Booij et al., 2010).

1.2.2 Oxidative stress

Cumulative oxidative damage contributes to aging (Adelman et al., 1988). The retina, on the other hand, through its daily exposure to visible light, high oxygen consumption, and enrichment in docosahexaenoate, the most oxidizable polyunsaturated fatty acid (PUFA) in humans, offers a high oxidative stress environment (Fliesler and Anderson, 1983). It is not surprising therefore, that oxidative stress has been long suspected to play a role in the pathogenesis of AMD (Beatty et al., 2000). Convincing evidence in favour of this hypothesis came from epidemiological studies showing that smoking significantly increases the risk of AMD, whereas carotenoids and antioxidant vitamins may retard progression of the disease (Snodderly, 1995). By now numerous studies have explored the

mechanism, how oxidative modifications of diverse classes of molecules can act detrimentally to the POS, RPE and BrM. In particular, bisretinoid A2E has been shown to carry out its cytotoxic action via blue light and oxygen mediated mechanism (Sparrow et al., 2000; Sparrow et al., 2003). Already mentioned PUFAs, representing 50% of the lipids in POS membranes, can easily generate lipid peroxides that have the potential to oxidize, thus damage further molecules. Docosahexaenoate-derived oxidative modifications of proteins (i.e., CEP-protein adducts) have been found at higher concentrations in AMD drusen compared to drusen derived from healthy aged individuals, which implicates their involvement in the "pathological aging" (Crabb et al., 2002). Similarly, AMD drusen contain protein modifications generated from lipoxidation and glyoxidation (AGEs). By cross-linking common drusen proteins (TIMP3 and vitronectin) and structural proteins in BrM, AGEs prevent normal protein turnover, accelerate drusen formation and promote progression of AMD (Crabb et al., 2002; Glenn et al., 2009; Handa et al., 1999; Yamada et al., 2006).

1.2.3 Central role of the immune response

In the late 1990-ties and at the beginning of the XXI century a number of immuno-histochemical studies has consistently identified various plasma proteins in drusen, including acute phase reactants: amyloid P component, complement C5, α1-anti-trypsin, and proteins mediating immune response, such as vitronectin, activated complement components (Fig. 9) and apolipoprotein E (Mullins et al., 2000). These findings together with the fact that immune and inflammatory response appeared to play a role in formation of other pathologic, age-related deposits, led to a concept that similar mechanism may be involved in the development and/or regression of drusen (Johnson et al., 2000). Nevertheless, at that stage of research on AMD and understanding its pathogenesis, there was no general consensus regarding the origin of drusen, and the importance of the immune pathways in drusen formation. The last 15 years of research have been constantly delivering strong evidence positioning immunological responses in the center of the AMD etiology. A strong line of evidence in favour of this hypothesis came from genetic analyses revealing that sequence variants in complement-related genes have large contribution to the AMD heritability (Klein et al., 2005) (more detailed information in section 1.2.4, "Genetic susceptibility to AMD"). Additionally, in a recent study at the systems-level involving comparative transcriptome profiling combined with interactome analysis, Newman and colleagues showed that cell-mediated immune response is a common feature of all examined AMD phenotypes, whereas apoptosis and angiogenesis related genes are overrepresented in GA and CNV, respectively

(Newman et al., 2012). Similarly, a comparative quantitative proteomics analysis of AMD and control BrM/choroid samples revealed elevated levels of complement proteins, various damage-associated molecular patterns (DAMPs), and other immune system stimulators at all stages of AMD, again demonstrating a central role of the immunity (Yuan et al., 2010). Latest findings have established pattern recognition receptors (PRRs), which are part of the innate immune response, as key sensors recognizing various DAMPs and controlling further molecular pathways, including vascular growth and RPE cell survival. Specifically, activation of NLRP3 inflammasome by CEP-protein adducts and C1Q drusen component was shown to be protective against CNV, whereas priming of this PRR by *Alu* RNA was demonstrated to induce RPE cell degeneration, and thus to contribute to the pathogenesis of GA (Doyle et al., 2012; Tarallo et al., 2012). Toll-like receptors (TLRs) are other "immune-hubs" known to control both angiogenesis and development of geographic atrophy in response to oxidative stress or siRNA (Kleinman et al., 2008; West et al., 2010; Yang et al., 2008).

Taken together, a model is supported where aging, environmental and genetic factors accelerate the onset and progression of cell-based immunological events, leading to chronic local inflammation and promoting atrophic and/or neovascular changes characteristic of advanced AMD. Furthermore, these findings suggest key components of the immune system to be promising targets for therapeutic intervention at all stages of the disease.

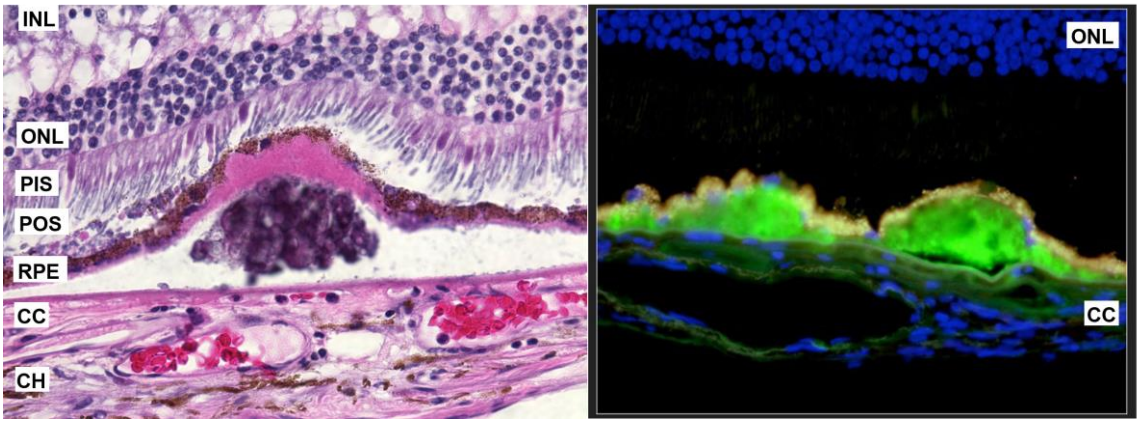

Figure 9. Drusen.
Left panel: Histology of a human retina with a druse localized between the retinal pigment epithelium (RPE) and the Bruch's membrane. Right panel: Drusen from a human donor eye with AMD immunofluorescently labelled with an antibody directed against terminal complement complex C5b-9 (green fluorescence) illustrate involvement of immune-mediated processes in AMD. Nuclei are stained with DAPI visible in blue. INL, inner nuclear layer; ONL, outer nuclear layer; PIS, photoreceptor inner segments; POS photoreceptor outer segments; CC, choriocapillaris; CH, choroid.
Adapted from http://webeye.ophth.uiowa.edu/mullinslab/

1.2.4 Genetic susceptibility to AMD

It is now beyond the question that genes play a significant etiological role in AMD. Some of the early suggestions of genetic predisposition originated from familial aggregation studies. For example, a high concordance of clinical features was observed in monozygotic twins (Hammond et al., 2002). Additionally, first-degree relatives of affected probands displayed higher incidence of AMD in comparison to controls, with siblings of affected individuals having a three to six-fold increase in disease risk (Klaver et al., 1998; Seddon et al., 1997). These initial indications established the need for further characterization of the genetic component of AMD. To date various classical genetic analyses and novel state-of-the art genotyping and sequencing techniques were utilized for this purpose. In particular, genome-wide linkage analysis of large families led to the discovery of the major AMD-susceptibility loci on chromosome 1 (1q31) and on chromosome 10 (10q26), which was replicated in several independent studies, and further validated through a meta-analysis of whole genome scans (Abecasis et al., 2004; Barral et al., 2006; Fisher et al., 2005; Iyengar et al., 2004; Klein et al., 1998; Majewski et al., 2003; Seddon et al., 2003; Weeks et al., 2004). Testing of these two AMD-susceptibility loci in a single nucleotide polymorphism (SNP)-association studies on case-control populations identified specific genetic variants associated with AMD, among them the p.Tyr402His polymorphism in the complement factor H (*CFH*) gene (Edwards et al., 2005). Subsequent analysis of the complement pathway identified SNPs conferring risk/protection for AMD in other complement genes: complement factor *C2*, *CFB*, *C3*, and *CFI*, supporting a critical role for complement regulation in the pathology of AMD (Fagerness et al., 2009; Gold et al., 2006; Maller et al., 2007; Spencer et al., 2007; Yates et al., 2007). While the pathogenicity of variants in the complement genes has been well characterized, the functional pathway involving the 10q26 locus has not yet been understood (Swaroop et al., 2007).

Advances in genotyping technology enabled high-throughput genome-wide association scans (GWAS) for AMD on large cohorts, aiming to explain the unrevealed heritability of AMD. In 2010 two large consortia of researchers conducted two independent GWASs with subsequent replication of risk factor findings. These studies identified several new genes associated with advanced AMD such as *LIPC* (hepatic lipase), *CEPT* (cholesterylester transfer protein), *LPL* (lipoprotein lipase), and *ABCA1* (ATP-binding cassette, sub-family A, member 1). Interestingly, these genes encode proteins involved in high-density lipoprotein (HDL) and cholesterol metabolism, pathways that were previously indicated in drusenogenesis (Chen et al., 2010; Curcio et al., 2005; Li et al., 2005; Neale et al., 2010).

For complete benefit from the genetic studies, discovery of direct casual mechanisms for particular genes and their protein products are essential. Recently, a couple of studies have beautifully explained the molecular consequence of single nucleotide variants, previously shown to be associated with risk to develop AMD. Weissman and colleagues demonstrated that malondialdehyde (MDA), a common lipid peroxidation product present at elevated concentrations in plasma of AMD patients, directly interacts with CFH (Baskol et al., 2006; Weismann et al., 2011). Moreover, the CFH p.His402 variant conferring high risk of AMD markedly reduces ability of CFH to bind MDA, which shifts the active-inactive complement balance toward the active state and promotes chronic inflammation. Another study provided insights into the pathogenicity of the highly penetrant risk variant p.Gly119Arg in CFI, a complement factor which similarly to CFH can inactivate the alternative pathway of the complement system (van de Ven et al., 2013). The Gly119Arg substitution resulted in a lower factor I proteolytic activity, and led to defects in the morphology of hyaloids vessels in the developing retina of zebrafish. A further recent finding showed that the rare allele in complement component C3 posing risk of AMD that encodes p.Lys155Gln amino acid exchange results in resistance to proteolytic inactivation by CFH and CFI (Seddon et al., 2013). All risk alleles in the complement system investigated to date share common molecular mechanism, namely they lead to an excessive alternative pathway activation, which may eventually cause RPE cell death.

1.2.5 Animal models in AMD research

Expanded understanding of the mechanisms of human disease leading to the formulation of efficient and safe therapeutic strategies would not be feasible without employing appropriate animal models. The animal models are particularly useful due to their relatively unlimited supply, ease of manipulation, and closely controlled experimental conditions. A perfect model organism should display high similarity to humans in terms of genetics, anatomy, and physiology. Considering AMD, one could propose the primates as a preferable model organism, because they are the only mammals possessing a macula. Despite this obvious anatomical prerequisite, other factors like the slow course of disease, limited supply of animals, economic constrains, and ethical challenges in generating genetically modified monkeys restrict their utilization in AMD research (Ramkumar et al., 2010).

Since 1924 when the first inherited retinal degeneration has been identified in mice, these rodents have become the main model organism to study retinal degeneration, and helped to discover genes causing retinal dystrophies in humans

(Hafezi et al., 2000; Keeler, 1924). The mouse retina closely resembles that of the human nasal and peripheral retina, thus is well suitable to model defects in these parts of the retina. AMD, however is a disease affecting the macula, a functional area that is not distinguishable in mouse. As nocturnal animals, mice have rod-dominated retinas with rods comprising 97% of photoreceptor cells and 3% of cones spread through the retina (Carter-Dawson and LaVail, 1979). Furthermore, murine Burch's membrane structure, its age-related changes, and RPE lipofuscin metabolism differ from the one present in humans (Mishima and Hasebe, 1978). Despite those differences in the retinal anatomy and physiology, there are numerous mouse models showing partial features of AMD like drusenoid lesions, sub-RPE basal deposits, Bruch's membrane thickening, A2E accumulation, RPE atrophy, choroidal neovascularization, and electroretinogram (ERG) abnormalities (Ramkumar et al., 2010). Most murine models for dry AMD are genetically engineered mice with modified genes that either are causative for the juvenile macular dystrophies in humans or have been implicated in the pathogenesis of AMD. These models include *Abca4*$^{-/-}$ (Stargardt disease) (Mata et al., 2001; Weng et al., 1999) and transgenic *ELOVL4* mice (Stargardt-3 dominant inherited disease) (Vasireddy et al., 2009), as well as models targeting the immune pathway such as *Cfh*$^{-/-}$, *Ccl2*$^{-/-}$, *Ccr2*$^{-/-}$, *Cx3cr1*$^{-/-}$, *Ccr2*$^{-/-}$/*cx3cr1*$^{-/-}$ mice (Ambati et al., 2003; Coffey et al., 2007; Combadiere et al., 2007; Combadiere et al., 2013; Luhmann et al., 2013a; Luhmann et al., 2013b; Tuo et al., 2007); oxidative stress associated genes like in *Sod1*$^{-/-}$, *Sod2*$^{-/-}$ and *Nrf2*$^{-/-}$ knockout mice (Imamura et al., 2006; Justilien et al., 2007; Zhao et al., 2011); or metabolic pathways related genes, for example in *ApoE4* transgenic mice on high fat and high cholesterol diet (lipid metabolism) (Malek et al., 2005). Features of dry AMD were also observed in CEP-immunized wild type mice (C57BL/6J) and in a few natural mouse strains such as "age-related retinal degeneration" mouse (arrd2) and the Senescence-Accelerated Mouse (SAM) (Chang et al., 2008; Hollyfield et al., 2010; Majji et al., 2000; Takeda et al., 1994). In some of the above-mentioned models dry AMD-like changes are accompanied by CNV (*ApoE4* transgenic mouse, SAM). The best-established model for wet AMD, however, is a laser-induced CNV (Bora et al., 2003).

An alternative *in vivo* model system to investigate photoreceptor and RPE cell death involves exposure to the high intensities of white fluorescent light or blue light (light damage, LD) (Grimm and Reme, 2013; Wenzel et al., 2005). This experimental model provides an opportunity to explore the light-induced cytotoxity as a mechanism contributing to AMD pathology (Sparrow and Boulton, 2005; Sparrow et al., 2000). Light exposure was shown to cause RPE damage and altered Bruch's membrane structure in the golden hamster (Thumann et al., 1999). Photoreceptor apoptosis, followed by RPE cell death upon light illumination was

observed in rats (Hafezi et al., 1997). On the contrary, mouse RPE stayed preserved after LD (Reme et al., 2000), it displayed, however, several dysfunctionalities, like tight and adherent junctions disassembly, increased permeability and abnormal polarity of VEGF (vascular endothelial growth factor) secretion (Cachafeiro et al., 2013). Additionally, activation of proinflammatory signalling followed by the macrophage infiltration into the subretinal space was observed (Joly et al., 2009). These molecular events, known to play a role in inflammatory angiogenesis which contributes to AMD, could be further studied using the light damage model in mice.

1.3 Paraoxonase-1

1.3.1 Paraoxonase family

Paraoxonase-1 (PON1) is the best studied member of the paraoxonase (PON) gene family composed of 3 genes: *PON1*, *PON2* and *PON3* aligned next to each other on the evolutionary conserved region on chromosome 7 in human and on chromosome 6 in mouse (Humbert et al., 1993; Sorenson et al., 1995). The human paraoxonases share approximately 70% identity at the nucleotide level and 65% identity at the amino acid level (Primo-Parmo et al., 1996). Based on the structural homology, PON2 appears to be the oldest member of the family, followed by PON3 and more recently by PON1 (Draganov and La Du, 2004). All three PON proteins are lactonases with antioxidant properties, which differ in their site of synthesis and in the mechanisms of action (Draganov et al., 2000; Rosenblat et al., 2003). While *PON2* is commonly expressed in various organs/cell types, the *PON1* and *PON3* production is limited almost exclusively to the liver (Ng et al., 2005) (Fig. 10). Additionally, the PON1 and PON3 proteins have signal sequences that route them for secretion. Both PON1 and PON3 are being secreted to the blood where they bind HDL, enabling its transport and protecting it from oxidation (Draganov et al., 2000; Mackness, 1989). PON2 on the contrary, is an intracellular protein important in protecting endoplasmic reticulum (ER) and mitochondria from reactive oxygen species (ROS) mediated damage (Altenhofer et al., 2010; Horke et al., 2007).

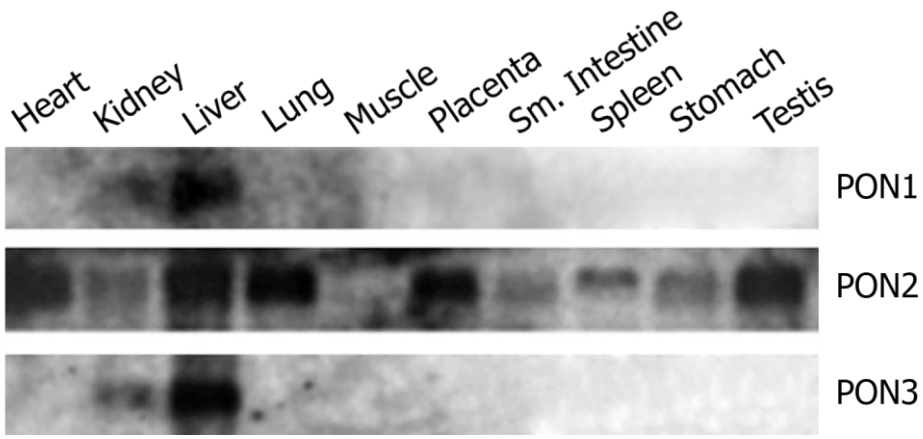

Figure 10. Tissue distribution of the human *PON* transcripts.
Northern blot analysis of human tissue containing 2 μg of mRNA per lane. Sm, small.
Adapted from Ng et al., 2005.

1.3.2 Regulation of *PON1* gene expression

The human *PON1* gene (ID: 5444) extends over approximately 26 kb at 7q21.3 and consists of 9 exons and 8 introns (Fig. 11). Mouse *Pon1* (ID: 18979) located at chromosome 6 displays the same gene structure as its human ortholog (Sorenson et al., 1995). Transcription of *PON1* can be initiated from the multiple transcription start sites located within the TATA-less promoter (Gouedard et al., 2003). Peroxisome proliferator-activated receptor gamma (PPARγ) and the aryl hydrocarbon receptor (AhR) are two ligand-activated transcription factors that have been shown to regulate *PON1* expression. Statins, pharmacological compounds widely used for the treatment of hyperlipidemia, up-regulate *PON1* expression via activation of PPARγ that results in higher serum PON1 activity in hypercholesterolemic patients (Tomas et al., 2000). Similarly, plant-derived polyphenols increase *PON1* expression upon binding to PPARγ in human hepatocytes *in vitro* (Khateeb et al., 2010). Resveratrol, a natural phenol, and aspirin have been shown to induce *PON1* expression through an AhR-mediated mechanism in human liver cell lines (Gouedard et al., 2004a; Jaichander et al., 2008).

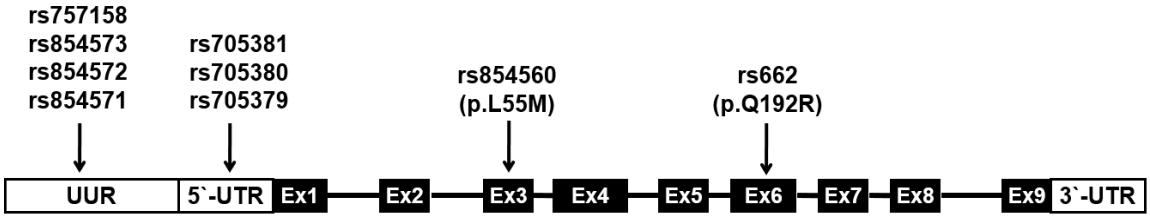

Figure 11. Schematic representation of the human *PON1* gene.
Single nucleotide polymorphisms within upstream regulatory region of *PON1* gene and missense SNPs in exon 3 and exon 6 are indicated: rs757158, C(-1740)T; rs854573, T(-1075)C; rs854572, C(-908)G; rs854571, C(-831)T; rs705381, G(-162)A; rs705380, G(-126)C; rs705379, T(-107)C; rs854560, p.L55M; rs662, p.Q192R. UUR, upstream untranscribed region; UTR, untranslated region; ex, exon.

Five single nucleotide polymorphisms (SNPs) have been identified in the first 1000 bases upstream of the *PON1* coding region at positions -107/-108, -126, -160/-162, -824/-832, and -907/-909 (Brophy et al., 2001a; Leviev and James, 2000; Suehiro et al., 2000). Several of these SNPs -107, -162 and -909 exerted functional effects on *PON1* expression *in vitro* (Brophy et al., 2001a), whereas the -909 polymorphism appeared to have little or no effect on PON1 levels in human plasma (Brophy et al., 2001b). The -107 polymorphism, which displayed a dominant effect on expression of *PON1* gene both *in vitro* and *in vivo* (Brophy et al., 2001a; Brophy et al., 2001b), lies within the consensus sequence of the binding site for the transcription factor Sp1, and affects interaction between this factor and

PON1 promoter (Deakin et al., 2003). The -107 variant was found to be associated with increased risk of coronary artery disease and AMD (James et al., 2000; Oczos et al., 2013).

Four SNPs and variant poly(A) signal sequences have been identified in the 3'UTR of PON1 transcript (Brophy et al., 2001b). To date no experimental evidence has clarified whether they affect the addition of the poly(A) tail or otherwise alter the stability of the PON1 mRNA.

1.3.3 PON1 enzymatic activities

Human paraoxonase-1 (PON1) is a serum glycosylated protein consisting of 355 amino acids with a molecular mass of approximately 45kDa (Draganov et al., 2005; Hassett et al., 1991). Mouse *Pon1* cDNA encodes a 355-amino acid long protein, that shares 83% identity with the human PON1 amino acid sequence (Primo-Parmo et al., 1996). Human PON1 forms a six-bladed beta-propeller structure containing two Ca(2+) ions necessary for the protein stability, as shown in figure 12 (Erdos et al., 1959; Harel et al., 2004).

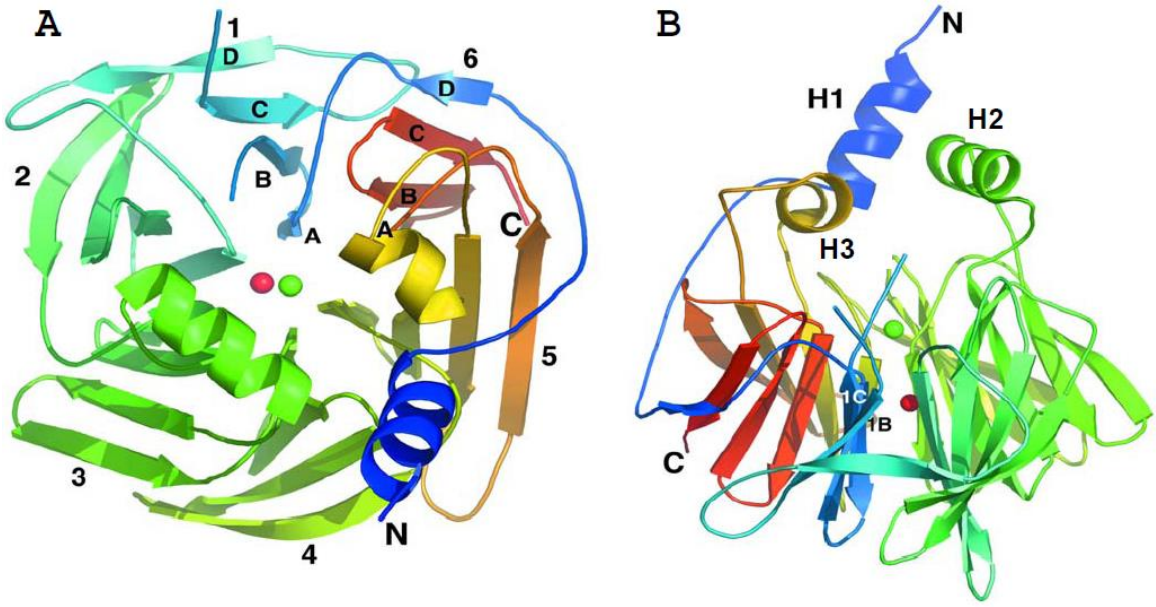

Figure 12. 3D model of the structure of human PON1.
(A) A view of the 6-bladed β-propeller from the top. Shown are N- and C-termini, the six blades (labelled 1-6) each of which is comprised of 4 β-strands (labelled A-D) and the two calcium atoms in the central tunnel of the propeller (red and green spheres). (B) A side view of the propeller. The top calcium ion (green sphere) is a key part of the enzyme's active site. Three helices at the top (H1-H3) comprise an active site lid. Helix H1 contains N-terminal hydrophobic signal sequences that is retained after PON1 secretion. Helixes H1 and H2 are believed to participate in the binding of PON1 to HDL.
Adapted from Harel et al., 2004.

The name “paraoxonase” indicates hydrolyzing activity (E.C. 3.1.8.1) toward paraoxon, the active metabolite of the organophosphorous insecticide, parathione (Aldridge, 1953). PON1 can hydrolyze a broad range of molecules: toxic metabolites of a number of other insecticides (phosphotriesterase activity), as well as aromatic esters (arylesterase activity) and aromatic or long-chain aliphatic lactones (lactonase activity) (Billecke et al., 2000). Despite the long list of various PON1 substrates that have been identified, its “major” physiological function and the endogenous substrates remain uncertain (La Du et al., 1999; Teiber et al., 2007). The fact that other members of the PON family lack, or have very limited paraoxonase and arylesterase activity implies that the name “paraoxonases” is purely historical, and suggests the lactonase activity to be the one, for which the PONs may have evolved. Comprehensive structure-reactivity studies with PON1 and PON1 variants generated from directed evolution have supported this hypothesis (Khersonsky and Tawfik, 2005, 2006). Furthermore, Dragnov and colleagues have characterized PONs enzymatic activities in detail and proposed lactone and hydroxy acid derivatives of polyunsaturated fatty acids (PUFAs) as the endogenous substrates (Draganov et al., 2005). Homocystein thiolactones, the toxic homocystein metabolites involved in the pathogenesis of the cardiovascular disease in humans, are another group of lactones that have been described as likely natural PON1 substrates (Jakubowski et al., 2001).

1.3.4 Polymorphic forms of PON1

The PON1 activity polymorphisms have been subject of numerous studies for more than 20 years before Humbert and colleagues found the actual genetic determinant of those variants (Geldmacher-von Mallinckrodt, 1973; Humbert et al., 1993). The two known PON1 allozymes differ in paraoxonase activity, originating from the amino acid exchange at position 192 (p.Q192R). In addition to the amino acid substitution at position 192, a large interindividual variability in the amount of serum PON1 contributes to the reported differences in paraoxonase activity (Furlong et al., 1988; Playfer et al., 1976). Currently it is known that the level of PON1 in serum is determined by the genetic variants (leucine to metionine substitution at codon 55 (p.L55M); and T(-107)C polymorphisms), as well as disease state, dietary, life-style, and environmental factors (Costa et al., 2003; Leviev and James, 2000).

The two common coding *PON1* polymorphisms: p.L55M (rs854560), p.Q192R (rs662) have been investigated for genetic association with a number of pathophysiological conditions, including atherosclerosis, hyperlipidemia, coronary artery disease (CAD), stroke, type 2 diabetes, Parkinson`s disease, Alzheimer`s

disease, and AMD; frequently giving contradictory results (Baird et al., 2004; Esfandiary et al., 2005; Ikeda et al., 2001; Ng et al., 2005; Pauer et al., 2010). Nevertheless, independent of PON1 genotype, low serum PON1 activity levels have been implicated in hyperlipidemia, type I diabetes, CAD, chronic renal failure, metabolic syndrome, rheumatoid arthritis, thyroid dysfunction, uremia, and AMD (Ates et al., 2009; Baskol et al., 2006; Ng et al., 2005). The inconsistence between various genetic and physiological studies led to the suggestion, that PON1 status (activity and level) may be more important in determining the PON1 involvement in disease than paraoxonase genetic polymorphisms (Brophy et al., 2000; Jarvik et al., 2003; Jarvik et al., 2000; Mackness et al., 2001; Richter and Furlong, 1999).

1.3.5 Anti-oxidant and anti-inflammatory properties of PON1

In 1991 Mackness and colleagues discovered that PON1 purified from human HDL may be responsible for destroying pro-inflammatory oxidized lipids present in oxidized low-density lipoprotein (oxLDL), and thus may act anti-atherogenic (Mackness et al., 1991). This study has stimulated further investigations, which provided further evidence that PON1 protects vascular tissue from oxidative damage (Aviram et al., 1998; Mackness et al., 1993; Watson et al., 1995). Additional confirmation of the *in vitro* findings came from characterization of mice lacking PON1 (*Pon1*$^{-/-}$) (Shih et al., 1998). Relative to their control littermates, HDL from PON1-deficient mice was more susceptible to oxidation and was unable to prevent LDL from oxidation in a co-cultured cell model of the artery wall. On the contrary, HDL isolated from transgenic mice overexpressing human or mouse PON1 exhibited enhanced ability to protect LDL against oxidation, further confirming anti-oxidant function of PON1 (Oda et al., 2002; Tward et al., 2002).

Another mechanism by which PON1 contributes to the anti-atherogenic properties of HDL is its anti-inflammatory activity. PON1 can decrease oxLDL-mediated secretion of monocyte chemotactic protein-1 (MCP-1) and monocyte transmigration, as demonstrated by studies on PON1-knockouts (Shih et al., 1998). Furthermore, PON1 inhibits monocyte-to-macrophage differentiation and directly suppresses macrophage pro-inflammatory responses (Aharoni et al., 2013; Rosenblat et al., 2011).

1.3.6 Implications for involvement of PON1 in AMD

Atherosclerosis and AMD are complex diseases that share similar aetiology, environmental risk factors, and underlying molecular mechanisms. In particular, in both conditions oxidative stress and inflammation are involved in formation of

pathological extracellular lesions, plaques in atherosclerosis or drusen in AMD (Curcio et al., 2010; Curcio et al., 2011). As described above, diverse studies have demonstrated beneficial, anti-atherogenic function of PON1, whereas its role in development of drusen or other ocular changes characteristic to AMD has not been described to date. There exist, however, several lines of evidence for the involvement of PON1 in AMD. Decreased serum paraoxonase activity levels were found in patients with neovascular and nonexudative AMD (Ates et al., 2009). Also cigarette smoking, one of the strongest environmental risk factors to develop AMD, reduces serum PON1 activities (Isik et al., 2007; Solak et al., 2005). Furthermore, association between the two missense *PON1* gene polymorphisms (p.L55M and p.Q192R) and AMD was found in Japanese and Caucasian populations (Ikeda et al., 2001). Though, in different patient cohorts of European origin no association has been detected (Baird et al., 2004; Brion et al., 2011; Esfandiary et al., 2005).

II. SPECIFIC AIMS

The overall goal of the thesis was to understand the role of PON1 in complex human diseases (age-related macular degeneration and coronary artery disease), as well as in development, maintenance and function of the mouse retina.
The thesis had three specific aims:

1. To determine whether SNPs in *PON1* contribute to AMD.

2. To determine whether SNPs and private mutations in *PON1* contribute to coronary artery disease.

3. To determine function of PON1 in the retina using *Pon1*$^{-/-}$ mice.

III. RESULTS and DISCUSSION

3.1 The role of upstream regulatory SNPs of *PON1* in AMD

3.1.1 Regulatory regions of the paraoxonase 1 (PON1) gene are associated with neovascular age-related macular degeneration (AMD)

Jadwiga Oczos[1,2,3], Christian Grimm[2,3,4], Daniel Barthelmes[5,6], Florian Sutter[5], Moreno Menghini[5], Barbara Kloeckener-Gruissem[1,7,*,‡] and Wolfgang Berger[1,3,4,*,‡]

[1] Institute of Medical Molecular Genetics, University of Zurich, Schwerzenbach, Switzerland
[2] Lab for Retinal Cell Biology, Department of Ophthalmology, University of Zurich, Zurich, Switzerland
[3] Zurich Center for Integrative Human Physiology (ZIHP), University of Zurich, Zurich, Switzerland
[4] Zurich Center of Neuroscience (ZNZ)
[5] Department of Ophthalmology, University Hospital Zurich, Zurich, Switzerland
[6] University of Sydney, Sydney, Australia, Save Sight Institute
[7] Department of Biology, ETH Zurich, Zurich, Switzerland

Published in Age. 2013 Oct;35(5):1651-62. Epub 2012 Sep 7.

Personal contribution

In silico RNA secondary structure predictions, genotyping, haplotype analysis, cloning, expression studies, statistical analysis

Regulatory regions of the paraoxonase 1 (*PON1*) gene are associated with neovascular age-related macular degeneration (AMD)

Jadwiga Oczos · Christian Grimm · Daniel Barthelmes · Florian Sutter · Moreno Menghini · Barbara Kloeckener-Gruissem · Wolfgang Berger

Received: 23 March 2012 / Accepted: 20 August 2012

Abstract Physiological stress response and oxidative damage are factors for aging processes and, as such, are thought to contribute to neovascular age-related macular degeneration (AMD). Paraoxonase 1 (PON1) is an enzyme that plays an important role in oxidative stress and aging. We investigated association of DNA sequence variants (SNP) within the upstream regulatory region of the *PON1* gene with neovascular AMD in 305 patients and 288 controls. Four of the seven tested SNPs (rs705379, rs705381, rs854573, and rs757158) were more frequently found in AMD patients compared to controls (P=0.0099, 0.0295, 0.0121, and 0.0256, respectively), and all but one (SNP rs757158) are in linkage disequilibrium. Furthermore, haplotype TGGCCTC conferred protection (odds ratio (OR)=0.76, (CI)=0.60–0.97) as it was more frequently found in control individ-

Barbara Kloeckener-Gruissem and Wolfgang Berger contributed equally to this work.

Electronic supplementary material The online version of this article (doi:10.1007/s11357-012-9467-x) contains supplementary material, which is available to authorized users.

J. Oczos · B. Kloeckener-Gruissem (✉) · W. Berger (✉)
Institute of Medical Molecular Genetics,
University of Zurich,
Schwerzenbach, Switzerland
e-mail: kloeckener@medgen.uzh.ch
e-mail: berger@medgen.uzh.ch

J. Oczos · C. Grimm
Lab for Retinal Cell Biology,
Department of Ophthalmology, University of Zurich,
Zurich, Switzerland

J. Oczos · C. Grimm · W. Berger
Zurich Center for Integrative Human Physiology (ZIHP),
University of Zurich,
Zurich, Switzerland

C. Grimm · W. Berger
Zurich Center of Neuroscience (ZNZ),
Zurich, Switzerland

D. Barthelmes · F. Sutter · M. Menghini
Department of Ophthalmology, University Hospital Zurich,
Zurich, Switzerland

D. Barthelmes
Save Sight Institute, University of Sydney,
Sydney, Australia

B. Kloeckener-Gruissem
Department of Biology, ETH Zurich,
Zurich, Switzerland

AGE
DOI 10.1007/s11357-012-9467-x
Published online: 07 September 2012

uals, while haplotype CGATGCT increased the risk (OR=1.55, CI=1.09–2.21) for AMD. These results were also reflected when haplotypes for the untranscribed and the 5′untranslated regions (5′UTR) were analyzed separately. To assess haplotype correlation with levels of gene expression, the three SNPs within the 5′UTR were tested in a luciferase reporter assay. In retinal pigment epithelium-derived ARPE19 cells, we were able to measure significant differences in reporter levels, while this was not observed in kidney-derived HEK293 cells. The presence of the risk allele A (SNP rs705381) caused an increase in luciferase activity of approximately twofold. Our data support the view that inflammatory reactions mediated through anti-oxidative activity may be relevant to neovascular age-related macular degeneration.

Keywords Paraoxonase 1 · Gene regulation · SNP association · Age-related macular degeneration (AMD)

Introduction

Age-related macular degeneration (AMD) is a progressive degenerative disease, which in its advanced stages leads to severe visual impairment. It is the major cause of loss of vision in elderly patients in developed countries (Deangelis et al. 2011). Advanced stages of AMD manifest either as atrophic changes in the macula (dry/atrophic/nonexudative AMD) or as choroidal neovascularization (wet/neovascular/exudative AMD). Although the neovascular AMD represents only 10–20 % of all AMD cases, it accounts for the vast majority of cases with severe and rapid vision loss (~90 %) (Jager et al. 2008).

The etiologic complexity of AMD arises from an interplay of genetic and environmental factors. Recent progress in AMD genetics has established several important risk loci, among them the complement factor H (*CFH*) on chromosome 1 (1q31) (Edwards et al. 2005; Hageman et al. 2005, 2006; Hughes et al. 2006; Klein et al. 2005; Li et al. 2006) and the age-related maculopathy susceptibility 2 (*ARMS2*/*HTRA1*) on chromosome 10 (10q26) (Dewan et al. 2006; Jakobsdottir et al. 2005; Rivera et al. 2005; Schmidt et al. 2006; Tanimoto et al. 2007; Weger et al. 2007; Yang et al. 2006). Both loci combined are thought to account for more than 50 % of AMD cases (Edwards et al. 2005; Klein et al. 2005; Maller et al. 2006; Swaroop et al. 2007; Thakkinstian et al. 2006). Their association with AMD has been replicated across multiple ethnic groups worldwide and further validated through a meta-analysis of whole genome scans (Fisher et al. 2005). The discovery of *CFH* as a genetic risk factor for AMD was supported by functional studies revealing a role of the alternative complement pathway in drusen formation (Hageman et al. 2005). Following the discovery of genetic susceptibility loci, an impressive number of further genes has been reported that either increase or lower the risk towards AMD development (Katta et al. 2009). Despite the strong associations established, it is still not possible to predict the onset or course of AMD (Swaroop et al. 2007). Hence, it is necessary to identify other genes involved in the pathogenesis and understand their interactions.

To date, several additional candidate genes have been studied for their association with AMD, including lipid metabolism and oxidative stress genes (*APOE* (Baird et al. 2004b; Pang et al. 2000), *VLDLR* (Conley et al. 2005; Haines et al. 2006), *LRP5* (Kloeckener-Gruissem et al. 2011), *LRP6* (Haines et al. 2006), *PON1* (Baird et al. 2004a; Brion et al. 2011; Esfandiary et al. 2005; Ikeda et al. 2001; Pauer et al. 2010), *LIPC* (Neale et al. 2010), and *SOD2* (Gotoh et al. 2008; Kimura et al. 2000). Discordant results across multiple studies indicate the existence of additional factors that influence the development of AMD in different populations.

Oxidative stress is implicated in the development of AMD (AREDS 2001; Beatty et al. 2000; Khandhadia and Lotery 2010); thus, identification of enzymes conferring antioxidant protection is of interest. During the last decade, paraoxonase 1 (PON1), an enzyme with antioxidant properties, has been extensively investigated in several disorders, including age-related pathologies such as hyperlipidemia, atherosclerosis, coronary artery disease, metabolic syndrome, type 2 diabetes, as well as Alzheimer's disease (Androutsopoulos et al. 2011; Mackness et al. 1998b, c; Paragh et al. 1998; Senti et al. 2003). PON1 is a protein mainly synthesized in the liver, and most studies have focused their analysis on this fact. The enzyme is secreted into the blood where it binds high-density lipoprotein (HDL) (Aviram 2004). One of the functions of PON1 is to protect low-density lipoprotein (LDL) from oxidative damage and to inactivate oxidized LDL by hydrolyzing its oxidized phospholipids (Deakin and James 2004).

PON1 serum concentration and activity are highly variable across the general population (Deakin and James 2004). This variability is attributed to environmental factors, such as smoking, diet, alcohol consumption,

but also to the genetic polymorphisms in the *PON1* gene. There are two annotated missense SNPs within the *PON1* coding region: p.L55M (rs854560), where the major allele L leads to elevated PON1 protein levels, and p.Q192R (rs662), affecting substrate specificity as well as enzyme activity (Garin et al. 1997; Humbert et al. 1993). These two missense polymorphisms affect also the ability of HDL to protect LDL from oxidative modifications, with MM/QQ genotype being most effective (Mackness et al. 1998a). The level of PON1 concentration in serum is also affected by sequence variants within the promoter of the *PON1* gene. In particular, the C allele at position −107 (SNP rs705379) yields the highest level of PON1 in the serum among all alleles that have been investigated so far (Leviev and James 2000).

The antioxidant properties of PON1 stimulated research for association of DNA sequence variants within the *PON1* coding region and AMD (Baird et al. 2004a; Brion et al. 2011; Esfandiary et al. 2005; Ikeda et al. 2001; Pauer et al. 2010). Much focus has been on studying the effects of the two above-mentioned polymorphisms, p.L55M and p.Q192R. In a Japanese AMD patient cohort, the 55L and the 192R variants were found more frequently (Ikeda et al. 2001), while in one Caucasian cohort, the 55Q variant was associated with the disease (Pauer et al. 2010). This association could not be confirmed in further three Caucasian patient groups suggesting the influence of other factors as well (Baird et al. 2004a; Brion et al. 2011; Esfandiary et al. 2005). No information has been published on associations of sequence variants within upstream regulatory regions of the gene and diseases. It was our goal to expand the knowledge of effects of *PON1* gene sequences beyond protein isoforms and to investigate the influence of the upstream regulatory regions on AMD. We report here the identification of protective and risk haplotypes with effects on gene expression, which displays cell-type specificity.

Materials and methods

Patients

Patients with neovascular AMD were diagnosed at the Department of Ophthalmology at the University Hospital Zurich. Inclusion criteria regarding age, visual acuity, and lesion type (minimally classic, predominantly classic, and occult) were based on the MARINA (Rosenfeld et al. 2006) and ANCHOR (Brown et al. 2006) trials. The patients were given a full explanation of the nature and purpose of the study. The study was conducted according to the Declaration of Helsinki and was approved by the local ethics committee. Clinical and demographic description as well as the analysis of several common AMD risk factors of this patient cohort has been published previously (Kloeckener-Gruissem et al. 2011). Data from 305 neovascular AMD patients are reported in the current study. The average age of the patients was 79.41 years (±6.97); female to male ratio, 1.95. All were of European descent, living in Switzerland. DNA of 288 individuals representing the general population was used as the control group (Moskvina et al. 2005). These individuals were not age-matched and did not undergo clinical assessment for the present study. They were of European descent, living in Switzerland. The female/male ratio was 2.1.

Genotyping

Venous blood was collected in EDTA tubes, and genomic DNA was extracted as described (Kloeckener-Gruissem et al. 2011). DNA concentration was adjusted to 10 ng/μl. SNP genotyping was performed either by DNA sequencing (primer 1 CCTCCCCGACTGGACTAGG and primer 2 AGGGAGTGAGGAGGACGAAG were used for genotyping SNPs rs705379, rs705380, and rs705381; primer 3 CCAAAAGCCTTGAGAAGGAA and primer 4 TGCTCTAGGTGATGCATGTG were used for genotyping SNPs rs854571 and rs854572) or by TaqMan technology (SNPs rs854571, rs854573, and rs757158), using ABI chemistry (Applied Biosystems, Inc. [ABI], Rotkreuz, Switzerland). Sequencing primers were designed by Primer3 (v. 0.4.0; http://frodo.wi.mit.edu/primer3, provided in the public domain by Massachusetts Institute of Technology, Cambridge, MA) and synthesized by Microsynth (http://www.microsynth.ch; Balgach, Switzerland). Annealing temperatures varied between 54 and 60 °C. For PCR, 50-ng genomic DNA and primers were cycled 35 times, each cycle lasting 1 min. For TaqMan assay, probes from ABI were used. Genotype calling was performed on SDS2.2 software, ABI. The allele calling of SNP assay was verified by DNA sequencing analysis for 10 % of all samples, yielding 100 % concordance. In addition, genotyping of 10 % of all samples was repeated for each SNP.

Selection of SNPs and haplotype analysis

Seven SNPs, namely rs705379, rs705380, rs705381, rs854571, rs854572, rs854573, and rs757158 (Fig. 1 and Table 1), within *PON1* gene (NG_008779.1) were chosen for association studies based on the linkage disequilibrium (LD) data in the HapMap Caucasion (CEU) population panel, using a tagging criteria of $R2>0.8$. Since there is no LD information available for SNPs in the 5′UTR (rs705379, rs705380, and rs705381), we included them in the analysis.

Individual haplotypes and their estimated population frequencies were inferred using PHASE program, v2.1.1 (http://stephenslab.uchicago.edu/software.html), with all parameters set at the default values (Stephens and Donnelly 2003; Stephens et al. 2001).

In silico analysis of 5′UTR variants on RNA folding

Putative RNA folding structures were predicted using the Mfold online software with standard settings (http://mfold.rna.albany.edu/?q=mfold/RNA-Folding-Form) (Zuker 2003). RNA structures were predicted for the *PON1* transcript (transcript: PON1-001 *ENST00000222381*) containing eight possible combinations of alleles at the SNPs within 5′UTR.

Cloning

A 400-bp fragment of *PON1* exon 1 containing the 5′ UTR was PCR-amplified (primer 1 and primer 2) and cloned into the intermediate pJET1.2/blunt cloning vector using the CloneJET PCR Cloning Kit (Fermentas International Inc, Glen Burnie, MD, USA). Fragments containing four of the eight possible haplotypes were obtained directly through PCR from patients' genomic DNA (CCA, CGA, CGG, and TGG; SNPs' order from left to right, rs705379, rs705380, and rs705381). DNA fragments containing the other four haplotypes were obtained by site-directed mutagenesis with the primer extension approach. For all substitutions, primer 1 and primer 2 served as outside flanking primers. Each mutation was obtained using additional pairs of inside primers (sequences are written from 5′to 3′) as primer 5 CCGACCCGGCGGGGAGGGGTGGGGCGG GCC with primer 6 GCAGCGCCGATTGGCCC GCCCCACCCCTCCC, primer 7 GGGGCTGA CCGCAAGCCGCGCCTTCTGTGC with primer 8 GACCAGGTGCACAGAAGGCGCGGCT TGCGG, primer 9 GGGGCTGACCGCAAGC CACGCCTTCTGTGC with primer 10 GACCAGGTG CACAGAAGGCGTGGCTTGCGGTC, and primer 11 TGGTCGGCCCAGCTAGCTGCCGACCCGGCGGG with primer 12 CCACCCCTCCCCGCCGGGTCGG CAGCTAGC. Subsequently, the *PON1* fragments representing each of the haplotype were cloned into pGL3-Control vector (Promega, Madison, WI, USA). In the first step, PCR reaction was performed to create a *Hind*III restriction site upstream of the three 5′UTR SNPs using primer 2 and primer 13 TATAAGCTTGTTGGAAG GAGCAAAATG. In the second step, 238-bp fragments spanning from the constructed *Hind*III site to the translational start codon ATG (*Nco*I site) were cloned into the pGL3-Control vector using *Hind*III and *Nco*I restriction enzymes (Fermentas). DNA sequences of all constructs were verified by Sanger sequencing.

Expression studies

HEK293 cells were seeded on 24-well plates (10^5 cells/well) in 1 ml DMEM, 10 % FBS, and 1 % penicillin/streptomycin and incubated under standard conditions (37 °C, 5 % CO_2). After 24 h, cells were transfected using 1.5-μl branched polyethylenimine, PEI (1 μg/μl), 600-ng pFirefly construct, and 15-ng pRenilla construct per well. Twenty-four hours later, the cells were harvested, and luciferase activities were analyzed using Dual-Glo Luciferase Assay System according to the protocol provided by Promega and measured on a Bio-Tek Synergy microplate reader (BioTek Instruments,

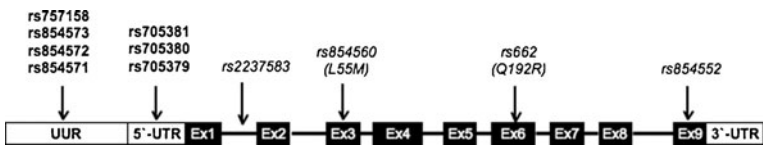

Fig. 1 Schematic representation of the *PON1* gene. Positions of SNPs that were analyzed in this study are printed in *bold*. They map to the upstream untranscribed region (*UUR*) and the 5′untranslated region (5′UTR). SNPs in exon 3 (*Ex3*), exon 6 (*Ex6*), and exon 9 (*Ex9*), investigated by other groups, are printed in *italics* (Baird et al. 2004a; Brion et al. 2011; Esfandiary et al. 2005; Ikeda et al. 2001; Pauer et al. 2010)

Table 1 Allele frequencies of SNPs in the upstream regulatory region of *PON1*

Marker	Major/minor allele	Position	Region	MAF			*P* value	OR	CI (95 %)
				HapMap	AMD (n=305)	Controls (n=288)			
rs705379	T/C	−107	5′UTR	0.425	0.517	0.440	0.0099	1.36	1.08–1.73
rs705380	G/C	−126	5′UTR	0.042	0.056	0.044	0.3566	1.29	0.75–2.21
rs705381	G/A	−162	5′UTR	0.167	0.253	0.199	0.0295	1.37	1.03–1.81
rs854571	C/T	−831	UUR	0.302	0.284	0.257	0.3009	1.14	0.89–1.49
rs854572	C/G	−908	UUR	0.425	0.471	0.419	0.0759	1.23	0.98–1.56
rs854573	T/C	−1075	UUR	0.230	0.255	0.194	0.0121	1.42	1.08–1.88
rs757158	C/T	−1740	UUR	0.376	0.444	0.380	0.0256	1.30	1.03–1.64

Comparison between patients with neovascular AMD (n=305) and control individuals (n=288). Three SNPs map to the 5′untranslated region while four of the SNPs lie within the upstream untranscribed region (Fig. 1). Minor allele frequencies for a Caucasian population were taken from the HapMap website (http://www.hapmap.org) and were calculated for our patient (AMD) and control groups. Statistical analyses are displayed as odds ratios (OR) with confidence intervals (CI) and *P* values, with α=0.05

5′UTR 5′untranslated region, *UUR* upstream untranscribed region, MAF minor allele frequencies

Winooski, VT, USA). Data were normalized for transfection efficiency by Renilla luciferase activity. The experiment was performed three times with three replicates each. ARPE19 cells (ATCC, Manassas, VA, USA) were seeded on 24-well plates (8×10^4cells/well) in 1 ml DMEM, 10 % FBS, 1 % penicillin/streptomycin, and 7.5 % Na_2CO_3 and cultured under standard conditions (37 °C, 5 % CO_2). Twenty-four hours later, transfection was performed; for each well, 0.75-µl X-tremeGENE 9 transfection reagent (Roche Diagnostics, Indianapolis, IN, USA), 250-ng pFirefly construct, and 6.25-ng pRenilla construct were used. Luciferase activities were measured and analyzed 24 h after transfection as described above. The experiment was repeated four times. Three of these repeats included three technical replicates while one of them included eight.

Statistical analysis

Pairwise LD analysis was performed on phased haplotype data generated from the control group according to the following formulas: $R2=D^2/(p_{A1}p_{A2}p_{B1}p_{B2})$, where $D=p_{A1B1}p_{A2B2}-p_{A1B2}p_{A2B1}$; $D'=D/D_{max}$, with $D_{max}=\min(p_{A1}p_{B2}, p_{A2}p_{B1})$ if $D>0$ and $D_{max}=\min(-p_{A1}p_{B1}, -p_{A2}p_{B2})$ if $D<0$ (Mueller 2004). For association studies, odds ratios and significance were calculated using 2×2 contingency table provided on an open access Internet portal (http://faculty.vassar.edu/lowry/odds2x2.html). Odds ratios were displayed with 95 % confidence intervals and Chi-square and *P* values according to Pearson. Statistical significance was assumed at $P<0.05$. For expression studies, eight technical replicas were measured and averages with confidence intervals at 95 % were computed. Fold-change differences were determined after normalizing the data to those obtained for the TCG haplotype. This haplotype was chosen because it yielded the lowest luciferase activity in the ARPE19 cell line. The Shapiro–Wilk test was applied to assess normal distribution of the data. For statistical analysis, the two-tailed *t* test was used.

Results

Linkage disequilibrium revealed two DNA blocks within the upstream regulatory region of *PON1*

Linkage disequilibrium data are crucial for the design of association studies. If two SNPs share high linkage disequilibrium, with $R2>0.8$ one of them can be used as tagged SNP. The region of *PON1* investigated in our study contains seven annotated SNPs (Fig. 1 and Table 1). LD data on the HapMap website are available only for four of them (rs854571, rs854572, rs854573, and rs757158). To complete this information, we performed LD analysis on phased genotype data of the control individuals (Table 2). Our analysis confirms already annotated data in a larger group of individuals (haplotype number n=500 in our study, n=224 in HapMap) and also provides pairwise *R*2 and *D*′ values for SNPs which are not included in HapMap. Among the seven analyzed SNPs, six belong to one haplotype block

as they revealed high pairwise *D′* values (rs705379, rs705380, rs705381, rs854571, rs854572, and rs854573). SNP rs757158 belongs to a separate haplotype block (Fig. 2). Among the analyzed SNPs, only two pairs (rs705381 with rs854573, and rs854572 with rs757158) fulfill tagging criteria of $R2>0.8$ (Table S1).

Association studies showed risk and protection potential for AMD

Genotypes of seven SNPs within regulatory, non-coding regions of the *PON1* locus were determined from 305 patients with neovascular AMD and compared to those from 288 control individuals (Table 1). The patients' AMD phenotype has been reported in detail previously (Kloeckener-Gruissem et al. 2011). Three SNPs within the 5′UTR and four SNPs within the upstream untranscribed region (UUR) (Fig. 1) were genotyped and analyzed. Note that as the transcriptional promoter region has not been defined experimentally, we chose to name this region "UUR", rather than "promoter region". Statistically significant association was found at two SNP loci within the 5′UTR and two within the UUR: rs705379 (OR=1.36, CI=1.08–1.73, P=0.0099), rs705381 (OR=1.37, CI=1.03–1.81, P=0.0295), rs854573 (OR=1.42, CI=1.08–1.88, P=0.0121), and rs757158 (OR=1.30, CI=1.03–1.64, P=0.0256) (Table 1).

To strengthen the significance of the association, we included analyses of haplotypes. For the seven SNP haplotypes (rs705379 at −107, rs705380 at −126 and rs705381 at −162, rs854571 at −831, rs854572 at −908, rs854573 at −1075, and rs757158 at −1740), PHASE predicted 18 different combinations. Haplotypes with fewer than five counts in PHASE (11 haplotypes) were not taken into account for statistical analyses. The haplotype TGGCCTC, comprising exclusively major alleles, was more frequently found in the control group, suggesting a protective function (OR=0.76, CI=0.60–0.97, P=0.0293), whereas the haplotype CGATGCT was more frequent in AMD patients (OR=1.55, CI=1.09–2.21, P=0.0141), posing a risk for the disease (Table 2). Similar results were found when SNPs from the 5′UTR and the upstream untranscribed region (UUR) were analyzed separately. The PHASE program revealed the presence of four possible haplotypes for SNPs in the 5′UTR (TGG, CGG, CGA, CCA; order of SNPs from left to right, rs705379 at −107, rs705380 at −126, and rs705381 at −162). Carriers of the haplotype TGG, representing the major alleles within a population, were more frequently found in the control group compared to the patient group, and, hence, this haplotype confers a protection against AMD (OR=0.72, CI=0.57–0.91, P=0.0063), while conversely the haplotype CGA indicates a risk for AMD (OR=1.35, CI=0.99–1.85, P=0.0564) (Table 3). For the four SNPs in the UUR, PHASE predicted seven different haplotypes. Three haplotypes showed statistically significant differences between patient and control group

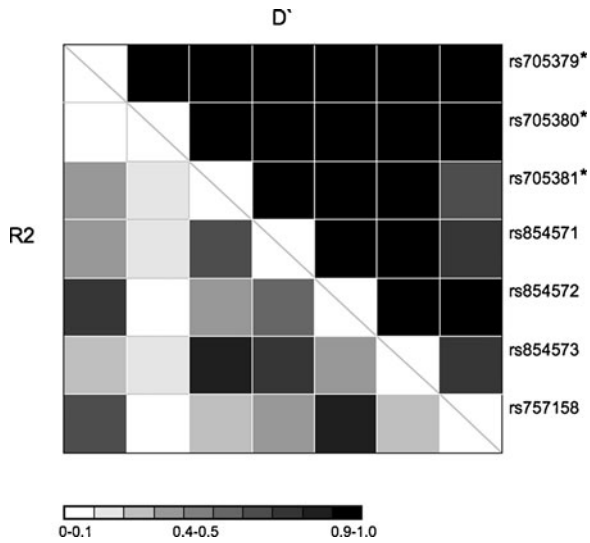

Fig. 2 Pairwise linkage analysis of SNPs within the *PON1* 5′ UTR and upstream untranscribed region. *R2* and *D′* values are depicted by the *grayscale color code* according to the legend. *Asterisks* indicate SNPs for which no data are available on the HapMap website

Table 2 Haplotype analysis for all seven SNPs

Haplotype	AMD (n=556) n (%)	Controls (n=500) n (%)	P value	OR	CI (95 %)
TGGCCTC	264 (47.5)	271 (54.2)	0.0293	0.76	0.60–0.97
CGGCGTT	100 (18.0)	74 (14.8)	0.1637	1.26	0.91–1.75
CGATGCT	94 (16.9)	58 (11.6)	0.0141	1.55	1.09–2.21
CCATGCT	25 (4.5)	22 (4.4)	0.9203	1.02	0.57–1.84
CGGCCTC	26 (4.7)	18 (3.6)	0.3833	1.31	0.71–2.43
CGGTGTT	17 (3.1)	25 (5.0)	0.1069	0.60	0.32–1.12
CGATGCC	12 (2.2)	14 (2.8)	0.5023	0.77	0.35–1.67

SNP order for each haplotype, from left to right is as follows: -107, -126, -162, -831, -908, -1075, and −1740. Haplotype counts (n) and percentages (%) are given. Haplotypes with less than five counts in PHASE were not taken into account for statistical analysis. Odds ratios (OR) with confidence intervals (CI) and P values (alpha=0.05) are shown

frequencies (Table 3). The haplotype TGCT (rs854571 at −831, rs854572 at −908, rs854573 at −1075, and rs757158 at −1740) was associated with the disease (OR=1.44, CI=1.07–1.95, P=0.0165), whereas the two haplotypes CCTC and TGTT were more frequently found in the control group (OR=0.79, CI=0.63–0.99, P=0.0492 and OR=0.48, CI=0.27–0.84, P=0.0092, respectively) (Table 3).

Sequence variants in the 5′UTR alter predicted structure of the *PON1* mRNA

It is known that SNPs within the 5′UTR of genes can affect its mRNA folding and consequently change translational efficiency (Zuercher et al. 2010). We simulated the influence of the 5′UTR polymorphisms on secondary RNA structures using the web server Mfold. RNA structures of the entire *PON1* mRNA (5′UTR, coding sequences, and 3′UTR) were predicted (Fig. 3). The predicted structure of the reference sequence carrying the minor alleles at three analyzed positions (−107C, -126C, and -162A) was not different from that containing only one major T allele at position −107 (Fig. 3a). In contrast, predicted folding of RNA containing the major alleles at position −126 and −162, singly, or in combination, assumed a strikingly different structure (Fig. 3b). Based on these bioinformatic predictions, we hypothesized that SNPs within the 5′UTR of *PON1* may have different effects on protein synthesis.

AMD risk haplotype altered reporter gene activity in cell culture

To correlate our association data and the structural predictions with potential effects on gene expression, we designed experiments to test whether different *PON1* 5′ UTR haplotypes influence luciferase reporter gene expression in cell culture. We generated the eight possible haplotypes in DNA constructs, containing the *PON1* 5′ UTR region fused to the *Luciferase* coding region, both transcribed from the SV40 promoter. Since tissue-specific effects on gene expression are likely to occur, we included two different cell lines in this test: the embryonic kidney-derived cell line HEK293 and the retinal pigment epithelium-derived cell line ARPE19. Both cell lines were transiently transfected with the various *PON1* 5′UTR haplotypes in front of the luciferase reporter. In ARPE19 cells, we found statistically significant differences in luciferase levels (Fig. 4). To assess contribution of each individual SNP to increased protein expression, we performed a pairwise comparison of luciferase levels between haplotypes differing at only one position (Table 4). This analysis revealed that SNP rs705381 at position −162 is mostly responsible for

Table 3 Haplotype analysis of the upstream untranscribed and untranslated region

Region	Haplotype	AMD *n* (%)	Controls *n* (%)	*P* value	OR	CI (95 %)
5′UTR[a]						
	TGG	280 (48.4)	297 (56.7)	0.0063	0.72	0.57–0.91
	CGG	150 (26.0)	121 (23.1)	0.2713	1.17	0.89–1.54
	CGA	116 (20.1)	82 (15.6)	0.0564	1.35	0.99–1.85
	CCA	32 (5.5)	24 (4.6)	0.4708	1.22	0.71–2.10
UUR[b]						
	CCTC	308 (52.4)	320 (58.2)	0.0492	0.79	0.63–0.99
	TGCT	128 (21.8)	89 (16.2)	0.0165	1.44	1.07–1.95
	CGTT	109 (18.5)	87 (15.8)	0.2253	1.21	0.89–1.65
	TGTT	19 (3.2)	36 (6.5)	0.0092	0.48	0.27–0.84
	TGCC	19 (3.2)	17 (3.1)	0.8875	1.05	0.54–2.04

Four haplotypes in the 5′untranslated region (5′UTR) and five haplotypes in the upstream untranscribed region (UUR) were analyzed in our patient and control population. The order of SNPs, from left to right is −107, -126, and −162 (5′UTR) and −831, -908, -1075, and −1740 (UUR). Haplotype counts (*n*) and percentages (%) are given. Odds ratios (OR) with confidence intervals (CI) and *P* values (alpha=0.05) are shown. Haplotypes with fewer than five counts in PHASE were not taken into account for statistical analysis

[a] AMD, n=578; controls, n=524

[b] AMD, n=588; controls, n=550

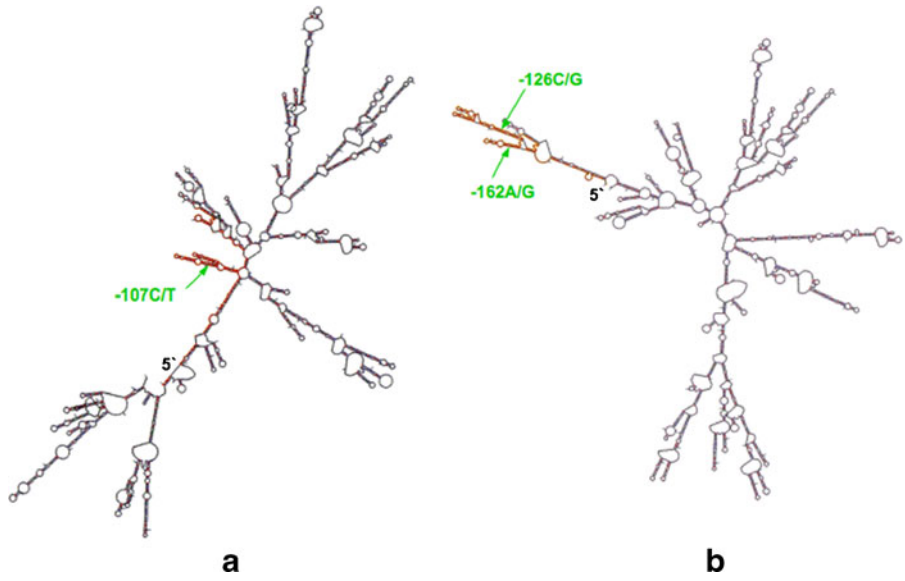

Fig. 3 Predicted *PON1* mRNA foldings. **a** The structure represents folding of the *PON1* mRNA containing the minor alleles CCA in the 5′untranslated region. It was indistinguishable from the allele combination TCA. **b** The structure depicts mRNA folding in the presence of the other six allelic combinations: CGA, TGA, CCG, TCG, CGG, and TGG (SNP order from left to right, -107,-126, and −162)

the observed difference in luciferase activity. The presence of the minor allele A leads to increase in the reporter activity up to 2.1-fold. Small contribution to the protein expression regulation has been found for two other SNPs (rs705379 at −107, and rs705380 at −126), with minor allele C at position −107 and minor allele C at position −126, causing up to 1.6- and 1.4-fold increase in luciferase level, respectively. Interestingly, in HEK293 cells, we did not find statistically significant differences in luciferase activity between the different constructs (data not shown), supporting our initial assumption of cell-specific effects on gene expression.

Discussion

This is the first report to show association of SNPs in the upstream regulatory region of *PON1* with neovascular AMD. Previous studies have investigated association between SNPs within the *PON1* coding region and AMD (Brion et al. 2011; Baird et al. 2004a; Esfandiary et al. 2005; Pauer et al. 2010; Ikeda et al. 2001). The focus was on two missense polymorphisms p.L55M and p.Q192R. Conflicting results were obtained when comparing different patient cohorts; while association with wet AMD has been found for both variants in a Japanese population (Ikeda et al. 2001), only the p.Q192R variant was associated in only one of the four Caucasian cohorts (Pauer et al. 2010). Furthermore, in the Japanese study, the arginine at position 192 of the PON1 protein has been found more frequently in the patient group, whereas in Caucasians, the glutamine (192Q) variant has been associated with the disease. Possible explanations encounter different allele frequencies in the different ethnic groups but also a diverse phenotype of AMD (Bird 2003; Oshima et al. 2001). Specifically for SNP p.Q192R in Caucasians, the minor variant is R with a frequency of 0.332, whereas in Japanese, the arginine is the major variant with an allele frequency of 0.706 (HapMap). As there is no linkage disequilibrium between p.Q192R variant and the promoter polymorphisms (Leviev and James 2000) (HapMap), a direct comparison between our data and those reported from other Caucasian patient cohorts, which examined p.Q192R (Baird et al. 2004a; Brion et al. 2011; Esfandiary et al. 2005; Pauer et al. 2010) is not meaningful.

In contrast to p.Q192R, the variant 55L is in linkage disequilibrium with the allele -107C (Leviev and James 2000), which is associated with AMD in our study. It has been shown that these two alleles lead to increased levels of PON1 in serum (Leviev and James 2000). Thus, it may be difficult to understand how higher levels of a protein that is known to have antioxidant properties can be associated with AMD. For a possible explanation, we would like to emphasize that variant p.L55M has been reported to affect PON1 activity towards lipid peroxides, with the LL genotype being less effective than MM at protecting LDL against oxidation (Mackness et al. 1998a). Since alleles at position -107C and -162A are in linkage disequilibrium with variant 55L, they are likely to be also associated with the less effective protection against oxidation, thus can confer the risk for AMD and

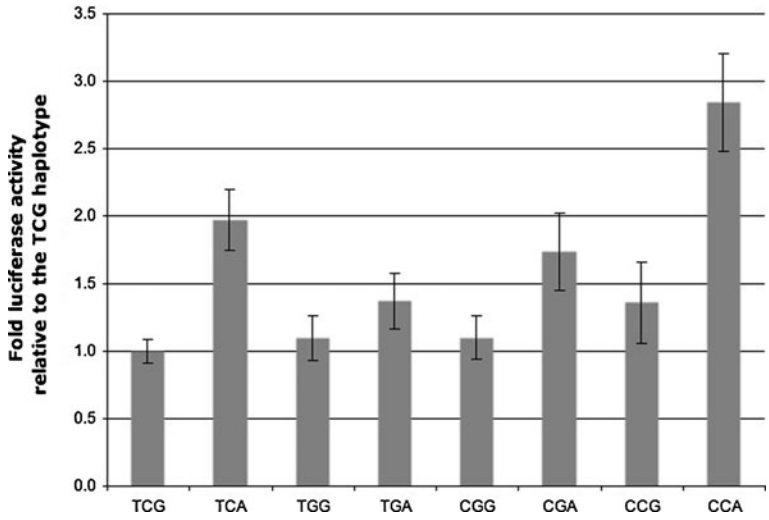

Fig. 4 Fold increase of luciferase activity for the eight *PON1* 5′UTR haplotypes in ARPE19 cells. The luciferase activity of the reporter construct containing the TCG haplotype was set to 1. SNP order in haplotypes from left to right: -107, -126, and −162. Error bars show confidence intervals, CI=95 %. Displayed are results from a representative experiment with eight technical replicates

be responsible for increased oxLDL levels (Ikeda et al. 2001) in AMD patients.

To strengthen the significance of the association found with individual SNPs, we performed haplotype association analysis. We discovered two seven-SNP haplotypes associated with AMD. The most abundant haplotype (54.2 % in controls), TGGCCTC, was more frequently found in controls conferring a protection against AMD, whereas haplotype CGATGCT was a risk factor. Interestingly, the two haplotypes CGATGCC and CCATGCT, each differing at only one position in comparison to CGATGCT, appeared not to be associated with the disease. These data imply a possible interplay between the analyzed loci and underlines the importance of haplotype analysis to assess risk factors. Similar results were obtained when analyzing haplotypes within the 5′UTR and UUR separately.

Table 4 Effects of 5′UTR haplotypes on luciferase reporter activity

SNP	Haplotype[a]		Fold increase in luciferase activity[b]	*P* value[c]
	1	2		
−107	CCA	TCA	1.4	<0.001
	CCG	TCG	1.4	0.016
	CGA	TGA	1.3	0.030
	CGG	TGG	1.0	0.984
−126	CCA	CGA	1.6	<0.001
	CCG	CGG	1.2	0.094
	TCA	TGA	1.4	<0.001
	TCG	TGG	0.9	0.242
−162	CCA	CCG	2.1	<0.001
	CGA	CGG	1.6	<0.001
	TCA	TCG	2.0	<0.001
	TGA	TGG	1.2	0.030

The comparison is based on haplotypes that differ at a single position. Displayed are results for a representative experiment shown in Fig. 4

[a] SNP order in haplotype, from left to right is −107, -126, and −162

[b] Fold increase in luciferase activity, haplotype 1 versus haplotype 2

[c] Two-tailed *t* test

It is known that sequence variants within the 5′UTR can regulate gene expression at the level of protein translation. We asked whether this would also apply to the *PON1* gene. To support our notion, we performed in silico RNA folding predictions for the different allelic combinations and found that the presence of the major alleles for two SNPs in the 5′UTR would lead to a striking difference in the folding properties of the entire *PON1* transcript. Furthermore, these alleles also appear to have an effect on reporter gene expression as measured by luciferase enzyme activity. Specifically, in the retinal pigment epithelium-derived cell line ARPE19, the protective TGG haplotype yielded the lowest level of luciferase activity, while the CCA haplotype resulted in the highest reported expression levels. When comparing those haplotypes differing at only one position, we discovered that the SNP at position −162 provided the largest contribution, with the A nucleotide causing up to 2.1-fold increase in luciferase reporter activity. Previous reports have shown that this allele

caused up-regulation of transcription in cultured kidney and liver cell lines (Brophy et al. 2001). These data, together with our findings, indicate that the position at −162 has regulatory function at both steps of gene expression, transcription, as well as translation. Alternatively, a sole effect on transcription of the luciferase reporter cannot be excluded. In our study, the two other investigated SNPs at positions −107 and −126 caused only minor changes in luciferase activity. In the literature, no effect of the SNP at −126 has been reported, but the minor allele C at position −107 has been shown to increase transcription of a luciferase reporter gene in HepG2 and HEK293 cells (Brophy et al. 2001). Taking these data together, we conclude that the three SNPs support different activities for *PON1* gene expression.

It is important to note that the luciferase reporter assays did not yield the same results in the two different cell lines tested. As cell and tissue-specific regulation of gene expression is a well-known phenomenon, it is not surprising that gene expression control potential within the 5′UTR of *PON1* is manifested in ARPE19 cells, but not in HEK293 cells. The latter cells, derived from kidney, do not seem to be implicated in the AMD pathology, while ARPE19 cells, derived from retinal pigment epithelium, do (Kinnunen et al. 2012). In this context, it is plausible that the relevant SNP at position −162 exerts a cell type-specific effect in favor of AMD. Since *Pon1* is expressed in the retinal pigment epithelium in mice (data not shown), further studies will provide crucial information to clarify these assumptions.

A number of factors such as blood pressure, usage of antihypertensive medication, blood cholesterol, or blood levels of high-density lipoprotein were shown to be associated with the development of neovascular AMD (Hyman et al. 2000). As the mean age of the population studied here is 79.5 years, it can be expected that some of the factors (e.g., increased arterial blood pressure) are present in the study population—assumingly randomly distributed across the participants. An influence of the proposed cardiovascular risk factors on the outcome of the treatment of neovascular AMD using ranibizumab has not yet been shown. Hence, it remains speculative whether or not such risk factors may have had an impact in the current study population and the reported outcomes.

Many open questions remain on the involvement of PON1 in AMD pathology. As our patients were diagnosed with the end stage neovascular AMD, our results cannot account for a potential role of *PON1* as a trigger for the onset of AMD or as an accelerator during the progression of the disease, or maybe both. Our and other previous association studies imply the involvement of *PON1* at the late stage of the disease. An alternative mechanism may exist, where PON1 enzyme changes are secondary to other events, present at early stages of AMD. For example, paraoxonase activity in serum is decreased in AMD patients. As AMD is considered to be a chronic inflammatory disease and the *PON1* transcription levels in liver are known to be down-regulated in response to infections, it seems feasible that *PON1* down-regulation and decreased activity are the outcome of primarily inflammation events. Cross talk between PON1 levels and inflammatory response could be mediated by the oxLDL, which can induce expression of genes involved in an inflammation by stimulating various transcription factors (Maziere and Maziere 2009). Our results provide insights in the action of PON1, but further investigation is required for a deeper understanding of the contribution of PON1 in the pathology of AMD.

Acknowledgments We would like to thank Marijana Samardzija for help with Excel macros to ease data entry in PHASE. We appreciate the genomic DNA preparations by Esther Glaus. Financial support by a cooperative project grant by the Zurich Center for Integrative Human Physiology (ZIHP) of the University of Zurich, Zurich, Switzerland, is greatly acknowledged. DB was supported by a grant from the Swiss National Foundation (SNF/SSMBS), a grant from the Holcim Foundation, and the Walter and Gertrud Siegenthaler Foundation Zürich, Switzerland.

References

Androutsopoulos VP, Kanavouras K, Tsatsakis AM (2011) Role of paraoxonase 1 (PON1) in organophosphate metabolism: implications in neurodegenerative diseases. Toxicol Appl Pharmacol 256:418–424

AREDS (2001) A randomized, placebo-controlled, clinical trial of high-dose supplementation with vitamins C and E and beta carotene for age-related cataract and vision loss: AREDS report no. 9. Arch Ophthalmol 119:1439–1452

Aviram M (2004) Introduction to the serial review on paraoxonases, oxidative stress, and cardiovascular diseases. Free Radic Biol Med 37:1301–1303

Baird PN, Chu D, Guida E, Vu HT, Guymer R (2004a) Association of the M55L and Q192R paraoxonase gene polymorphisms with age-related macular degeneration. Am J Ophthalmol 138:665–666

Baird PN, Guida E, Chu DT, Vu HT, Guymer RH (2004b) The epsilon2 and epsilon4 alleles of the apolipoprotein gene are associated with age-related macular degeneration. Investig Ophthalmol Vis Sci 45:1311–1315

Beatty S, Koh H, Phil M, Henson D, Boulton M (2000) The role of oxidative stress in the pathogenesis of age-related macular degeneration. Surv Ophthalmol 45:115–134

Bird AC (2003) The Bowman lecture. Towards an understanding of age-related macular disease. Eye (Lond) 17:457–466

Brion M, Sanchez-Salorio M, Corton M, de la Fuente M, Pazos B et al (2011) Genetic association study of age-related macular degeneration in the Spanish population. Acta Ophthalmol 89:e12–e22

Brophy VH, Hastings MD, Clendenning JB, Richter RJ, Jarvik GP et al (2001) Polymorphisms in the human paraoxonase (PON1) promoter. Pharmacogenetics 11:77–84

Brown DM, Kaiser PK, Michels M, Soubrane G, Heier JS et al (2006) Ranibizumab versus verteporfin for neovascular age-related macular degeneration. N Engl J Med 355: 1432–1444

Conley YP, Thalamuthu A, Jakobsdottir J, Weeks DE, Mah T et al (2005) Candidate gene analysis suggests a role for fatty acid biosynthesis and regulation of the complement system in the etiology of age-related maculopathy. Hum Mol Genet 14:1991–2002

Deakin SP, James RW (2004) Genetic and environmental factors modulating serum concentrations and activities of the antioxidant enzyme paraoxonase-1. Clin Sci (Lond) 107:435–447

Deangelis MM, Silveira AC, Carr EA, Kim IK (2011) Genetics of age-related macular degeneration: current concepts, future directions. Semin Ophthalmol 26:77–93

Dewan A, Liu M, Hartman S, Zhang SS, Liu DT et al (2006) HTRA1 promoter polymorphism in wet age-related macular degeneration. Science 314:989–992

Edwards AO, Ritter R 3rd, Abel KJ, Manning A, Panhuysen C et al (2005) Complement factor H polymorphism and age-related macular degeneration. Science 308:421–424

Esfandiary H, Chakravarthy U, Patterson C, Young I, Hughes AE (2005) Association study of detoxification genes in age related macular degeneration. Br J Ophthalmol 89:470–474

Fisher SA, Abecasis GR, Yashar BM, Zareparsi S, Swaroop A et al (2005) Meta-analysis of genome scans of age-related macular degeneration. Hum Mol Genet 14:2257–2264

Garin MC, James RW, Dussoix P, Blanche H, Passa P et al (1997) Paraoxonase polymorphism Met-Leu54 is associated with modified serum concentrations of the enzyme. A possible link between the paraoxonase gene and increased risk of cardiovascular disease in diabetes. J Clin Invest 99:62–66

Gotoh N, Yamada R, Matsuda F, Yoshimura N, Iida T (2008) Manganese superoxide dismutase gene (SOD2) polymorphism and exudative age-related macular degeneration in the Japanese population. Am J Ophthalmol 146:146, author reply 146–147

Hageman GS, Anderson DH, Johnson LV, Hancox LS, Taiber AJ et al (2005) A common haplotype in the complement regulatory gene factor H (HF1/CFH) predisposes individuals to age-related macular degeneration. Proc Natl Acad Sci U S A 102:7227–7232

Hageman GS, Hancox LS, Taiber AJ, Gehrs KM, Anderson DH et al (2006) Extended haplotypes in the complement factor H (CFH) and CFH-related (CFHR) family of genes protect against age-related macular degeneration: characterization, ethnic distribution and evolutionary implications. Ann Med 38:592–604

Haines JL, Schnetz-Boutaud N, Schmidt S, Scott WK, Agarwal A et al (2006) Functional candidate genes in age-related macular degeneration: significant association with VEGF, VLDLR, and LRP6. Investig Ophthalmol Vis Sci 47:329–335

Hughes AE, Orr N, Esfandiary H, Diaz-Torres M, Goodship T et al (2006) A common CFH haplotype, with deletion of CFHR1 and CFHR3, is associated with lower risk of age-related macular degeneration. Nat Genet 38:1173–1177

Humbert R, Adler DA, Disteche CM, Hassett C, Omiecinski CJ et al (1993) The molecular basis of the human serum paraoxonase activity polymorphism. Nat Genet 3:73–76

Hyman L, Schachat AP, He Q, Leske MC (2000) Hypertension, cardiovascular disease, and age-related macular degeneration. Age-Related Macular Degeneration Risk Factors Study Group. Arch Ophthalmol 118:351–358

Ikeda T, Obayashi H, Hasegawa G, Nakamura N, Yoshikawa T et al (2001) Paraoxonase gene polymorphisms and plasma oxidized low-density lipoprotein level as possible risk factors for exudative age-related macular degeneration. Am J Ophthalmol 132:191–195

Jager RD, Mieler WF, Miller JW (2008) Age-related macular degeneration. N Engl J Med 358:2606–2617

Jakobsdottir J, Conley YP, Weeks DE, Mah TS, Ferrell RE et al (2005) Susceptibility genes for age-related maculopathy on chromosome 10q26. Am J Hum Genet 77:389–407

Katta S, Kaur I, Chakrabarti S (2009) The molecular genetic basis of age-related macular degeneration: an overview. J Genet 88:425–449

Khandhadia S, Lotery A (2010) Oxidation and age-related macular degeneration: insights from molecular biology. Expert Rev Mol Med 12:e34

Kimura K, Isashiki Y, Sonoda S, Kakiuchi-Matsumoto T, Ohba N (2000) Genetic association of manganese superoxide dismutase with exudative age-related macular degeneration. Am J Ophthalmol 130:769–773

Kinnunen K, Petrovski G, Moe MC, Berta A, Kaarniranta K (2012) Molecular mechanisms of retinal pigment epithelium damage and development of age-related macular degeneration. Acta Ophthalmol 90:299–309

Klein RJ, Zeiss C, Chew EY, Tsai JY, Sackler RS et al (2005) Complement factor H polymorphism in age-related macular degeneration. Science 308:385–389

Kloeckener-Gruissem B, Barthelmes D, Labs S, Schindler C, Kurz-Levin M et al (2011) Genetic association with response to intravitreal ranibizumab in patients with neovascular AMD. Investig Ophthalmol Vis Sci 52:4694–4702

Leviev I, James RW (2000) Promoter polymorphisms of human paraoxonase PON1 gene and serum paraoxonase activities and concentrations. Arterioscler Thromb Vasc Biol 20:516–521

Li M, Atmaca-Sonmez P, Othman M, Branham KE, Khanna R et al (2006) CFH haplotypes without the Y402H coding variant show strong association with susceptibility to age-related macular degeneration. Nat Genet 38:1049–1054

Mackness B, Mackness MI, Arrol S, Turkie W, Durrington PN (1998a) Effect of the human serum paraoxonase 55 and 192 genetic polymorphisms on the protection by high density lipoprotein against low density lipoprotein oxidative modification. FEBS Lett 423:57–60

Mackness B, Mackness MI, Arrol S, Turkie W, Julier K et al (1998b) Serum paraoxonase (PON1) 55 and 192 polymorphism and

paraoxonase activity and concentration in non-insulin dependent diabetes mellitus. Atherosclerosis 139:341–349
Mackness MI, Mackness B, Durrington PN, Fogelman AM, Berliner J et al (1998c) Paraoxonase and coronary heart disease. Curr Opin Lipidol 9:319–324
Maller J, George S, Purcell S, Fagerness J, Altshuler D et al (2006) Common variation in three genes, including a noncoding variant in CFH, strongly influences risk of age-related macular degeneration. Nat Genet 38:1055–1059
Maziere C, Maziere JC (2009) Activation of transcription factors and gene expression by oxidized low-density lipoprotein. Free Radic Biol Med 46:127–137
Moskvina V, Holmans P, Schmidt KM, Craddock N (2005) Design of case-controls studies with unscreened controls. Ann Hum Genet 69:566–576
Mueller JC (2004) Linkage disequilibrium for different scales and applications. Brief Bioinform 5:355–364
Neale BM, Fagerness J, Reynolds R, Sobrin L, Parker M et al (2010) Genome-wide association study of advanced age-related macular degeneration identifies a role of the hepatic lipase gene (LIPC). Proc Natl Acad Sci U S A 107:7395–7400
Oshima Y, Ishibashi T, Murata T, Tahara Y, Kiyohara Y et al (2001) Prevalence of age-related maculopathy in a representative Japanese population: the Hisayama study. Br J Ophthalmol 85:1153–1157
Pang CP, Baum L, Chan WM, Lau TC, Poon PM et al (2000) The apolipoprotein E epsilon4 allele is unlikely to be a major risk factor of age-related macular degeneration in Chinese. Ophthalmologica 214:289–291
Paragh G, Seres I, Balogh Z, Varga Z, Karpati I et al (1998) The serum paraoxonase activity in patients with chronic renal failure and hyperlipidemia. Nephron 80:166–170
Pauer GJ, Sturgill GM, Peachey NS, Hagstrom SA (2010) Protective effect of paraoxonase 1 gene variant Gln192Arg in age-related macular degeneration. Am J Ophthalmol 149:513–522
Rivera A, Fisher SA, Fritsche LG, Keilhauer CN, Lichtner P et al (2005) Hypothetical LOC387715 is a second major susceptibility gene for age-related macular degeneration, contributing independently of complement factor H to disease risk. Hum Mol Genet 14:3227–3236
Rosenfeld PJ, Brown DM, Heier JS, Boyer DS, Kaiser PK et al (2006) Ranibizumab for neovascular age-related macular degeneration. N Engl J Med 355:1419–1431
Schmidt S, Hauser MA, Scott WK, Postel EA, Agarwal A et al (2006) Cigarette smoking strongly modifies the association of LOC387715 and age-related macular degeneration. Am J Hum Genet 78:852–864
Senti M, Tomas M, Fito M, Weinbrenner T, Covas MI et al (2003) Antioxidant paraoxonase 1 activity in the metabolic syndrome. J Clin Endocrinol Metab 88:5422–5426
Stephens M, Donnelly P (2003) A comparison of bayesian methods for haplotype reconstruction from population genotype data. Am J Hum Genet 73:1162–1169
Stephens M, Smith NJ, Donnelly P (2001) A new statistical method for haplotype reconstruction from population data. Am J Hum Genet 68:978–989
Swaroop A, Branham KE, Chen W, Abecasis G (2007) Genetic susceptibility to age-related macular degeneration: a paradigm for dissecting complex disease traits. Hum Mol Genet 16(Spec No. 2):R174–R182
Tanimoto S, Tamura H, Ue T, Yamane K, Maruyama H et al (2007) A polymorphism of LOC387715 gene is associated with age-related macular degeneration in the Japanese population. Neurosci Lett 414:71–74
Thakkinstian A, Han P, McEvoy M, Smith W, Hoh J et al (2006) Systematic review and meta-analysis of the association between complement factor H Y402H polymorphisms and age-related macular degeneration. Hum Mol Genet 15:2784–2790
Weger M, Renner W, Steinbrugger I, Kofer K, Wedrich A et al (2007) Association of the HTRA1–625G>A promoter gene polymorphism with exudative age-related macular degeneration in a Central European population. Mol Vis 13:1274–1279
Yang Z, Camp NJ, Sun H, Tong Z, Gibbs D et al (2006) A variant of the HTRA1 gene increases susceptibility to age-related macular degeneration. Science 314:992–993
Zuercher J, Neidhardt J, Magyar I, Labs S, Moore AT et al (2010) Alterations of the 5′untranslated region of SLC16A12 lead to age-related cataract. Investig Ophthalmol Vis Sci 51:3354–3361
Zuker M (2003) Mfold web server for nucleic acid folding and hybridization prediction. Nucleic Acids Res 31:3406–3415

Regulatory regions of the paraoxonase 1 (*PON1*) gene are associated with neovascular age-related macular degeneration (AMD)

Jadwiga Oczos[1,2,3], Christian Grimm[2,3,4], Daniel Barthelmes[5,6], Florian Sutter[5], Moreno Menghini[5], Barbara Kloeckener-Gruissem[1,7,*,‡] and Wolfgang Berger[1,3,4,*,‡]

[1] Institute of Medical Molecular Genetics, University of Zurich, Schwerzenbach, Switzerland
[2] Lab for Retinal Cell Biology, Department of Ophthalmology, University of Zurich, Zurich, Switzerland
[3] Zurich Center for Integrative Human Physiology (ZIHP), University of Zurich, Zurich, Switzerland
[4] Zurich Center of Neuroscience (ZNZ),
[5] Department of Ophthalmology, University Hospital Zurich, Zurich, Switzerland
[6] University of Sydney, Sydney, Australia, Save Sight Institute
[7] Department of Biology, ETH Zurich, Zurich, Switzerland

SUPPLEMENTARY INFORMATION

Supplementary Table S1. Linkage disequilibrium measurements for seven SNPs within the regulatory region of the *PON1* gene.

Data calculated using the control dataset (Table 2). D` is given in the upper right half and the R2 in the lower left half.

SNP	rs705379	rs705380	rs705381	rs854571	rs854572	rs854573	rs757158
rs705379	—	1	1	0.90	0.91	0.93	0.93
rs705380	0.06	—	1	1	1	1	0.93
rs705381	0.33	0.19	—	0.93	0.93	0.94	0.693
rs854571	0.36	0.14	0.63	—	1	0.99	0.79
rs854572	0.76	0.07	0.31	0.49	—	1	1
rs854573	0.28	0.19	0.88	0.71	0.36	—	0.73
rs757158	0.67	0.07	0.20	0.35	0.87	0.22	—

3.1.2 *PON1* 5'UTR haplotypes regulate gene expression in Caco-2 cells

Unpublished data

Contributors

Jadwiga Oczos[1], Barbara Kloeckener-Gruissem[1] and Wolfgang Berger[1]

[1] Institute of Medical Molecular Genetics, University of Zurich, Schwerzenbach, Switzerland

Personal contribution

Cloning, expression studies, statistical analysis

PURPOSE

Our previous study has shown that various *PON1* 5'UTR haplotypes exert cell-specific regulation of gene expression *in vitro* (section 3.1.1 of this thesis, Oczos et al., 2013). To further investigate this phenomenon, we tested DNA constructs containing different *PON1* 5'UTR haplotypes in the colon epithelium-derived cell line, Caco-2. We chose Caco-2 cells because of their epithelial characteristics and since they are known to express PON1 protein (Shamir et al., 2005).

METHODS

Eight DNA constructs containing all possible haplotypes of the *PON1* 5'UTR cloned into the pFirefly vector (pGL3-Control vector; Promega, Madison, WI, USA) were obtained as previously reported (section 3.1.1), and used in a functional assay in Caco-2 cells, a colon carcinoma-derived cell line (American Type Culture Collection (ATCC), Manassas, VA, USA; product ATCC-HTB-37). Of note, the *PON1* 5'UTR fragment was inserted downstream of the SV40 promoter. Therefore, we assume that both the *PON1* 5'UTR and the *Luciferase* coding sequence were transcribed from the strong viral promoter and we could assay an effect of the *PON1* fragment on mRNA folding and consequently on the protein synthesis, as measured by luciferase reporter activity.

Caco-2 cells at passage 90-92 were seeded on 24-well plates (8×10^4 cells/well) in 1 ml DMEM, 10% FBS, and 1% penicillin/streptomycin and cultured at 37°C in 5% CO_2 in air. Twenty-four hours later, cells were transfected using 0.75 μl X-tremeGENE9 transfection reagent (Roche Diagnostics, Indianapolis, IN, USA), 250 ng pFirefly construct, and 25 ng pRenilla construct per well. Forty-eight hours after transfection cells were harvested and luciferase activity was analyzed

using Dual-Glo Luciferase Assay System according to the manufacturer's protocol (Promega) and measured on a BioTek Synergy microplate reader (BioTek Instruments, Winooski, VT, USA). Data were normalized to the Renilla luciferase activity. The experiment was conducted four times with four replicates each.

RESULTS

Various *PON1* 5'UTR haplotypes affected differently gene expression in Caco-2 cells, as measured by luciferase reporter activity (Fig. 13). To assess contribution of each individual SNP to observed alterations, we performed a pairwise comparison between haplotypes differing at only one position. The SNP at position -162 appeared to be responsible for detected differences, with the A nucleotide causing an up to 1.6-fold increase in luciferase activity (Fig. 13 and Table 1). Effect of the two other polymorphisms on the gene expression was negligible and not consistent between repeated experiments.

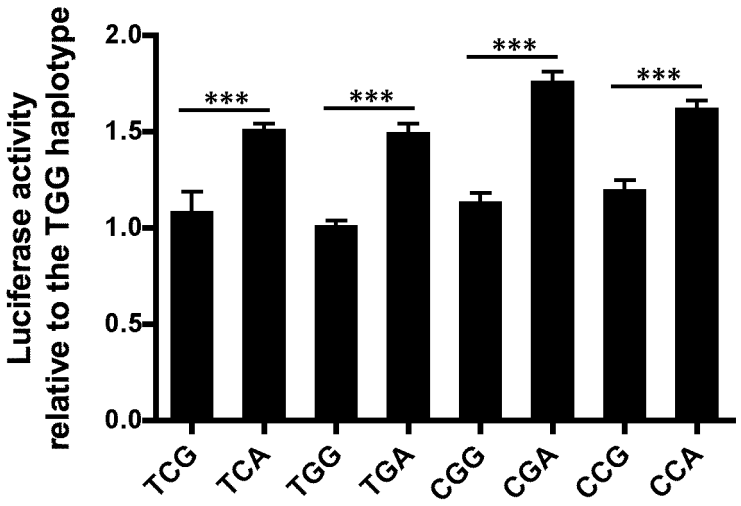

Figure 13. Luciferase activity for the eight *PON1* 5'UTR haplotypes in Caco-2 cells.
SNP order in haplotypes from left to right: -107, -126, -162. Luciferase activity of the reporter construct containing the TGG haplotype was set to 1. Shown are mean values ± SD of N = 4. Two-tailed *t* test revealed highly significant differences in luciferase activity between haplotypes differing at SNP -162. A p-value of less than 0.05 was considered significant; ***p<0.001.

DISCUSSION

PON1 5'UTR haplotypes affected gene expression in Caco-2 and ARPE19 cells (section 3.1.1) in a similar way. In both cell lines the SNP at position -162 caused alterations in luciferase reporter activity. In contrast, tested *PON1* haplotypes did not affect expression levels in HEK293 cells (section 3.1.1). Detected differences

between the three cell lines may be attributed to cell-specific *trans*-acting factors controlling translation (Di Liegro et al., 2014). Since both Caco-2 and ARPE19 cells are of epithelial origin, factors specific to epithelium might be involved. It is also possible that such regulatory mechanisms contribute to the previously reported tissue-specific differences in the expression of human PON1 (Ng et al., 2005).

SNP	Haplotype*		Fold increase in luciferase activity†	P value‡
	1	2		
-107	CCA	TCA	1.1	0.014
	CCG	TCG	1.1	ns
	CGA	TGA	1.2	0.001
	CGG	TGG	1.1	0.010
-126	CCA	CGA	0.9	0.018
	CCG	CGG	1.1	ns
	TCA	TGA	1.0	ns
	TCG	TGG	1.1	ns
-162	CCA	CCG	1.4	<0.001
	CGA	CGG	1.6	<0.001
	TCA	TCG	1.4	<0.001
	TGA	TGG	1.5	<0.001

Table 1. Effects of the *PON1* 5'UTR haplotypes on the luciferase reporter activity in Caco-2 cells.

Numerical representations of the results shown in figure 13. Compared are haplotypes differing at a single position: -107, -126, or -162. * SNP order in haplotypes from left to right: -107, -126, -162. † Fold increase in luciferase activity of haplotype 1 versus haplotype 2. ‡ Two-tailed *t* test was used to analyze statistical significance. A p-value of less than 0.05 was considered significant; ns, non-significant.

3.2 The contribution of SNPs and private mutations in *PON1* gene to coronary artery disease (CAD)

Unpublished data

Contributors

Jadwiga Oczos[1], Meliana Riwanto[2,3], Ulf Landmesser[2,3], Barbara Kloeckener-Gruissem[1] and Wolfgang Berger[1]

[1] Institute of Medical Molecular Genetics, University of Zurich, Schwerzenbach, Switzerland
[2] Cardiology, Cardiovascular Center, University Hospital Zurich, Zurich, Switzerland
[3] Cardiovascular Research, Institute of Physiology, University of Zurich, Zurich, Switzerland

Personal contribution

Design of the case-control study, genotyping, statistical analysis

PURPOSE

Studies on *Pon1*$^{-/-}$, *Pon1*$^{-/-}$*/ApoE*$^{-/-}$ and transgenic mice expressing human PON1 have demonstrated protective, anti-atherosclerotic function of PON1 (Rozenberg et al., 2003; Shih et al., 1998; Shih et al., 2000; Tward et al., 2002). Additionally, lower serum paraoxonase activity levels have been implicated in CAD (MacKness et al., 2000b). However, association studies between SNPs within *PON1* coding sequence and atherosclerosis or CAD led to contradictory results (Wheeler et al., 2004). To clarify the interplay between PON1 genotype, serum PON1 activities and the disease status we performed a comprehensive study in collaboration with the Cardiovascular Center at the University Hospital Zurich. The project had the following specific aims: (i) to examine whether SNPs within the *PON1* are associated with CAD in the Swiss population; (ii) to identify possible novel DNA sequence alterations in *PON1* that contribute to CAD; (iii) to study correlation between *PON1* genotypes, HDL-associated PON1 enzymatic activities and CAD (Besler et al., 2011).

METHODS

Patients

Patients with stable coronary artery disease (CAD) or acute coronary syndrome (ACS) between 40 and 70 years of age were consecutively recruited into the study at the University Hospital of Zurich (ethics committee approval: KEK-1471). The diagnosis of CAD and ACS was made according to guidelines of the American Heart Association (Anderson et al., 2007). Age- and sex-matched control subjects were enrolled by the Blood Donation Service of the University Hospital Zurich and had no cardiovascular risk factors or accompanying disorders. A detailed description of the recruitment criteria has been published previously (Besler et al., 2011).

Genotyping

Genomic DNA extraction and genotyping were performed as described in section 3.1.1 above (Oczos et al., 2013). Additionally, the entire *PON1* coding region including splice sites was sequenced by Sanger DNA sequencing using primer pairs listed in table 2.

Exon	Forward 5' → 3'	Reverse 5' → 3'
1	CCTTTCCCATGGCAATTTAC	TTAACAGCCTGGACCCAACT
2	CCTGGAAAAATTGCAGGAAA	GGACAGAATTGAACAGGCACA
3	CCAGTTTCAAGTGAGGTGTGA	TTTATTTGAAAGTGGGCATGG
4	CTGTGGTTTGGAGCAGTCAA	TTGGCATGTTTTTCTGTTTTTG
5	ATTCCATCTGCCTGACATCC	CCTACTCTGGCCAAAAGGAA
6	AGACAGTGAGGAATGCCAGTT	TCTCCTGAGAATCTGAGTAAATCC
7	GGGTTCCATTTTCCATTCCT	TCTCACCCACCCCAATTAAG
8	GACCAAGGACAAGAGGCAAC	AAAACAGTAGCTGGGAATAAAGTCA
9	GGCTTCTTATGGAGGATGACC	CACTGGGTCCTCGGAATATG

Table 2. DNA sequence of primers used for Sanger DNA sequencing.
Sequencing primers were designed by Primer3 (v. 0.4.0; http://frodo.wi.mit.edu/primer3, provided in the public domain by Massachusetts Institute of Technology, Cambridge, MA), and synthesized by Microsynth (http://www.microsynth.ch; Balgach, Switzerland). Annealing temperatures were established empirically and varied between 54 and 60°C.

Design of the case-control study

An online sample size calculator (http://sampsize.sourceforge.net/iface/s3.html) was used to estimate number of samples needed to collect in order to achieve 80% power to detect the minimum odds ratio (OR) of 2 with the error rate $\alpha = 0.05$. We designed our study based on the power calculation for the polymorphism rs705381 characterized by relatively low minor allele frequency (MAF = 0.167, dbSNP, https://www.ncbi.nlm.nih.gov/SNP/, HapMap-CEU European population) among

the analysed SNPs, for which collection of 193 cases and 193 controls would ensure desired power. The same sample size would enable detection of the minimum OR = 3.1 for the polymorphism rs705380 with the lowest minor allele frequency (MAF = 0.042), and the minimum OR = 1.8 for the rs705379 and rs854572 with the highest MAF = 0.425 among the analysed SNPs.

Statistical analysis

For association studies, odds ratios and significance were calculated using 2×2 contingency table provided on an open access Internet portal (http://faculty.vassar.edu/lowry/odds2x2.html). Odds ratios are given with 95% confidence intervals and Chi-square and P-values according to Pearson. Statistical significance was assumed at $p<0.05$.

RESULTS

This study in collaboration with the Cardiovascular Center at the University Hospital Zurich is an ongoing project that has not come to a completion. Preliminary results obtained until January 2013 will be presented.

Association of the *PON1* SNPs with coronary artery disease

Genotypes of 9 SNPs: 2 within the coding region (rs662, rs854560), 3 within the 5'UTR (rs705379, rs705380, rs705381), and 4 within the UUR (rs854571, rs854572, rs854573, rs757158) were determined from 39 CAD patients, 31 ACS patients, and 24 healthy control individuals (Table 3A, B). As described in the methods section, we would have to examine roughly 200 samples per each group to achieve sufficient power to detect differences in frequencies of the analysed alleles between the patient and the control groups. Analysis of the current sample size has the power to detect an OR of 4.5 and higher, thus only a relatively strong effect size. Nevertheless, we compared minor allele frequencies (MAFs) in the control group with the MAFs in both affected groups (CAD and ACS) by means of the odds ratio. Results of the statistical analysis presented in table 3 show lack of association between the analysed alleles with either CAD or ACS.

A

Marker	Major/ minor allele	Position	Region	MAF dbSNP	MAF Controls (n=24)	MAF CAD (n=39)	P value	OR	CI (95%)
rs662	A/G	c.575A>G (p.Q192R)	Ex6	0.332	0.295	0.250	0.75	0.79	0.34-1.86
rs854560	T/A	c.163T>A (p.L55M)	Ex3	0.375	0.370	0.448	0.54	0.72	0.33-1.59
rs705379	T/C	-107	5'UTR	0.425	0.476	0.500	0.81	0.91	0.43-1.93
rs705380	G/C	-126	5'UTR	0.042	0.045	0.039	—	1.15	0.19-7.22
rs705381	G/A	-162	5'UTR	0.167	0.227	0.224	0.86	1.02	0.42-2.48
rs854571	C/T	-831	UUR	0.302	0.300	0.231	0.38	1.43	0.64-3.19
rs854572	C/G	-908	UUR	0.425	0.438	0.423	1.00	0.94	0.46-1.95
rs854573	T/C	-1075	UUR	0.230	0.271	0.205	0.40	1.44	0.62-3.34
rs757158	C/T	-1740	UUR	0.376	0.420	0.395	0.78	0.90	0.44-1.86

B

Marker	Major/ minor allele	Position	Region	MAF dbSNP	MAF Controls (n=24)	MAF ACS (n=31)	P value	OR	CI (95%)
rs662	A/G	c.575A>G (p.Q192R)	Ex6	0.332	0.295	0.224	0.55	0.69	0.28-1.69
rs854560	T/A	c.163T>A (p.L55M)	Ex3	0.375	0.370	0.435	0.62	0.76	0.35-1.66
rs705379	T/C	-107	5'UTR	0.425	0.476	0.466	0.92	1.04	0.47-2.31
rs705380	G/C	-126	5'UTR	0.042	0.045	0.083	—	0.52	0.10-2.83
rs705381	G/A	-162	5'UTR	0.167	0.227	0.233	0.86	0.97	0.38-2.44
rs854571	C/T	-831	UUR	0.302	0.300	0.274	0.76	1.13	0.50-2.58
rs854572	C/G	-908	UUR	0.425	0.438	0.414	1.00	0.91	0.42-2.00
rs854573	T/C	-1075	UUR	0.230	0.271	0.226	0.58	1.27	0.53-3.04
rs757158	C/T	-1740	UUR	0.376	0.420	0.387	0.73	0.87	0.41-1.86

Table 3. Allele frequencies of the *PON1* SNPs in CAD and ACS patients.
Analysis of the allele frequencies in CAD patients (Table 3A) and ACS patients (Table 3B) compared to the healthy control individuals. Two analysed SNPs lie within the coding region (Ex6, exon6; and Ex3, exon3), another 3 within the 5' untranslated region (5'UTR), and additional 4 SNPs map to the upstream untranscribed region (UUR). Minor allele frequencies (MAF) for a Caucasian population were taken from the dbSNP database (https://www.ncbi.nlm.nih.gov/SNP/, HapMap-CEU European population), and were calculated for the control and both patient (CAD and ACS) groups. Odds ratios (OR) with confidence intervals (CI) and P-values ($\alpha = 0.05$) revealed no association between any of the analysed SNPs and any of the patient groups. For the polymorphism rs705380, P-value was not obtained because of too few counts for the minor allele C ($n<5$).

Screening for novel DNA sequence variants in *PON1* in patients with CAD

Sequencing of the entire *PON1* coding region including splice sites and 5'UTR was performed for 5 healthy individuals and 9 CAD patients. No unknown sequence variants were discovered. We confirmed several of the 18 annotated SNPs within the *PON1* gene that map to 5'UTR, coding and intronic regions. Genotype results for the three polymorphisms: T(-107)C within the 5'UTR, p.L55M in exon 3 and p.Q192R in exon 8, which are crucial from a functional and regulatory point of view (Furlong et al., 1988; Leviev and James, 2000), are presented in table 4.

Sample ID	Status	rs705379 T(-107)C	rs854560 c.163T>A (p.L55M)	rs662 c.575A>G (p.Q192R)
70682A	Healthy	CC	TT (LL)	AA (QQ)
70683A	Healthy	CT	TA (LM)	AA (QQ)
70684A	Healthy	CT	TA (LM)	AA (QQ)
70685A	Healthy	CT	TT (LL)	AG (QR)
70686A	Healthy	TT	TA (LM)	AA (QQ)
70687A	CAD	CC	TT (LL)	AA (QQ)
70688A	CAD	CT	TA (LM)	AG (QR)
70689A	CAD	TT	AA (MM)	AA (QQ)
70690A	CAD	CT	TT (LL)	AG (QR)
70691A	CAD	CT	TA (LM)	AA (QQ)
70692A	CAD	CT	TA (LM)	AA (QQ)
70693A	CAD	CT	TT (LL)	AG (QR)
70694A	CAD	CC	TT (LL)	AA (QQ)
70695A	CAD	CT	TT (LL)	AA (QQ)

Table 4. Genotyping results for selected SNPs within *PON1* gene.
For the two non-synonymous *PON1* SNPs (rs854560 and rs662) both genotypes and corresponding amino acids are given. L, leucine; M, methionine; Q, glutamine; R, arginine.

DISCUSSION

The study presented here showed no association between the genotyped *PON1* SNPs and either CAD or ACS patient groups. However, since analysis was performed only on a relatively small sample size, which enabled detection of a large (OR ≥ 4.5) but not a small effect, we can only make a clear statement on the lack of such a strong effect. Contribution of SNPs to a complex disease could be much smaller, e.g. OR = 1.5, as for the association between the *PON1* SNPs and AMD described in section 3.1.1. Therefore, we plan to analyse additional cases and controls. CAD and ACS patients, as well as control subjects are consecutively

recruited at the Cardiovascular Center, University Hospital Zurich. Additional blood samples are collected for DNA extraction and the following genotyping to reach the planned sample size of 193 controls and 193 affected individuals.

In parallel, for a subset of subjects, from whom HDL-associated PON1 activity will be measured, we will perform sequencing of the entire *PON1* coding region. Correlation analysis between the biochemical and genetic data will give an insight into the interaction between these factors in CAD pathology.

3.3 Function of PON1 in the mouse retina

3.3.1 Lack of paraoxonase-1 alters phospholipid composition but not morphology and function of the mouse retina

Jadwiga Oczos[1,2,3,*], Iryna Sutter[3,4,*], Barbara Kloeckener-Gruissem[2,6], Wolfgang Berger[2,3,5], Katharina Rentsch[7], Thorsten Hornemann[3,4], Arnold von Eckardstein[3,4] and Christian Grimm[1,3,5]

* These authors contributed equally to the work
[1] Lab for Retinal Cell Biology, Department of Ophthalmology, University of Zurich, Zurich, Switzerland
[2] Institute of Medical Molecular Genetics, University of Zurich, Schlieren, Switzerland
[3] Zurich Center for Integrative Human Physiology (ZIHP), University of Zurich, Zurich, Switzerland
[4] Institute of Clinical Chemistry, University of Zurich, Zurich, Switzerland
[5] Zurich Center of Neuroscience (ZNZ)
[6] Department of Biology, ETH Zurich, Zurich, Switzerland
[7] Laboratory Medicine, University Hospital Basel, Basel, Switzerland

Financial Support: Supported by a cooperative project grant by the Zurich Center for Integrative Human Physiology (ZIHP) of the University of Zurich, Zurich, Switzerland and by a matching fund of the Center for Clinical Research of the University Hospital Zurich, Zurich, Switzerland.

Manuscript submitted to IOVS, the Journal of *Investigative Ophthalmology & Visual Science*

First authors' contribution

JO: Laser capture microdissection, fundus imaging and fluorescein angiography, light and transmission electron microscopy, RPE flat mounts, RNA preparation and real-time PCR

IS: Lipid extraction, LC-MS

Purpose. Biochemical and genetic analyses established a contribution of lipid metabolism to AMD pathology. *PON1* (*Paraoxonase 1*) encodes an anti-oxidative protein involved in high density lipoprotein (HDL) function and was found to be associated with AMD. Here we used *Pon1*$^{-/-}$ mice to study the influence of PON1 on retinal physiology and to reveal the potential impact of PON1 on AMD aetiology.

Methods. Laser capture microdissection served to isolate single retinal layers. Retinal function was assessed by ERG. Retinal and RPE morphology were monitored by fundus imaging, fluorescein angiography, light and transmission electron microscopy, and immunofluorescence microscopy. Levels of mRNA and composition of phospholipid species were determined by real-time PCR and LC-MS, respectively.

Results. Adult (8-week old) *Pon1*$^{-/-}$ mice displayed normal retinal function and morphology, but their retinas contained reduced amounts of lysophosphatidyl-cholines (LPCs) compared to controls. Aged (12-month old) *Pon1*$^{-/-}$ animals did not show any morphological or molecular signs of photoreceptor or RPE degeneration, or of accelerated aging. Photoreceptors of *Pon1*$^{-/-}$ and control mice were similarly susceptible to light damage.

Conclusions. PON1 is not essential for normal development, function, ageing and the defense against light damage of the mouse retina. Reduced levels of LPCs in eyes of *Pon1*$^{-/-}$ mice may reflect a decreased activity of phospholipase A2 or altered anti-oxidative activity in aged eyes.

INTRODUCTION

Age-related macular degeneration (AMD) is the leading cause of irreversible blindness and visual disability in the elderly population of industrialized countries. Various environmental risk factors, such as advanced age, cigarette smoking, diet, obesity, atherosclerosis, hypertension, inflammatory disease, as well as genetic predisposition have been implicated in this complex disease (Guymer and Chong, 2006; Smith et al., 2001; Swaroop et al., 2007). The epidemiological risk factors point towards various molecular mechanisms that might be involved in the aetiology of AMD. Among those, cellular and extracellular oxidative stress, along with chronic inflammation are best-known to play a role in disease development and/or progression (Ambati et al., 2013; Handa, 2012; Khandhadia and Lotery, 2010).

Aging, the strongest risk factor for AMD is associated with structural and functional changes in Bruch's membrane and the retinal-pigment epithelium (RPE). Drusen, a hallmark of AMD (Booij et al., 2010) are formed between RPE and Bruch's membrane and contain polymorphous material. Major components of this material are lipid aggregates containing numerous lipoproteins and cholesterol (Curcio et al., 2011; Wang et al., 2010). These results established a connection between lipid metabolism and AMD aetiology, which was further confirmed by genetic studies. Genome-wide association scans identified several genes contributing to HDL metabolism to be associated with AMD, among them *LIPC* (hepatic lipase), *CEPT* (cholesterylester transfer protein), *LPL* (lipoprotein lipase), and *ABCA1* (ATP-binding cassette, sub-family A1) (Chen et al., 2010; Neale et al., 2010). We and others have also found an association of *PON1* (paraoxonase 1), a gene involved in HDL function, with advanced AMD in single populations (Baird et al., 2004; Ikeda et al., 2001; Oczos et al., 2013).

PON1 together with PON2 and PON3 forms a family of lactonases with antioxidant properties, which differ in sites of synthesis and mechanisms of action (Draganov and La Du, 2004). *PON1* is mainly expressed in liver (Ng et al., 2005) and encodes a secreted enzyme with a broad spectrum of functions that favor the involvement of PON1 in AMD pathology. In particular, PON1 present in serum HDL inhibits LDL oxidation, or "neutralizes" oxidized LDL by hydrolyzing lipid peroxides (Mackness et al., 1991; Mackness and Durrington, 1995). Additionally, PON1 acts in an anti-inflammatory manner by reducing monocyte chemotaxis and adhesion to endothelial cells (Ahmed et al., 2003), inhibiting monocyte-to-macrophage differentiation (Rosenblat et al., 2011), and directly suppressing macrophage pro-inflammatory responses (Aharoni et al., 2013). The anti-oxidant as well as the anti-inflammatory activities of PON1 suppress the formation of

atherosclerotic plaques, pathological lesions that share several properties with drusen (Curcio et al., 2010; Tabas et al., 2007). Whereas PON2 is an ubiquitous intracellular protein that can protect endoplasmic reticulum and mitochondria against reactive oxygen species (ROS) mediated damage (Altenhofer et al., 2010; Horke et al., 2007), PON3 acts similarly to PON1, as it is transported by HDL and protects HDL from oxidation (Draganov et al., 2000).

The genetic studies mentioned above, biochemical analyses reporting lower serum paraoxonase activity in patients with AMD (Baskol et al., 2006), and reports showing that smoking reduces PON1 activity in serum (Isik et al., 2007; Solak et al., 2005) are indications for a potential involvement of PON1 in the pathophysiology of AMD. Nevertheless, the role of PON1 in the eye has not been studied. Here we used *Pon1*$^{-/-}$ mice to investigate the role of PON1 in the retina/RPE to elucidate its potential contribution to retinal lesions and eye pathology.

MATERIALS AND METHODS

Mice

Animals were treated in accordance with the regulations of the Veterinary Authority of Zurich and with the statement of *The Association for Research in Vision and Ophthalmology* for the use of animals in research. Wild type 129S6/SvEvTac mice were purchased from Taconics (Eiby, Denmark). *Pon1*$^{-/-}$ mice (B6.129X1-Pon1^{tm1Lus}/J) (Shih et al., 1998) were purchased from Jackson Laboratory (Bar Harbor, ME, USA), and genotyped by PCR using the following primers: common forward primer 5'-CTT GTC CAT CCT CAG CTT GT-3', wild type reverse primer 5'-CCG ATG GTT CTT GTA AAG TGC-3', mutant reverse primer 5'-CTT GGG TGG AGA GGC TAT TC-3'. *Pon1*$^{-/-}$ mice were backcrossed for 10 generations onto the 129S6/SvEvTac background prior to analyses. All mice were kept at the animal facility of the University Hospital Zurich in a dark-light cycle (12 h : 12 h) with 60 lux of light at cage level and a normal chow diet.

Light exposure

Six- to 8-week old mice were dark adapted overnight (16 h). Pupils were dilated with 1% cyclogyl (Alcon, Cham, Switzerland) and 5% phenylephrine (Ciba Vision, Niederwangen, Switzerland) 30 minutes before exposure to 17,000 lux of white light for 2 hours. After light exposure mice were kept in darkness until the next day before being returned to cyclic light. Mice were killed at different time points after light offset (N=3 for each group) and retinas, eyecups, or whole eyeballs were removed. Mice that were dark-adapted but not exposed to light served as controls.

Laser capture microdissection

Eyes of 8-week old wild type and *Pon1*$^{-/-}$ mice were enucleated, immediately embedded in tissue freezing medium (Leica Microsystems Nussloch GmbH, Nussloch, Germany), and frozen in a 2-methylbutane bath cooled in liquid nitrogen. Retinal sections (20 μm) were collected on Arcturus PEN Membrane Glass Slides (Applied Biosystems, Foster City, CA, USA), fixed (5 min acetone), air dried (5 min), and dehydrated (30 sec 100% ethanol, 5 min xylol). Retinal layers were isolated using an Arcturus XT Laser Capture Microdissection system (Bucher Biotec AG, Basel, Switzerland) and Arcturus CapSure Macro LCM Caps (Applied Biosystems). RNA was isolated using the Arcturus PicoPure RNA Isolation Kit (Applied Biosystems) according to the manufacturer's directions, including a DNase treatment to remove residual genomic DNA. cDNA was synthesized using random hexamer primers (High-Capacity cDNA Reverse Transcription Kit; Applied Biosystems), and further analyzed by real-time PCR as described in section `RNA preparation and semi-quantitative real-time PCR`.

Electroretinogram (ERG)

Electroretinograms were recorded from both eyes simultaneously following published protocols (Seeliger et al., 2001; Tanimoto et al., 2009). Briefly, mice were dark-adapted overnight and anesthetized the next day with ketamine (66.7 mg/kg; Ratiopharm GmbH, Ulm, Germany) and xylazine (11.7 mg/kg; Bayer HealthCare, Monheim, Germany). Pupils were dilated with 1% cyclogyl and 5% phenylephrine 30 min before performing single flash ERG recordings under dark-adapted (scotopic) and light adapted (photopic) conditions. Light adaptation was accomplished with low background illumination starting 5 min before photopic recordings. Single white-flash stimulus intensities ranged from –3.7 to 1.9 log cd*s/m^2 under scotopic and from –0.6 to 2.9 log cd*s/m^2 under photopic conditions, divided into 12 and 8 steps, respectively. Ten responses per flash intensity were averaged with an interstimulus interval of either 4.95 sec or 16.95 sec (for 1.4, 1.9, 2.4, and 2.9 log cd*s/m^2).

Fundus imaging and fluorescein angiography

Pupils were dilated with 1% cyclogyl and 5% phenylephrine. After 30 min mice were anesthetized with ketamine (66.7 mg/kg) and xylazine (11.7 mg/kg) and corneas were moistened with 2% methocel (OmniVision, Puchheim, Germany). Fundi were monitored and photographed using a mouse imaging system (Micron III, Phoenix Research Laboratories, Pleasanton, CA, USA). Fluorescein solution (2% in PBS; AK-FLUOR; Lake Forest, IL, USA) was injected intraperitoneally and eyes were analyzed immediately.

Light and transmission electron microscopy

Eyes were enucleated and fixed in 2.5% glutaraldehyde in 0.1 M cacodylate buffer (pH 7.3) at 4˚C overnight. Cornea and lens were removed and eyecups cut dorso-ventrally through the optic nerve head. Trimmed tissue was washed in cacodylate buffer, incubated in osmium tetroxide for 1 hour at room temperature, dehydrated, and embedded in Epon 812. For light microscopy (Axioplan 2, Zeiss, Feldbach, Switzerland) semi-thin cross sections (500 nm) were cut and counterstained with toluidine blue. For transmission electron microscopy (TEM), ultra-thin sections (50 nm) were stained with uranyl acetate and lead citrate, and analyzed using a Philips CM100 transmission electron microscope.

RPE flat mount preparation and analysis

Unless stated otherwise, all procedures were conducted at room temperature. Eyes were enucleated and incubated in 2% paraformaldehyde (PFA) in 0.1 M phosphate buffer pH 7.4 (PB, 0.081M Na_2HPO_4, 0.019M $NaH_2PO_4 \times H_2O$) for 5 min. Cornea and lens were removed and the remaining tissue was left in PB-salt (PB containing 140 mM NaCl and 2.7 mM KCl) for 20 min to allow the retina to separate from the eyecup. The retina was gently removed and the eyecup containing the RPE cut into a “clover-leaf” shape and post-fixed in 4% PFA in PB for 1 hour. Flatmounts were blocked with blocking solution (3% normal goat serum, 0.3% Triton X-100 in PBS) for 1 hour and incubated with the primary antibody anti-β-catenin (1:300 in blocking solution; BD Biosciences, Allschwil, Switzerland) overnight at 4°C. After washing 3 × 10 min in PBS, Cy3-conjugated anti-mouse secondary antibody (1:200 in blocking solution; Jackson ImmunoResearch, Suffolk, UK) and Alexa Fluor 488-phalloidin (1.3 U/ml in blocking solution; Applied Biosystems) were applied for 2 hours. After washing, cell nuclei were stained with Hoechst (2 μg/ml in PBS; Sigma Aldrich, Buchs, Switzerland) for 30 min. Flatmounts were washed with PBS and mounted with anti-fade medium (10% Mowiol 4–88 (w/v); Calbiochem, San Diego, CA, USA; 25% glycerol (w/v); 0.1% 1,4-diazabicyclo[2.2.2]octane in 100 mM Tris, pH 8.5). RPE sheets were examined using a digitalized fluorescence microscope and an ApoTome module (Axioplan 2, Zeiss, Switzerland).

Morphometric measurements including eccentricity and form factor were performed with CellProfiler software (Carpenter et al., 2006). Phalloidin-stained images (magnification: 20x) were illumination corrected and analyzed using the “Tissue Neighbours” pipeline with the background adaptive thresholding method. At least N=700 RPE cells per group were examined. RPE cells were counted in 4 quadrants of 176.8 × 235.3 μm (1040 × 1384 pixels), approximately 800-900 μm temporal, dorsal, nasal and ventral of the optic nerve head. Three animals per genotype and condition were analyzed.

RNA preparation and semi-quantitative real-time PCR

Retinas were removed through a slit in the cornea and placed in an Eppendorf tube. The rest of the eye (eyecup without lens) was isolated separately. All samples were immediately frozen in liquid nitrogen and stored at -80°C. Total RNA from retina and eyecups was prepared using the High Pure RNA Isolation Kit (Roche Diagnostics, Mannheim, Germany) or the RNeasy kit (Qiagen, Hilden, Germany), respectively. RNA isolations included a DNase treatment to digest residual genomic DNA. Equal amounts of RNA were reverse transcribed using oligo(dT) primer and M-MLV reverse transcriptase (Promega, Madison, WI, USA). Real-time PCR with specific primer pairs (Table 1), a polymerase ready mix (LightCycler 480 SYBR Green I Master Mix; Roche Diagnostics, Basel, Switzerland), and a thermocycler (LightCycler, Roche Diagnostics) were used to study gene expression. Three animals per time point were analyzed in duplicates. Signals were normalized to *β-actin* and relative gene expression was calculated using the ΔΔCt method.

Lipid extraction

For most analyses, lipids were extracted from retinal and eyecup tissue together. We will refer to these samples as "retina/eyecup" samples from here on. In some instances retinas and eyecups were isolated separately and named accordingly. Isolated tissue samples were immediately frozen in liquid nitrogen and stored at -80°C. Retina/eyecup samples were homogenized in lysis buffer (PBS, 0.2% Triton X-100 [vol./vol.]) using a Precellys 24 tissue homogenizer (Bertin Technologies, Montigny-le-Bretonneux, France). The protein content was measured using the Bradford assay. Total lipids were extracted from aliquots of homogenized tissue containing 40 mg of protein. Extraction was conducted according to the Bligh and Dyer (Bligh and Dyer, 1959) procedure in the presence of 200 ng of the internal standards PG 17:0/17:0, PA 14:0/14:0, PE 14:0/14:0, PC 14:0/14:0, PC 24:0/24:0, LPC 17:0, SM d18:1/12:0 and Cer d18:1/17:0 (Avanti Polar Lipids, Alabaster, AL, USA). Samples were mixed with 375 µl of methanol/chloroform (2:1, v/v) and vortexed, followed by the addition of 100 ml water and 125 ml chloroform. The mixture was shaken for 15 minutes and centrifuged at 16100×g for 5 minutes at 25°C. The lower phase was collected, 250 ml chloroform added, shaken for 15 minutes and centrifuged at 16100×g for 5 minutes at 25°C. All lower phases were combined and evaporated to dryness under a stream of nitrogen. Dried material was reconstituted in 200 ml of a mixture of mobile phases A (80%) and B (20%) (see below). 10 ml was injected into the LC-MS system for PL analysis.

Table 1. Primers and conditions for real-time PCR

Gene	Froward 5′→ 3′	Reverse 5′→ 3′	Annealing temp. (°C)	Product (bp)
Pon1	GCATCTGAAAACCATCACACA	AAGCTCTCAGGTCCAATAGCA	60	72
Pon2	CAGAGGCTCTTCGTGTACCA	ATGTTCTGAATGCGGAGGAC	60	88
Pon3	TTGACCGTTGATCCAGCCAC	GAAGCACAGAGCCGTTGTTC	62	175
Sod1	GAGCAGAAGGCAAGCGGTGA	AGGTCCTGCACTGGTACAGC	62	126
Sod2	GACCTGCCTTACGACTATGG	CTGAAGAGCGACCTGAGTTG	62	168
Hmox1	CCGCCTTCCTGCTCAACATT	GACGAAGTGACGCCATCTGTG	62	99
Abca1	GCGTGAAGCCTGTCATCTAC	CATGAGAGGAGTGATCGACC	62	185
Scarb1	CGCACAGTTGGTGAGATCCT	CACCAGATGGATCCTGCTGA	62	183
Lif	AATGCCACCTGTGCCATACG	CAACTTGGTCTTCTCTGTCCCG	60	216
Edn2	AGACCTCCTCCGAAAGCTG	CTGGCTGTAGCTGGCAAAG	60	64
Fgf2	TGTGTCTATCAAGGGAGTGTGTGC	ACCAACTGGAGTATTTCCGTGACCG	62	158
Stat3	CAAAACCCTCAAGAGCCAAGG	TCACTCACAATGCTTCTCCGC	62	139
Socs3	ATTTCGCTTCGGGACTAGC	AACTTGCTGTGGGTGACCAT	58	126
Mct3	GGCTCAACCCTAAATCCAGA	CTTCGGAGTTTCCTCACCAG	58	75
Gnat1	GAGGATGCTGAGAAGGATGC	TGAATGTTGAGCGTGGTCAT	58	209
Vsx2	CCAGAAGACAGGATACAGGTG	GGCTCCATAGAGACCATACT	60	111
Opn4	CCAGCTTCACAACCAGTCCT	CAGCCTGATGTGCAGATGTC	62	111
Actb	CAACGGCTCCGGCATGTGC	CTCTTGCTCTGGGCCTCG	62	153

Analysis of the retina/eyecup lipidome: LC-MS instrumentation and chromato-graphic conditions

Analyses of six different phospholipid (PL) classes: phosphatidylcholines (PC), sphingomyelins (SM), phosphatidylethanolamines (PE), phosphatidylglycerols (PG), phosphatidic acids (PA) and ceramides/hexosylceramides (Cer/HexCer) were performed by utilizing liquid chromatography and mass spectrometry. Details of the method are described in the supplementary materials. Briefly, total lipid extracts were analyzed on a LC-MS system consisting of a Rheos 2200 pump (Flux Instruments, Reinach, Switzerland), an HTC PAL autosampler (CTC Analytics, Zwingen, Switzerland) and a TSQ Quantum Access triple quadrupole mass analyzer (Thermo Fisher Scientific, Waltham, MA, USA). Separation of lipid extracts was performed on a diol silica-based column (QS Uptisphere 6 OH, 150 × 2.1 mm, 5 μm, Interchim, France). Mobile phase A was a mixture of hexane/isopropanol/water (70:30:2, v/v) with 15 mM ammonium formate. Mobile phase B was isopropanol/ water (50:2, v/v) with 15 mM ammonium formate. The solvent-gradient was 0-7 min A/B (%) 80/20, 8-10 min A/B (%) 60/40, 11-23 min A/B (%) 40/60 and 25-30 min A/B (%) 80/20 at a flow rate of 0.35 ml/min. The column was maintained at 30°C. Mass spectrometry was performed in positive ionization mode with the following parameters: 4500 V spray voltage, skimmer voltage 2 - 14 V (depending on the scan mode), 250°C capillary temperature, and 10 and 6 (arbitrary units) sheath and auxiliary N_2 gas, respectively. Molecular masses provided by a neutral loss and precursor scan were used to selectively detect specific phospholipids. A neutral loss of masses m/z 115 and 189 from $[M+NH_4]^+$ ions were used for analysis of PA and PG lipids, respectively. A precursor ion scan of m/z 184 specific for phosphocholine containing lipids was used for PC, SM and LPC. A neutral loss scan of m/z 141 was used for PE and a precursor scanning of m/z 264 was applied for screening of Cer. Acquired data were analyzed using Xcalibur (version 2.0.6, Thermo Scientific). The structure of the head groups were determined from the type of MS/MS scanning. Molecular species were identified by using LIMSA (Haimi et al., 2006). All species were assigned to the lipid classes and species with a defined total number of carbon atoms and double bounds in O-linked fatty acids. Data were corrected for isotopic overlap. Quantification was based on calibration curves for seven PL standards including PC 16:0/18:2, SM d18:1/16:0, LPC 16:0, PE 18:0/18:0, Cer d18:1/14:0, PG 16:0/16:16 and PA 14:0/14:0. The calibration curves were constructed by plotting the PL/IS peak area ratios against the nominal concentration of the standards. The concentrations for the individual lipid classes were calculated from linear regressions of the calibration curves.

Statistical analysis

Semi-quantitative real-time PCR and morphometric analysis of the RPE flat mounts: Statistical analyses were performed using Prism4 software. All data are given as means ± standard deviation (SD) of three animals per group. Statistical differences of means were calculated using 2-way ANOVA followed by a Bonferroni post-hoc test. A p-value of less than 0.05 was considered significant.

Lipidomic analysis: Statistical analyses were performed using SPSS, version 19 (SPSS Switzerland, Zurich, Switzerland). Normality of the data was determined by using Kolmogorov-Smirnov test. Since not all lipid species had normally distributed values nonparametric Mann-Whitney U test was used. The Mann-Whitney U test was applied for comparison between *Pon1*$^{-/-}$ and wild type mice. Bonferroni correction was applied to adjust the p-value for multiple comparisons (37 statistical tests). A p-value of 0.001 or below was considered significant. Data are presented as median with lower and upper range values.

RESULTS

Paraoxonase-1 is highly expressed in the RPE

To evaluate the expression pattern of paraoxonases in the retina we isolated the retinal pigment epithelium (RPE), the outer nuclear layer (ONL), the inner nuclear layer (INL) and the ganglion cell layer (GCL) by laser capture microdissection and analyzed levels of *Pon1*, *Pon2* and *Pon3* mRNA by semi-quantitative real-time PCR (Fig. 1). Expression of monocarboxylate transporter, member 3 (*Mct3*; RPE), guanine nucleotide binding protein, alpha transducing activity polypeptide (*Gnat1*; ONL), visual system homeobox 2 (*Vsx2*; INL), and melanopsin (*Opn4*; GCL) were used as layer-specific markers and showed that cross-contamination between collected layers was minimal. In wild type mice, *Pon1* was highest expressed in the RPE with 267-, 590-, and 651-fold higher levels than in ONL, INL, and GCL, respectively. Similarly, *Pon3* was most abundant in the RPE (45-, 43-, 72-fold higher levels than in ONL, INL, and GCL, respectively). *Pon2* content was comparable in the RPE and the INL, approximately 25- and 9-fold higher than in ONL and GCL, respectively.

Even though *Pon1*$^{-/-}$ mice have a neomycin cassette inserted into exon 1 of *Pon1* and do not produce a functional PON1 protein (Shih et al., 1998), the RNA transcript can still be detected. Interestingly, we found differential effects of the neomycin insertion on *Pon1* expression in RPE and neuronal retina. Whereas expression of the disrupted *Pon1* gene was 33-fold decreased in the RPE, it was 15-fold increased in the INL and 6-fold in the GCL, indicating differential regulation of *Pon1* expression in RPE and neuroretina. Levels of *Pon2* and *Pon3* transcripts were not significantly affected by the lack of functional PON1.

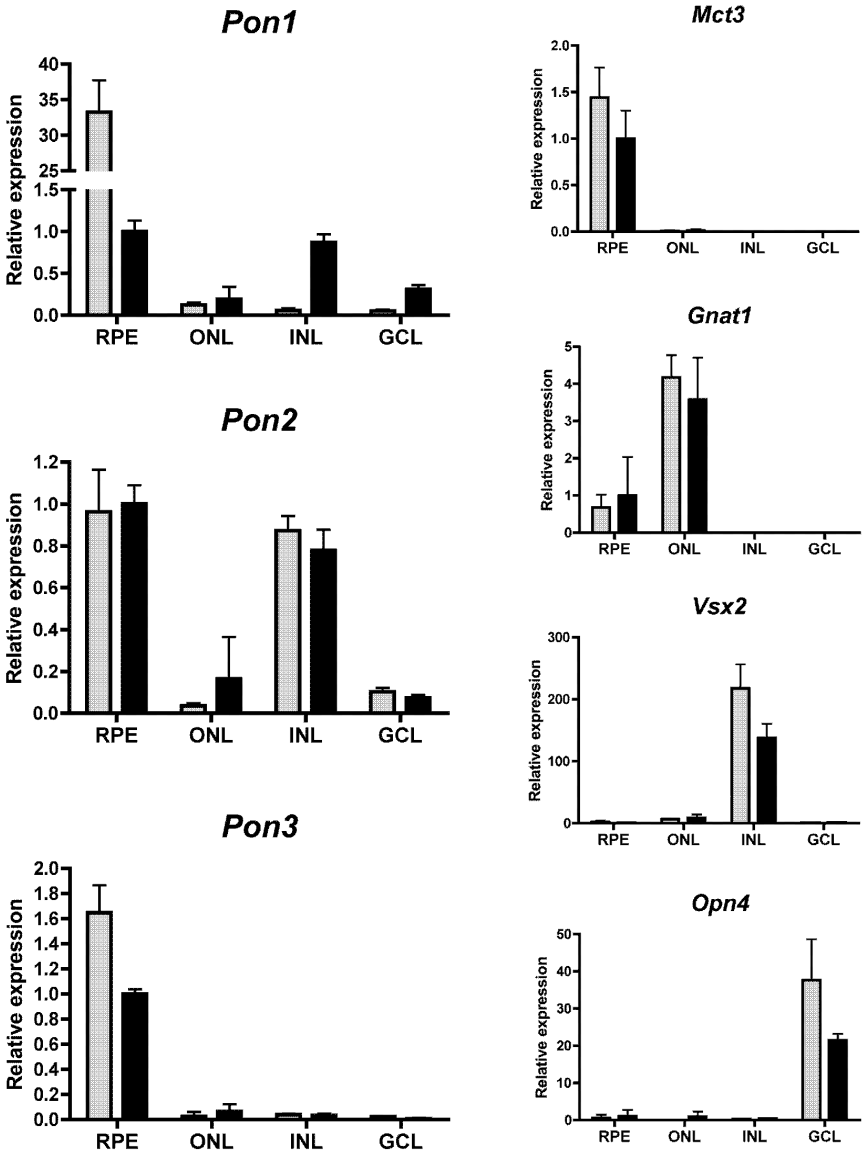

Figure 1. *Pon1* is highly expressed in the RPE.
Retinal pigment epithelium (RPE), outer nuclear layer (ONL), inner nuclear layer (INL) and ganglion cell layer (GCL) were isolated from wild type (grey bars) and *Pon1*$^{-/-}$ mice (black bars) using laser capture microdissection. Relative gene expression was determined by semi-quantitative real-time PCR in each individual layer. Values were normalized to *β-actin*, and expressed relative to levels in the RPE of *Pon1*$^{-/-}$ mice, which were set to 1. Shown are mean values ± SD of N=3. Expression of *Mct3* (marker for RPE), *Gnat1* (marker for ONL), *Vsx2* (marker for INL), and *Opn4* (marker for GCL) was determined to monitor contamination between the isolated retinal layers.

Absence of PON1 does not compromise retinal function and architecture

To evaluate whether PON1 is important for normal retinal development, ageing and function, we analyzed 8-week and 1-year old mice. *Pon1*$^{-/-}$ mice showed regular retinal architecture and no signs of RPE or photoreceptor degeneration at either age (Fig. 2A). Similarly, funduscopy and fluorescein angiography revealed no retinal or vascular defects in *Pon1*$^{-/-}$ mice (Fig. 2B). Normal scotopic and photopic ERGs with a- and b-wave amplitudes similar to wild types (Fig. 2C) supported the conclusion that *Pon1*$^{-/-}$ mice developed a normal and functional retina.

Lack of PON1 does not affect RPE morphology

Since we found high *Pon1* expression in the RPE and *PON1* was previously implicated in AMD (Baird et al., 2004; Baskol et al., 2006; Ikeda et al., 2001; Oczos et al., 2013), a disease strongly affecting RPE and Bruch's membrane, we examined these structures in young and old mice. Transmission electron microscopy did not detect any obvious differences in the ultrastructure of RPE and Bruch's membrane between *Pon1*$^{-/-}$ and wild type mice at any age (Fig. 3A). Also, RPE microvilli and basal infoldings appeared normal and no AMD-like features such as Bruch's membrane thickening or sub-RPE deposits (Ramkumar et al., 2010) were present in any of the analyzed animals up to one year of age.

To analyze RPE cell morphology on a larger scale, we prepared RPE flat mounts. The RPE monolayer is normally formed by a relatively uniform array of polygonal cells containing one to two centrally positioned nuclei. The regular shape is maintained by adherens and tight junctions, as well as by the actin-myosin cytoskeleton, whose components may serve as markers of epithelial integrity. We monitored the RPE cell boundaries by immunofluorescent staining for β-catenin (adherens junctions) and phalloidin (F-actin) and did not observe any abnormalities in mice lacking PON1 up to one year of age (Fig. 3B). This was further supported by morphometric analyses, which were used to quantitatively assess RPE cell shape. The eccentricity (ECC) and form factor (FF) are two measures of distortion from a circular shape, whose values vary between 0 and 1, with ECC=0 and FF=1 for a perfect circle. These factors did not differ significantly between cells in the RPE of *Pon1*$^{-/-}$ and age-matched wild type mice (Fig. 3C).

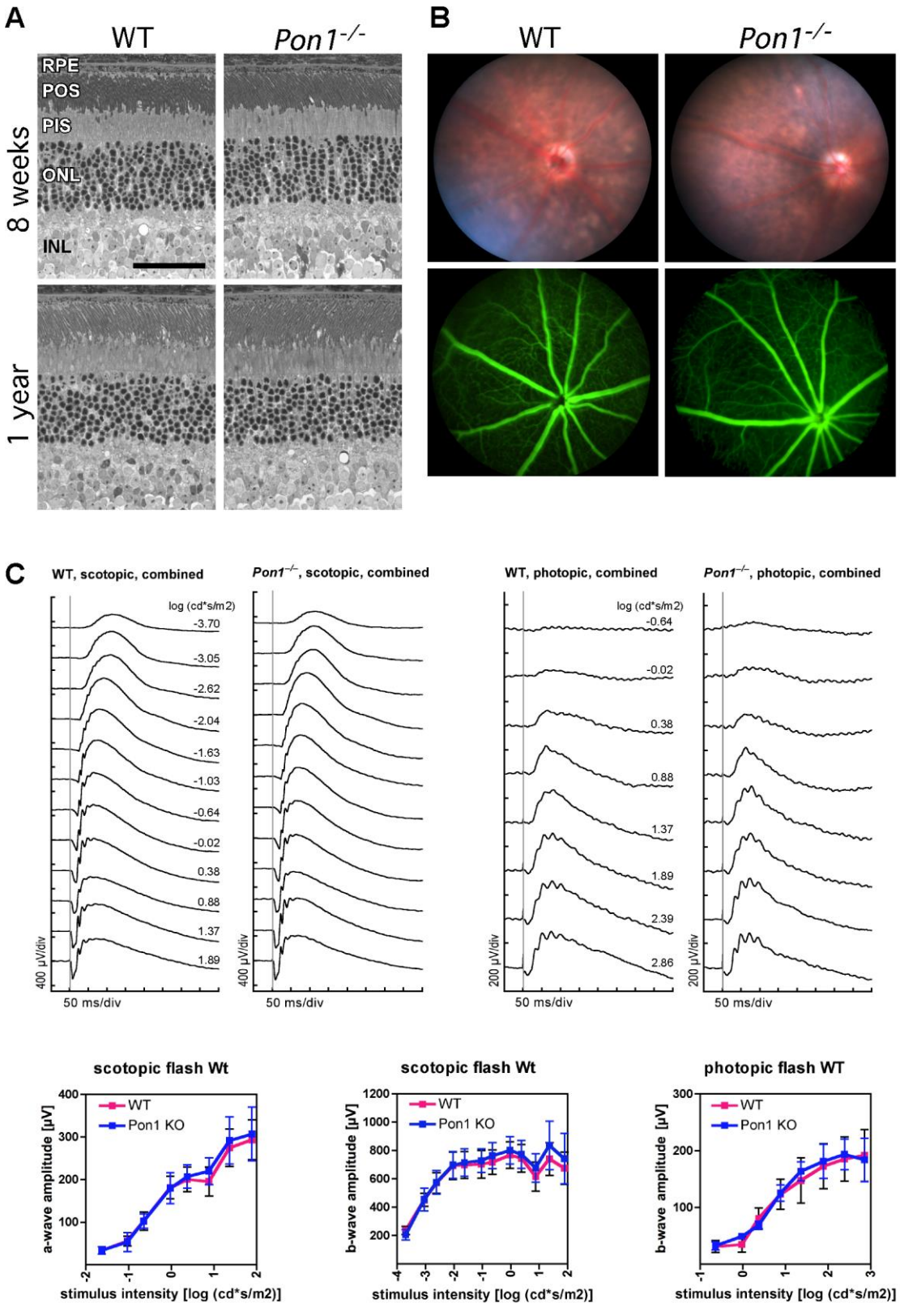

Figure 2. Lack of PON1 does not compromise retinal architecture and function
(A) Retinal morphology of *Pon1*$^{-/-}$ and control mice (WT) at 8 weeks and 1 year of age. Shown are representative sections of N=3. RPE, retinal pigment epithelium; POS, photoreceptor outer segments; PIS, photoreceptor inner segments; ONL, outer nuclear layer; INL, inner nuclear layer. Scale bar: 50 µm. **(B)** Funduscopy (top panels) and fluorescein angiography (bottom panels) of WT and *Pon1*$^{-/-}$ mice at 8 weeks of age. Shown are representative images of N=3. **(C)** Scotopic and photopic electroretinograms from WT and *Pon1*$^{-/-}$ mice at 8 weeks of age. Top panels: representative traces from individual mice. Bottom panels: scotopic a- and b-wave amplitudes, as well as photopic b-wave amplitudes as a function of light intensity. N=3.

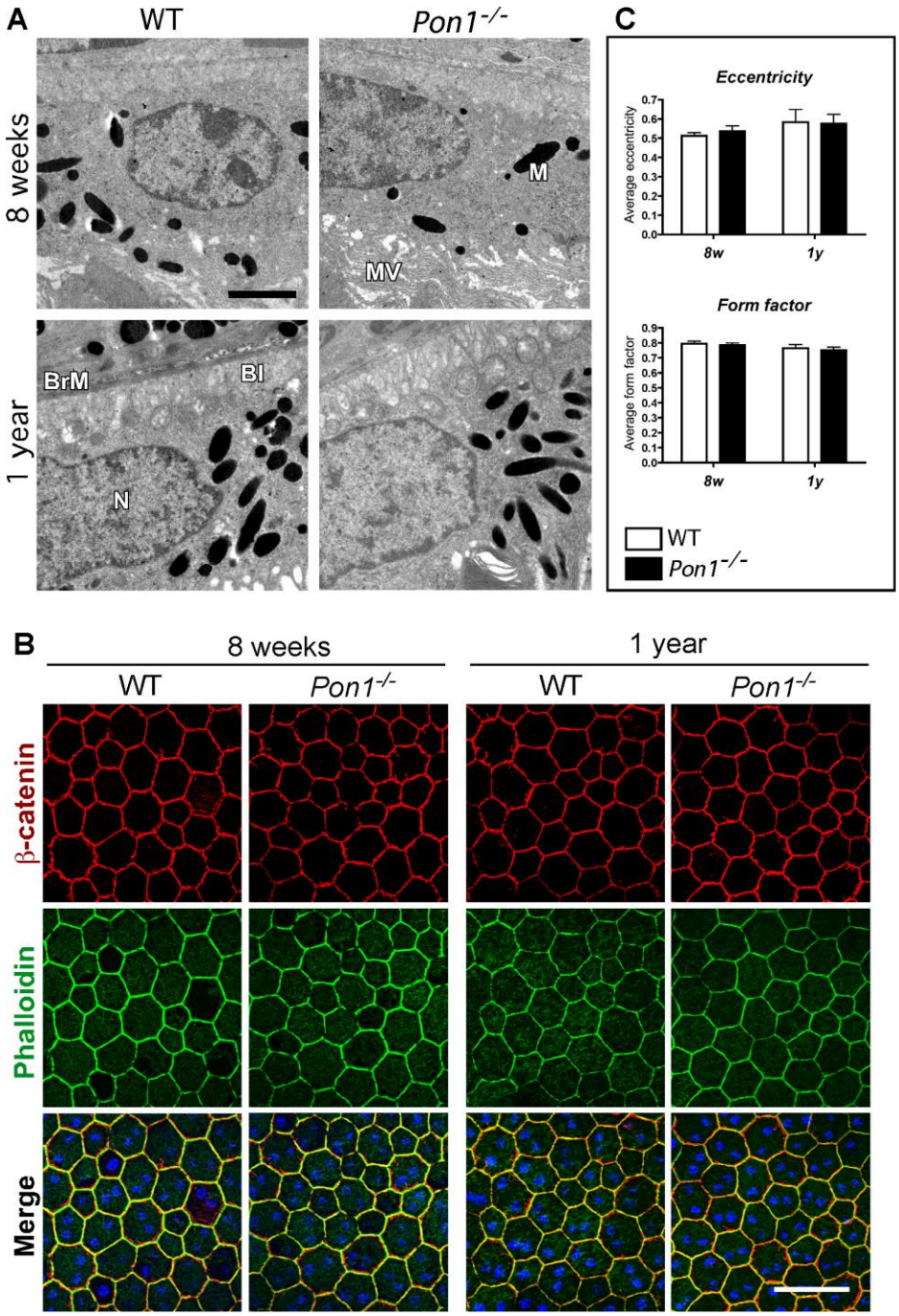

Figure 3. Lack of PON1 does not affect RPE morphology

The RPE was analyzed in *Pon1*$^{-/-}$ and control (WT) mice at 8 weeks (8w) and 1 year (1y) of age. **(A)** Transmission electron micrographs of the RPE and adjacent tissues. Shown are representative sections of N=3 for each panel. N, nucleus; BrM, Bruch's membrane; BI, basal infoldings; MV, apical microvilli; M, melanosomes. Scale bar: 2 μm. **(B)** RPE flat mounts immunostained for β-catenin (red) and phalloidin (green). Nuclear staining (Hoechst) is visible in blue. Shown are representative microphotographs of N=3 for each panel. Scale bar: 50 μm. **(C)** Morphometric analysis of RPE cells. Shown are mean values ± SD of at least N=700 RPE cells examined per group. Two-way ANOVA revealed no significant differences in RPE cell shape between WT and *Pon1*$^{-/-}$ mice at 8w and 1y of age ($p>0.05$).

Gene expression in *Pon1*$^{-/-}$ mice

To reveal whether the lack of PON1 influences expression of related genes or of genes encoding known PON1 interaction partners, we analyzed gene expression in retina and eyecup at 8 weeks and 1 year of age. Similar to the LCM data (Fig. 1), expression of *Pon1* was lower in the neuronal retina compared to that in the eyecup (Fig. 4). Cross-contamination between RPE and neuronal retina was minimal as shown by the relative expression of *Mct3* (RPE) and *Gnat1* (retina) in both isolated compartments (Supplementary Table 1).

In accordance with the LCM experiment, we found significant up-regulation of *Pon1* mRNA expression in the retina of 8 week old *Pon1*$^{-/-}$ mice and down-regulation in the eyecup. Since lack of the anti-oxidative PON1 protein may influence the oxidative balance in a tissue, expression of other anti-oxidative genes may be affected. However, both other members of the paraoxonase family (*Pon2* and *Pon3*), the two superoxide dismutases (*Sod1* and *Sod2*), as well as heme oxygenase 1 (*Hmox1*) were similarly expressed in control and *Pon1*$^{-/-}$ mice (Fig. 4). Remarkably, we detected an age-related moderate decrease in the expression of *Sod1*, *Sod2*, *Pon3* (retina and eyecup), *Pon2* (retina), *Pon1* and *Hmox1* (eyecup) independently of the *Pon1* genotype (Fig. 4 and Supplementary Table 1).

Previous studies showed that the role of PON1 in HDL transport and function involves interaction with partner proteins, such as scavenger receptor class B (SCARB1, also known as SR-BI) and ATP-binding cassette transporter (ABCA1). Whereas SCARB1 facilitates acquisition of PON1 secreted from hepatocytes (James et al., 2010), interaction between PON1 and ABCA1 transporter enhances HDL-mediated cholesterol efflux from macrophages (Rosenblat et al., 2005). Both SCARB1 and ABCA1 were previously shown to be involved in lipid efflux and reverse cholesterol transport in retina and RPE (Duncan et al., 2009), and this function might depend on interaction with PON1. Nevertheless, expression of *Scarb1* was similar in control and *Pon1*$^{-/-}$ mice at either age. The expression of *Abca1* was also similar in old control and knockout mice, whereas expression in young *Pon1*$^{-/-}$ mice was variable in different sets of animals (see also Fig. 5), suggesting the influence of other, yet unknown factors. Further studies are required to investigate a potential functional connection between *Pon1* and *Abca1* in the retina.

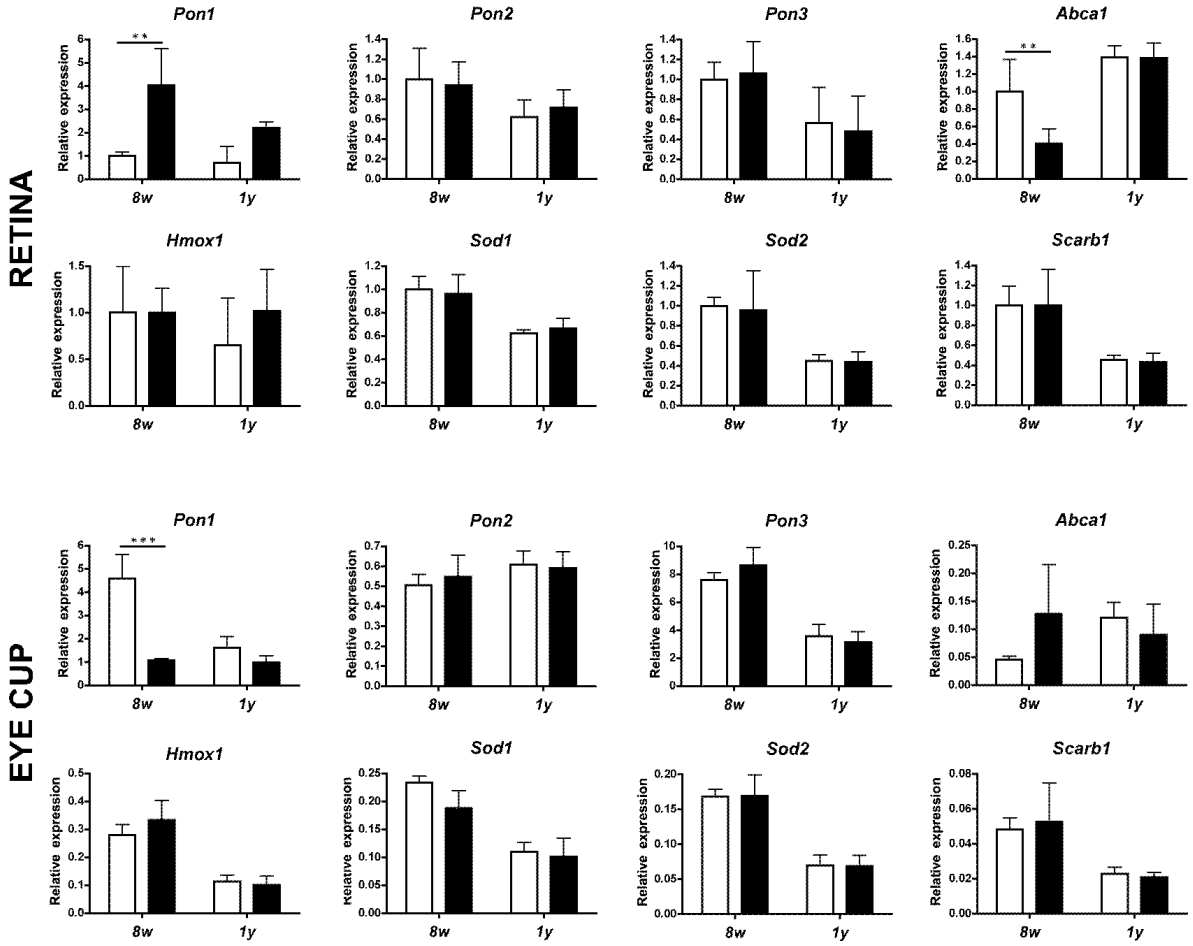

Figure 4. Expression of PON1-related genes

Expression of genes related to PON1 function was determined by semi-quantitative real-time PCR in retinas (upper panels) and eyecups (lower panels) of wild type (white bars) and *Pon1*$^{-/-}$ mice (black bars) at 8 weeks (8w) and 1 year (1y) of age as indicated. Shown are mean values ± SD of N=3. Values were normalized to *β-actin*, and levels in WT mice at 8w were set to 1. Two-way ANOVA with Bonferroni post-hoc analysis was used to test statistical significance. A p-value of less than 0.05 was considered significant; **p<0.01; ***p<0.001. Shown are statistics for the comparison of expression levels in wt and *Pon1*$^{-/-}$ mice at 8w or 1y of age. See supplementary Table 1 for statistical analysis of age-dependent expression in wt and *Pon1*$^{-/-}$ mice.

Alterations of phospholipid composition in retina/eyecup of *Pon1*$^{-/-}$ mice

The retina contains very high levels of polyunsaturated fatty acids (PUFAs). The majority of retinal PUFAs is esterified to phospholipids (PLs), which build up the membranous disks of photoreceptor outer segments (Giusto et al., 2000). Due to their molecular structure and constant exposure to a photo-oxidative environment (Handa, 2012; Khandhadia and Lotery, 2010), retinal PLs are particularly prone to oxidative modifications. Based on the fact that PON1 can reduce lipid peroxidation in LDL and cell membranes (Ahmed et al., 2003; Mackness et al., 1991), we

hypothesized that PON1 might have a similar effect on retinal PLs, and thus affect their composition. To test this assumption, we employed a combination of liquid chromatography (LC) and mass spectrometry (MS) for the identification and quantification of retina/eyecup PLs from wild type and *Pon1*$^{-/-}$ mice.

The overall phospholipid profile was similar in the retina/eyecup samples of *wt* and *Pon1*$^{-/-}$ mice at the age of 8 weeks. The most abundant PLs were phosphatidylcholines (PC) and phosphatidylethanolamines (PE) (Table 2). The most abundant PE species was PE 40:6, which possibly contained polyunsaturated $C_{22:6n-3}$ docosahexaenoic (DHA) fatty acid at the sn-1 or sn-2 position. PC 40:6 was the third most abundant PC species after PC 32:0 and PC 34:1. Interestingly, highly unsaturated PC 44:12 and PE 44:12 species were identified in both mouse strains. They probably represent PC and PE lipids that were esterified with two molecules of DHA at the sn-1 and sn-2 position. The third abundant lipid class was sphingomyelin (SM). Among lysophosphatidylcholines (LPC), the most abundant species contained a DHA fatty acid (LPC 22:6). Ceramides/hexosylceramides (Cer/HexCer), phosphatidylglycerols (PG) and phosphatidic acids (PA) were found at very low concentrations, therefore we report only total concentrations of these three lipid classes.

The major difference between 8-week old *Pon1*$^{-/-}$ and *wt* mice was seen for total LPC ($p=0.001$) and in particular for LPC 22:6 species ($p=0.001$), which were detected at significantly reduced levels in *Pon1*$^{-/-}$ mice (Table 2). These differences remained significant after Bonferroni correction for multiple testing. Analysis of PLs in wild type retinas and eyecups, which were isolated separately, revealed that LPC 22:6 was the most abundant LPC species in the retina, whereas it was almost absent in the eyecup (data not shown). Some polyunsaturated and mono-unsaturated PCs as well as polyunsaturated PEs were also decreased in *Pon1*$^{-/-}$ mice ($p<0.05$). However, these differences missed significance after Bonferroni correction (Table 2). Other PL species were also not significantly different in *Pon1*$^{-/-}$ as compared to controls.

Since aging is a major risk factor for the development of AMD, and lipid metabolism is known to be involved in the etiology of this disease, we characterized the PL profiles of 1-year old wild type and *Pon1*$^{-/-}$ mice. In contrast to young adults at 8 weeks of age, levels of total LPC and LPC 22:6 species in 1-year old mice did not differ between the two mice strains (Table 3). Interestingly, age-related changes in the PLs profiles showed different trends in wild type and *Pon1*$^{-/-}$ mice. While control animals showed a trend for decreased levels of total LPC and LPC 22:6 with age, *Pon1*$^{-/-}$ mice revealed almost no age-related changes in the content of those PLs (Table 3).

Table 2. Phospholipid species in the retina/eyecup samples from control (WT) and *Pon1*$^{-/-}$ mice at 8 weeks (8w) of age (page 77).

Phospholipid (PL) analysis was performed by LC-MS. Content of PL classes and species is shown as nmol of PL per one mg of retina and eyecup proteins. Total phospholipids represent sum of molecular species of a given class and are presented for ceramides/hexosylceramides (Cer/HexCer), phosphatidylglycerols (PG) and phospho-tungstic acids (PA). Species pattern is displayed for phosphatidylcholines (PC), phosphatidylethanolamines (PE), sphingomyelins (SM) and lysophosphatidylcholines (LPC). Data values are displayed as median with range. N=10 for both genotypes. Statistical significance was determined by the Man-Whitney U test. After Bonferroni correction a p-value of 0.001 corresponds to a significance level of 0.05. Statistically significant results are indicated in bold. An assignment of PL species includes number of carbon atoms and double bounds in both acyl chains (for example, PC 34:1 consist of 34 carbon atoms and one double bond and can correspond to the following species PC 16:0/18:1 or PC 18:0/16:1, etc.). Sphingomyelin assignment comprises the number of carbon atoms and double bonds in both sphingoid base and in N-linked fatty acid.

Table 2. Phospholipid species in the retina/eyecup samples from control (WT) and *Pon1*$^{-/-}$ mice at 8 weeks (8w) of age.

PLs	Content of PL in nmol / mg of retina and eyecup proteins		Mann-Whitney Test, p values
	WT 8w Median(min;max)	*Pon1*$^{-/-}$ 8w Median(min;max)	WT 8w vs *Pon1*$^{-/-}$ 8w
Total PC	143.5(92;170.5)	120.5(54.1;140.3)	0.023
Total SM	20(7.2;26.8)	17(7.2;23.7)	0.174
Total LPC	**5.2(2.1;5.9)**	**2.5(1.2;4.1)**	**0.001**
Total PE	26.5(16.2;29.8)	21.9(11.4;24.6)	0.013
Total Cer/HexCer	5.6(2.7;7.6)	6.1(2.6;9.4)	0.545
Total PG	1.2(0.2;1.9)	0.9(0.3;1.5)	0.253
Total PA	2.8(2.3;3.1)	2.9(2.5;3.2)	0.326
PC 32:0	27.3(15.5;31.5)	23.3(10.9;27.7)	0.070
PC 32:1	2.7(2.1;3.5)	2.1(1.1;2.6)	0.010
PC 34:0	6.4(3.7;8)	5.9(3;7.6)	0.257
PC 34:1	27.8(18.8;33.4)	23.4(10.9;28.9)	0.016
PC 34:2	4.7(3;5.9)	4.2(1.7;4.6)	0.096
PC 36:1	14.1(8;16.2)	11.1(5.3;13.3)	0.019
PC 36:2	5.6(4.3;7.2)	4.7(2.2;5.8)	0.023
PC 36:3	1.5(1;2)	1.3(0.4;1.7)	0.070
PC 36:4	6.4(4.1;7.2)	5.4(2.6;6.3)	0.059
PC 38:4	7.9(4.7;10.4)	6.6(2.8;8.3)	0.013
PC 38:5	2.5(1.6;2.8)	2.4(0.9;2.9)	0.450
PC 38:6	12.1(7.6;15.1)	9.5(4;12.3)	0.013
PC 40:5	1.7(0.7;2.3)	1.3(0.8;1.9)	0.023
PC 40:6	17.7(12.2;20.4)	13.7(5.7;15.6)	0.004
PC 40:7	1.4(1.2;2.4)	1.1(0.5;1.5)	0.008
PC 44:12	4.9(3.7;8.3)	3.9(1.4;5.7)	0.016
SM34:1	5.8(2.3;7.6)	5.2(2.4;7.2)	0.174
SM36:1	4.7(1.9;6.4)	3.9(1.9;5.5)	0.199
SM38:1	2.4(0.8;3.3)	2.2(0.7;2.9)	0.199
SM40:1	2.2(0.8;3.2)	2(0.8;2.9)	0.199
SM42:1	2.1(0.6;2.7)	1.7(0.5;2.6)	0.131
SM42:2	2.2(0.8;3.4)	1.8(0.7;2.7)	0.257
SM42:3	0.4(0.1;0.5)	0.3(0.1;0.4)	0.059
LPC 18:0	0.8(0.6;0.8)	0.7(0.4;0.9)	0.131
LPC 18:1	1.7(0.6;2)	0.7(0.4;1.2)	0.002
LPC 22:6	**2.8(0.9;3.1)**	**1.2(0.4;2)**	**0.001**
PE 34:1	0.8(0.6;0.9)	0.7(0.4;0.9)	0.290
PE 36:0	0.3(0.2;0.4)	0.3(0.2;0.4)	0.880
PE 36:2	0.9(0.8;1.2)	0.9(0.7;1.1)	0.151
PE 36:4	0.6(0.4;0.8)	0.6(0.4;0.8)	0.650
PE 38:4	3.3(1.8;3.7)	2.6(1.5;3.1)	0.019
PE 38:6	5(2.8;6.3)	4.2(2;5.1)	0.008
PE 40:6	12.2(7.6;13.8)	10.3(5.1;11.4)	0.013
PE 44:12	2.9(1.9;3.8)	2.3(1.1;2.7)	0.013

PLs	Median (min;max) [nmol/mg]						Mann-Whitney Test, p values					
	WT 8w	*Pon1*$^{-/-}$ 8w	WT 1y	*Pon1*$^{-/-}$ 1y	WT LD	*Pon1*$^{-/-}$ LD	WT 8w vs WT 1y	*Pon1*$^{-/-}$ 8w vs Pon1$^{-/-}$ 1y	WT 1y vs Pon1$^{-/-}$ 1y	WT 8w vs WT LD	*Pon1*$^{-/-}$ 8w vs Pon1$^{-/-}$ LD	WT LD vs Pon1$^{-/-}$ LD
Total LPC	5.2(2.1;5.9)	2.5(1.2;4.1)	1.9(1.5;6.8)	3.1(1.3;5.3)	5(2.2;6.5)	3.7(3;8.6)	0.086	0.745	1.000	0.940	0.002	0.059
LPC 22:6	2.8(0.9;3.1)	1.2(0.4;2)	0.7(0.5;3.8)	1.3(0.4;2.5)	2.6(1.3;3.2)	1.7(1.4;4.8)	0.066	0.745	1.000	1.000	0.005	0.049

Table 3. Levels of total LPCs and LPC 22:6 in the retina/eyecup samples from 8-week and 1-year old wild type (WT) and *Pon1*$^{-/-}$ mice, and from 8-week old mice exposed to the light.

Phospholipid (PL) analysis was performed by LC-MS. PL classes and species are shown as nmol of PL per one mg of retina and eyecup proteins. Displayed are median values with range. N=5 for WT (1y), N=6 for *Pon1*$^{-/-}$ (1y), N=10 for WT (LD), N=10 for *Pon1*$^{-/-}$ (LD). Statistical significance was determined by the Man-Whitney U test. After Bonferroni correction a p-value of 0.001 corresponds to a significance level of 0.05. An assignment of PL species includes numbers of carbon atoms and double bonds in both acyl chains. Total LPC represent sum of all species of a lysophosphatidylcholines class. Samples marked by asterisk * were analyzed in a separate LC-MS run.

PON1 does not influence photoreceptor degeneration or RPE survival after light exposure

To evaluate whether the lack of the anti-oxidative PON1 protein influences cell survival under oxidative stress conditions, we exposed wild type and *Pon1*$^{-/-}$ mice to high levels of white light (Wenzel et al., 2005). At 5 days after exposure, many photoreceptors were lost and large numbers of pyknotic nuclei were detected in the ONL of wild type and *Pon1*$^{-/-}$ mice (Fig. 5A). We also observed similar levels of subretinal macrophages in *Pon1*$^{-/-}$ and wild type mice, although previous reports suggested inhibitory effects of PON1 on monocyte transmigration (Shih et al., 1998). At 10 days after light exposure the photoreceptor layer was further degenerated, with only few pyknotic nuclei left in the ONL of both *Pon1*$^{-/-}$ and wild type mice. Additionally, some RPE cells displayed severe morphological changes in both mouse lines (Fig. 5B). Enlarged RPE cells with increased cytoplasmic β-catenin localization, as well as a global increase in cytoplasmic phalloidin (F-actin) staining were observed. The number of RPE cells before and after light exposure was comparable in wild type and *Pon1*$^{-/-}$ mice (data not shown).

Acute LD not only induces retinal degeneration, but also activates survival pathways to protect retinal cells from cell death. Leukemia inhibitory factor (LIF) is a key cytokine regulating an endogenous rescue pathway that involves activation of the Janus kinase signal transducer and activator of transcription (Jak-STAT) signaling pathway, and expression of protective factors like endothelin-2 (*Edn2*) and fibroblast growth factor-2 (*Fgf2*) (Joly et al., 2008; Samardzija et al., 2006). In line with the comparable extent of tissue damage (Fig. 5A, B), light exposure caused a similar expression pattern of these genes in retinas of wild type and *Pon1*$^{-/-}$ mice, even though *Edn2* and *Fgf2* were significantly stronger induced in mice lacking PON1 (Fig. 5C). No differences between the two genotypes were detected in eyecups. Remarkably, upon exposure to the light *Pon2*, *Sod1* and *Sod2* expression was reduced in the retina, but not in the eyecup, while *Hmox1* was up-regulated in both tissues (Fig. 5C; supplementary Table 2). Additionally, expression of *Socs3* was strongly up-regulated in the eyecup, suggesting that JAK/STAT signaling was also induced in the RPE. Whether this was a consequence of LIF signaling or whether other factors led to such activation needs to be established.

Untreated *Pon1*$^{-/-}$ mice had decreased levels of total LPCs and in particular of LPC 22:6 (see above). Since PON1 is an anti-oxidative enzyme, we tested whether its lack might impact the PL composition under oxidative stress induced by light exposure. At 2 hours after light exposure, PL profiles were comparable in wild type and in *Pon1*$^{-/-}$ retina/eyecups and showed increased levels of PE 34:1, PE 36:0 and PE 36:4 in both strains (Supplementary Table 3). In contrast, light exposure caused an increase in total LPC and LPC 22:6 in *Pon1*$^{-/-}$ but not in wild type mice (Table 3).

Although these differences did not remain statistically significant after Bonferroni correction, there was a clear trend for increased LPC in *Pon1*$^{-/-}$ compared to wild type mice. This suggests that PON1 protects from a raise of total LPC, especially of LPC 22:6 in light-induced oxidative stress.

Figure 5. PON1 does not protect against damage by acute light exposure (p. 81).

(A) Representative light micrographs of retinas of 8-week old control (WT) and *Pon1*$^{-/-}$ mice at 5 and 10 days after light exposure. Control mice (dark control, DC) were reared in normal cyclic light conditions (12 hours dark; 12 hours light) and not exposed to light. Arrows: pyknotic nuclei indicating photoreceptor cell death. Arrowheads: macrophages in the subretinal space. Shown are representative sections of N=3. Scale bar: 50 μm.

(B) Immunostaining of RPE flat mounts from 8-week old WT and *Pon1*$^{-/-}$ dark control (DC) mice and at 10 days after light exposure (10 d). Red: β-catenin; green: phalloidin; arrowheads: diffuse β-catenin staining in RPE cells of light exposed mice. Scale bar: 50 μm.

(C) Gene expression in retinas (upper panels) and eyecups (lower panels) of 8-week old WT (white bars) and *Pon1*$^{-/-}$ (black bars) mice at 12 hours after light exposure (12 h) or in dark controls (DC). Values were normalized to *β-actin* and expressed relative to the levels in the retina of unexposed wt animals, which were set to 1. Shown are mean values ± SD of N=3. Two-way ANOVA with Bonferroni post-hoc analysis was used to test significance. A p-value of less than 0.05 was considered significant; *p<0.05; **p<0.01; ***p<0.001. Shown are significantly different expression levels between WT and *Pon1*$^{-/-}$ mice in DC or light exposed mice. See supplementary Table 2 for statistical analysis of differences in gene expression between DC and light exposed WT and DC and light exposed *Pon1*$^{-/-}$ mice.

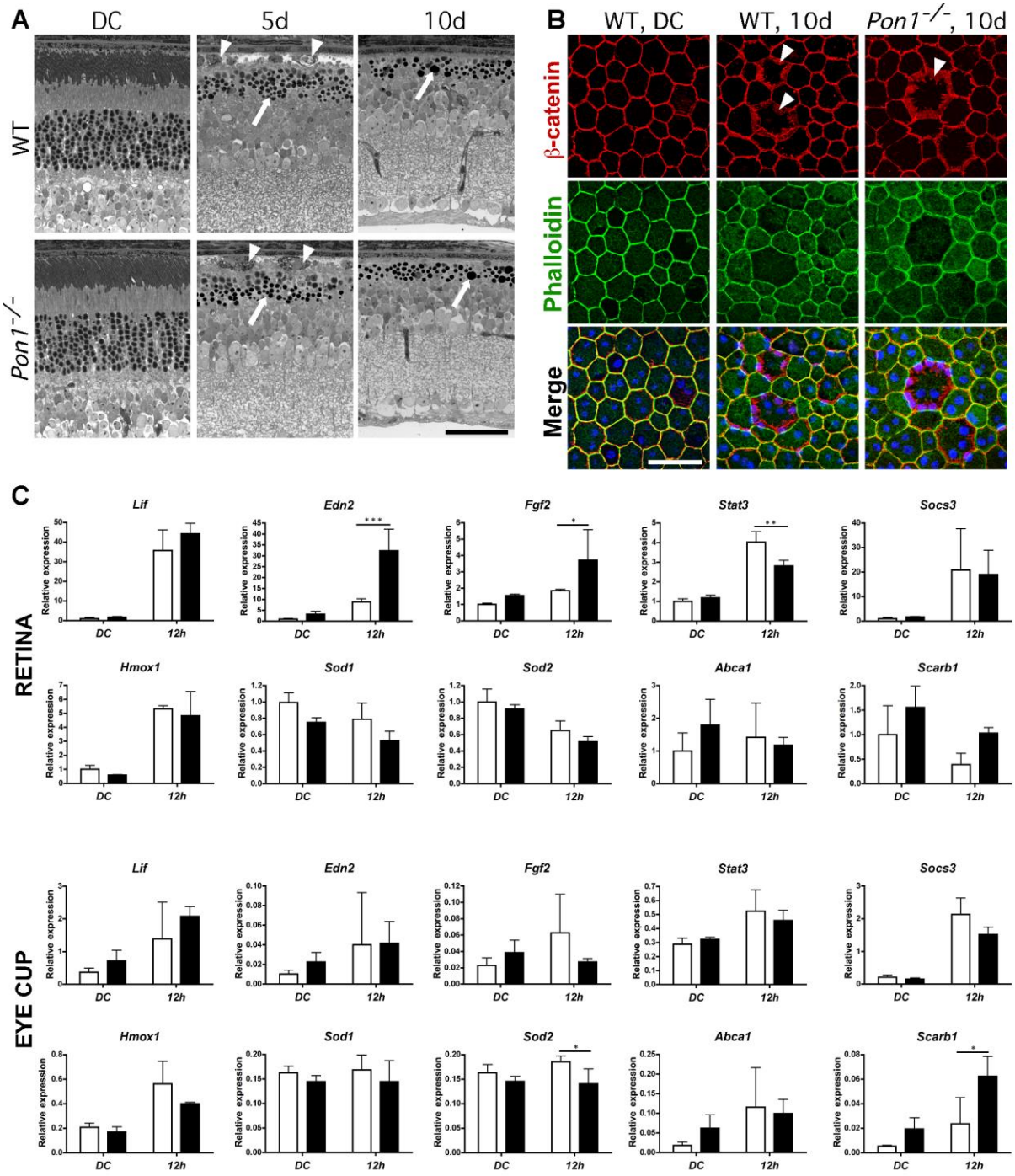
A
DC
5d
10d
WT
Pon1-/-
B
WT, DC
WT, 10d
Pon1-/-, 10d
β-catenin
Phalloidin
Merge
C
RETINA
EYE CUP
Lif
Edn2
Fgf2
Stat3
Socs3
Hmox1
Sod1
Sod2
Abca1
Scarb1
Relative expression
DC
12h

DISCUSSION

PON1 in the normal retina

Since PON1 has been implicated in AMD (Baird et al., 2004; Baskol et al., 2006; Ikeda et al., 2001; Oczos et al., 2013), we assessed whether lack of PON1 would alter retinal physiology in young and old *Pon1*$^{-/-}$ mice. We showed that PON1 is not essential for development and maintenance of a normal retinal structure, vasculature, or function. Similarly, RPE cells were morphologically indistinguishable between wild type and *Pon1*$^{-/-}$ mice, even though the RPE has the highest level of *Pon1* expression. Although PON1 has anti-oxidative activity, no signs of oxidative damage were detected and no compensatory increase in the expression of other anti-oxidative enzymes was observed. Lack of PON1 did also not influence the susceptibility of retina and RPE to light damage.

However, retina/eyecup samples of *Pon1*$^{-/-}$ mice showed decreased levels of LPCs in general and of LPC 22:6 in particular. LPCs are molecular species produced by the hydrolysis of PCs through enzymes of the phospholipase A2 (PLA2) superfamily. Previous studies have shown that PON1 has a PLA2-like activity leading to the formation and release of LPCs from macrophages (Rosenblat et al., 2006; Rosenblat et al., 2005). In wild type mice, PON1 may thus increase LPC production and modulate the content of phospholipids in the retina/RPE. In analogy to the stimulatory effect of PON1-generated LPCs on cholesterol efflux from macrophages (Hara et al., 1997; Rosenblat et al., 2006), LPCs might stimulate reverse lipid transport from RPE regulating lipid content in this cell layer (Ishida et al., 2006).

Since PON1 is a secreted protein that retains its hydrophobic signal peptide (James and Deakin, 2004), it may remain in the membrane of PON1 producing cells, or may reach membranes of neighboring cells. Thus, PON1 synthesized in the RPE might affect photoreceptors as well. The immunohistochemical detection of PON1 in the region of photoreceptor inner segments (and other nonnucleated areas of the retina) (Marsillach et al., 2008) and our observation that LPC 22:6, which was reduced in *Pon1*$^{-/-}$ mice, was very abundant in the retina but almost absent from the eyecup (data not shown) supports a role for a PLA2-like activity of PON1 in the neuronal retina.

We detected a general age-related decrease in the expression of anti-oxidative genes in retinas and especially eyecups of wild type mice. *Pon1* was among the affected genes and down-regulated about 65%. Remarkably, also levels of total LPCs and of LPC 22:6 were decreased in 1-year old wild type mice, by 63% and 75%, respectively (Table 3). This suggests a correlation between *Pon1* expression and LPC levels and indicates that reduced expression of *Pon1* resulted in reduced

PON1-related PLA2 activity and thus in a diminished PON1-mediated hydrolysis of PCs. Furthermore, increased lipid peroxidation and glycation in the aged eyes might have additionally compromised PON1 activity as it has been observed in metabolic syndrome and type II diabetes in humans (Garin et al., 2005; Mackness et al., 2000a; Mastorikou et al., 2008).

PON1 in the light-exposed retina

Even though PON1 has anti-oxidative and anti-inflammatory activities, *Pon1*$^{-/-}$ and wild type mice were similarly affected by light exposure: photoreceptors were equally susceptible to light induced degeneration; changes in RPE morphology after light exposure were comparable; expression of genes involved in anti-oxidative defense or the LIF-controlled cell survival pathway was similar; and levels of PE 34:1, PE 36:0 and PE 36:4 increased to the same extent. However, levels of total LPC and LPC 22:6 increased only in *Pon1*$^{-/-}$ but not in wild type mice after light exposure suggesting that presence of PON1 prevents generation of LPC upon light exposure. Whether this is a direct effect of PON1 or whether a differential activation of phospholipases A2 in the two mouse strains influences LPC production remains to be explored.

Several possible mechanisms may explain the lack of striking differences in response to light damage between *Pon1*$^{-/-}$ and wild type mice. Previous studies showed that PON1 may be inactivated by its own substrates such as oxidized lipids (Aviram et al., 1999). Thus, generation of a large amount of oxidized molecules by light exposure may substantially reduce PON1 activity in wild type mice. Alternatively, PON1 may "neutralize" only a subset of oxidized species produced in LD, such as oxidized PUFAs (Draganov et al., 2005). Other light-induced oxidation products may remain toxic and participate in the induction of cell death. It may also be of importance that PON1 is a secreted protein (James and Deakin, 2004) that may not be able to detoxify intracellular molecules that have been generated by light exposure and that are involved in the degenerative process.

PON1 in AMD

AMD is a complex, multifactorial disease. Most existing mouse models for AMD combine advanced age, which is the major risk factor to develop AMD, with genetic defects in key genes involved in AMD pathogenesis. Considering the complex nature of the disease, it may not be surprising that some models require the combination of more than two environmental or genetic risk factors to cause a pathological phenotype. An excellent example is a murine model that combines three known AMD risk factors: advanced age, high fat and cholesterol-rich diet, and mutations in *ApoE* (Malek et al., 2005). Importantly, neither age nor the diet alone

was sufficient to elicit changes that mimic human AMD pathology in the transgenic *ApoE4* mice.

The absence of an AMD-like phenotype in eyes of aged *Pon1*$^{-/-}$ mice suggests that even long-lasting absence of PON1 is not sufficient to cause detectable pathological changes like thickening of Bruch's membrane or sub-RPE deposits typical for AMD. Noteworthy, despite the well-established anti-atherogenic properties of PON1, *Pon1*$^{-/-}$ mice developed significantly larger atherosclerotic lesions than wild type controls only when raised on a high-fat/high-cholesterol but not on a regular diet (Rozenberg et al., 2003; Shih et al., 1998). This suggests that additional factors/stimuli may be needed to provoke phenotypes of complex diseases like atherosclerosis or AMD in *Pon1*$^{-/-}$ mice. This hypothesis is also supported by the observation that pathological processes in *ApoE*$^{-/-}$ mice were slowed in the presence of a human PON1 transgene (Tward et al., 2002), but accelerated by PON1 deficiency (Rozenberg et al., 2003; Shih et al., 2000).

These studies provide evidence that a co-existing chronic metabolic burden may be needed to reveal the role of PON1 in development and or progression of a complex disease. A long-lasting exposure to low levels of light (in contrast to the short-term exposure to high light levels used in present study), a high-fat diet or the inclusion of the *ApoE*-null genetic background might provide such an additional chronic stress to provoke AMD-like lesions in *Pon1*$^{-/-}$ mice.

We postulate that PON1 could be involved in AMD as a modulatory protein and that direct or indirect interactions with additional factors may influence its contribution to disease development and/or progression. Presence or absence of such factors may determine the association of PON1 with AMD in particular populations and may help to explain contradictory results regarding the implication of PON1 in AMD pathology. Nevertheless, the controversy on the role of PON1 in AMD still remains and there is a clear need for further studies to identify the precise function of PON1 in ocular tissues such as RPE and neuronal retina. Knowledge of these functions seems a prerequisite to understand how the anti-oxidative and anti-inflammatory properties of PON1 may influence AMD.

ACKNOWLEDGEMENTS

The authors thank Christel Beck, Andrea Gubler and Coni Imsand for excellent technical assistance, Meliana Riwanto for performing paraoxonase activity assays, and Marijana Samardzija for helpful discussions.

SUPPLEMENTARY MATERIAL

Supplementary Methods

Analysis of retina and eyecup lipidome: LC-MS instrumentation and chromatographic conditions

The liquid chromatography-mass spectrometry (LC-MS) method combining HPLC separation on normal phase column with multiple parent-ion or neutral loss scans on a triple quadrupole mass spectrometer is capable of the analysis of six different phospholipid (PL) classes: phosphatidylcholines (PC), sphingomyelins (SM), phosphatidylglycerols (PG), phosphatidyl-ethanolamines (PE), phosphatidic acids (PA) and ceramide/hexosylceramides (Cer/HexCer).

For PL analysis, 40 μg of total proteins from tissue homogenates were supplemented with 200 ng of internal standards (IS) and extracted by using the method by Bligh and Dyer (Bligh and Dyer, 1959). The mixture of ISs contained non-naturally occurring lipids: PG 17:0/17:0, PA 14:0/14:0, PE 14:0/14:0, PC14:0/14:0, PC24:0/24:0, LPC 17:0, SM d18:1/12:0 and Cer d18:1/17:0 (Avanti Polar Lipids, Alabaster, AL, USA).

For an adequate quantification, each series of measurements included calibration solutions of seven PL standards at six different concentrations in the range from 0.625 μg/ml to 12 μg/ml or from 0.8 μmol/l to 24.2 μmol/l, which were spiked with 200 ng of IS. Calibration solutions were composed of commercially available standards of PC 16:0/18:2, SM d18:1/16:0, LPC 16:0, PE 18:0/18:0, Cer d18:1/14:0, PG 16:0/16:16 and PA 14:0/14:0 (Avanti Polar Lipids, Alabaster, AL, USA). Two quality controls of a low and of a high concentration (2 μg/ml and 6 μg/ml for PC 16:0/18:2 and SM d18:1/16:0 versus 4 μg/ml and 12 μg/ml for LPC 16:0, PE 18:0/18:0, Cer d18:1/14:0, PG 16:0/16:16 and PA 14:0/14:0) were evaluated at the beginning and at the end of each samples series. Carry-over control was done by analyzing blank samples. The samples were prepared by adding methanol (DB) and IS (B) to 20 μl of water.

At first retina/eyecup samples were mixed with 375 μl of methanol/ chloroform (2:1, v/v) and vortexed. After that, 100 μl of water and 125 μl of chloroform were added. The mixture was shaken for 15 min and centrifuged at 16100×g for 5 min at 25°C. The lower phase was collected and an additional 250 μl of chloroform was added. The mixture was agitated for 15 min and centrifuged at 16100×g for 5 min at 25°C. All lower phases were combined and evaporated to dryness under a stream of nitrogen. The dried material was reconstituted in 200 μl of a mixture of mobile phases A (80%; hexane/isopropanol/water (70:30:2, v/v) containing 15 mM ammonium formate) and B (20%; isopropanol/water (50:2, v/v)

containing 15 mM ammonium formate). 10 µl of sample was injected into the LC-MS system for PL analysis.

The LC-MS system contained of a Rheos 2200 HPLC pump (Flux Instruments, Reinach, Switzerland), an HTC PAL autosampler (CTC Analytics, Zwingen, Switzerland) and a TSQ Quantum Access triple quadrupole mass analyzer (Thermo Fisher Scientific, Waltham, MA, USA). Separation of PLs was achieved by using a diol silica-based column (QS Uptisphere 6 OH, 150 × 2.1 mm, 5 µm) from Interchim (Montluçon, France). Gradient elution started with 80% mobile phase A and 20% of B and lasted for 7.0 min. Mobile phase B was increased to 40% within 1.0 min and kept constant for 2 min then mobile phase B was increased to 60% within 1 min and kept constant for 12 min. After that the column was re-equilibrated with 80% mobile phase A and 20% of B for 5.0 min. The solvent flow was 0.35 ml/min and the column was maintained at 30°C.

The MS parameters were set as follows: 4500 V spray voltage, skimmer voltage was constantly changing in range from 2 to 14 V depending on scan mode, 250°C capillary temperature, and 10 and 6 (arbitrary units) sheath and auxiliary N_2 gas, respectively. Tube lens voltages were tuned using a standard mixture of LPC 17:0, PC 14:0/14:0, PC 20:0/20:0 and PC 24:0/24:0, covering a wide molecular mass range. Both Q1 and Q3 resolution were set at 0.7 peak-width (at full-width half-maximum). Molecular masses provided by a neutral loss and precursor scans were used to selectively detect specific phospholipids. Multiple parent-ion and neutral loss scan events were performed in positive ionization mode by using 0.7 mTorr collision gas. A neutral loss of masses *m/z* 115 and 189 from $[M+NH_4]^+$ ions were used for analysis of PA and PG lipids, respectively. A precursor ion scan of m/z 184 specific for phosphocholine containing lipids was used for PC, SM and LPC. A neutral loss scan of m/z 141 was used for PE and a precursor scanning of m/z 264 was applied for screening of Cer and HexCer. Acquired data was analyzed using the Xcalibur software (version 2.0.6) from Thermo Scientific.

The identification of the molecular species was based on the molecular mass provided by MS, the structure of the head group was determined from the type of MS/MS scanning. From each scan segment, a mass-peak list containing parent-ion masses (*m/z*) and their intensities was generated by Xcalibur. The mass-peak list was entered into the lipid mass spectrum analysis software LIMSA (The Somerharju Lipid Group, Helsinki, Finland; Haimi et al., 2006) and lipid species were identified by using a mass tolerance of ±0.7 Da and list of theoretical PL species library prepared in our laboratory. Corrections were applied to the data for isotopic overlap in the species with mass difference Δ *m/z* of two Da. As a result all lipids were assigned to the individual lipid class and species with a defined total number of carbon atoms and double bounds in *O*-linked fatty acids. Identification of

SM resulted in the total number of carbon atoms in sphingoid base and N-linked fatty acid. Quantification was achieved by using the linear regression of the calibration curve of the related lipid class.

Lower limit of quantification (LLOQ) was defined as concentration of the first calibrator in standard curve. LLOQ was set at concentration levels of 0.8 μmol/L for PC, 0.9 μmol/L for SM, 2.45 μmol/L for Cer, 2.5 μmol/L for LPC, 2.0 μmol/L for PA, 1.7 μmol/L and 2.0 μmol/L for PG and PE, respectively. Intra- and inter-day accuracy (n=5) of LLOQ indicating difference between the mean result and expected value was within 20% of the expected value. Furthermore, intra- and inter-day precision (n=5) of the LLOQ measurements resulted in CV% better than 20%. Intra- and inter-day study (n=5) of quality controls at a low and a high concentration resulted in accuracy and precision within 15% for all lipid species. Extraction recovery of ISs from plasma varied from highest of 103% for PC to the lowest 68% for PA.

Supplementary Tables

Supplementary Table S1. Expression of PON1-related genes in retinas and eyecups of *Pon1*$^{-/-}$ and wild type (WT) mice at 8 weeks (8w) and one year (1y) of age (page 89).

Expression of genes related to PON1 function was determined by semi-quantitative real-time PCR. Shown are mean values ± SD of N=3. Values were normalized to *β-actin* and expressed relative to levels in the retina of WT mice at 8 weeks of age, which were set to 1. Two-way ANOVA with Bonferroni post-hoc analysis was used to test the statistical significance. A p-value of less than 0.05 was considered significant; ns, not significant. *Pon1*, paraoxonase 1; *Pon2*, paraoxonase 2; *Pon3*, paraoxonase 3; *Abca1*, ATP-binding cassette, sub-family A (ABC1), member 1; *Scarb1*, scavenger receptor class B, member 1; *Hmox1*, heme oxygenase 1; *Sod1*, superoxide dismutase 1; *Sod2*, superoxide dismutase 2, *Mct3*, monocarboxylate transporter, member 3 (marker for RPE); *Gnat1*, guanine nucleotide binding protein, alpha transducing activity polypeptide (marker for the neuronal retina).

		Mean ± SD				2-way ANOVA			
						WT vs. *Pon1*$^{-/-}$		8w vs. 1y	
	Gene	WT, 8w	*Pon1*$^{-/-}$, 8w	WT, 1y	*Pon1*$^{-/-}$, 1y	8w	1y	WT	*Pon1*$^{-/-}$
RETINA	***Pon1***	1 ± 0.16	4.04 ± 1.57	0.71 ± 0.7	2.21 ± 0.24	$p < 0.01$	ns	ns	ns
	Pon2	1 ± 0.31	0.94 ± 0.23	0.62 ± 0.17	0.72 ± 0.18	ns	ns	ns	ns
	Pon3	1 ± 0.18	1.06 ± 0.31	0.57 ± 0.36	0.48 ± 0.35	ns	ns	ns	ns
	Hmox1	1 ± 0.50	1 ± 0.26	0.65 ± 0.50	1.02 ± 0.44	ns	ns	ns	ns
	Sod1	1 ± 0.11	0.96 ± 0.16	0.62 ± 0.03	0.67 ± 0.09	ns	ns	$p < 0.01$	$p < 0.05$
	Sod2	1 ± 0.09	0.95 ± 0.40	0.45 ± 0.06	0.44 ± 0.1	ns	ns	$p < 0.05$	$p < 0.05$
	Scarb1	1 ± 0.19	1 ± 0.36	0.45 ± 0.05	0.44 ± 0.08	ns	ns	$p < 0.05$	$p < 0.05$
	Abca1	1 ± 0.18	0.4 ± 0.17	1.4 ± 0.13	1.39 ± 0.17	$p < 0.01$	ns	ns	$p < 0.001$
	Mct3	1 ± 0.75	5.1 ± 5.54	2.03 ± 2.12	0.38 ± 0.14	ns	ns	ns	ns
	Gnat1	1 ± 0.53	0.87 ± 0.32	1.74 ± 0.30	1.67 ± 0.5	ns	ns	ns	$p < 0.05$
EYECUP	***Pon1***	4.58 ± 1.04	1.08 ± 0.06	1.61 ± 0.47	0.98 ± 0.28	$p < 0.001$	ns	$p < 0.001$	ns
	Pon2	0.51 ± 0.05	0.55 ± 0.11	0.61 ± 0.07	0.59 ± 0.08	ns	ns	ns	ns
	Pon3	7.59 ± 0.52	8.64 ± 1.26	3.57 ± 0.85	3.15 ± 0.74	ns	ns	$p < 0.001$	$p < 0.001$
	Hmox1	0.28 ± 0.04	0.33 ± 0.07	0.11 ± 0.02	0.1 ± 0.03	ns	ns	$p < 0.01$	$p < 0.001$
	Sod1	0.23 ± 0.01	0.19 ± 0.03	0.11 ± 0.02	0.1 ± 0.03	ns	ns	$p < 0.001$	$p < 0.01$
	Sod2	0.17 ± 0.01	0.17 ± 0.03	0.07 ± 0.01	0.07 ± 0.02	ns	ns	$p < 0.001$	$p < 0.001$
	Scarb1	0.05 ± 0.01	0.05 ± 0.02	0.02 ± 0.00	0.02 ± 0.00	ns	ns	ns	$p < 0.05$
	Abca1	0.05 ± 0.01	0.13 ± 0.09	0.12 ± 0.03	0.09 ± 0.05	ns	ns	ns	ns
	Mct3	48.63 ± 3.78	46.75 ± 11.48	27.28 ± 6.25	19.38 ± 12.22	ns	ns	$p < 0.05$	$p < 0.01$
	Gnat1	0.004 ± 0.01	0.01 ± 0.02	0.01 ± 0.01	0.001 ± 0.001	ns	ns	ns	ns

Supplementary Table S1

Supplementary Table S2. Gene expression in retinas and eyecups of *Pon1*$^{-/-}$ and wild type (WT) mice after light damage (LD), page 91.

Gene expression was examined by semi-quantitative real-time PCR in retinas and eyecups of wild type and *Pon1*$^{-/-}$ mice, which either were (light damage, LD) or were not (dark control, DC) exposed to damaging light. Analysis was at 12 h after light exposure (12h). Values were normalized to *β-actin* and expressed relative to levels in retinas of dark control WT mice, which were set to 1. Shown are mean values ± SD of N=3. Two-way ANOVA with Bonferroni post-hoc analysis was used to test the statistical significance. A p-value of less than 0.05 was considered significant. *Lif*, leukemia inhibitory factor; *Edn2*, endothelin 2; *Fgf2*, fibroblast growth factor 2; *Stat3*, signal transducer and activator of transcription 3; *Socs3*, suppressor of cytokine signaling 3; *Hmox1*, heme oxygenase 1; *Sod1*, superoxide dismutase 1; *Sod2*, superoxide dismutase 2; *Abca1*, ATP-binding cassette, sub-family A (ABC1), member 1; *Scarb1*, scavenger receptor class B, member 1; *Mct3*, monocarboxylate transporter, member 3 (marker for RPE); *Gnat1*, guanine nucleotide binding protein, alpha transducing activity polypeptide (marker for the neuronal retina).

		Mean ± SD				2-way ANOVA			
						WT vs. *Pon1*$^{-/-}$		DC vs. LD	
	Gene	WT, DC	*Pon1*$^{-/-}$, DC	WT, 12h	*Pon1*$^{-/-}$, 12h	DC	12h after LD	WT	*Pon1*$^{-/-}$
RETINA	***Lif***	1 ± 0.47	1.73 ± 0.39	35.75 ± 10.41	44.29 ± 5.29	ns	ns	$p < 0.001$	$p < 0.001$
	Edn2	1 ± 0.23	3.18 ± 1.34	8.82 ± 1.39	32.3 ± 9.92	ns	$p < 0.001$	ns	$p < 0.001$
	Fgf2	1 ± 0.07	1.55 ± 0.09	1.85 ± 0.08	3.72 ± 1.85	ns	$p < 0.05$	ns	$p < 0.05$
	Stat3	1 ± 0.13	1.18 ± 0.14	4.02 ± 0.55	2.81 ± 0.29	ns	$p < 0.01$	$p < 0.001$	$p < 0.001$
	Socs3	1 ± 0.39	1.64 ± 0.17	20.71 ± 16.94	18.91 ± 9.82	ns	ns	ns	ns
	Hmox1	1 ± 0.29	0.6 ± 0.02	5.32 ± 0.22	4.83 ± 1.71	ns	ns	$p < 0.001$	$p < 0.001$
	Sod1	1 ± 0.12	0.76 ± 0.06	0.8 ± 0.20	0.53 ± 0.12	ns	ns	ns	ns
	Sod2	1 ± 0.16	0.92 ± 0.05	0.65 ± 0.12	0.51 ± 0.06	ns	ns	$p < 0.01$	$p < 0.01$
	Scarb1	1 ± 0.59	1.56 ± 0.43	0.39 ± 0.23	1.03 ± 0.11	ns	ns	ns	ns
	Abca1	1 ± 0.55	1.8 ± 0.79	1.42 ± 1.05	1.18 ± 0.24	ns	ns	ns	ns
	Mct3	1 ± 0.35	0.64 ± 0.30	0.54 ± 0.24	1.79 ± 0.69	ns	$p < 0.01$	ns	$p < 0.05$
	Gnat1	1 ± 0.11	1.14 ± 0.28	0.2 ± 0.06	0.3 ± 0.05	ns	ns	$p < 0.001$	$p < 0.001$
EYECUP	***Lif***	0.37 ± 0.13	0.72 ± 0.32	1.39 ± 1.12	2.07 ± 0.30	ns	ns	ns	ns
	Edn2	0.01 ± 0.004	0.02 ± 0.01	0.04 ± 0.05	0.04 ± 0.02	ns	ns	ns	ns
	Fgf2	0.02 ± 0.01	0.04 ± 0.02	0.06 ± 0.05	0.03 ± 0.004	ns	ns	ns	ns
	Stat3	0.29 ± 0.04	0.32 ± 0.01	0.52 ± 0.15	0.46 ± 0.07	ns	ns	$p < 0.05$	ns
	Socs3	0.21 ± 0.06	0.15 ± 0.03	2.13 ± 0.50	1.52 ± 0.22	ns	ns	$p < 0.001$	$p < 0.001$
	Hmox1	0.21 ± 0.03	0.17 ± 0.04	0.56 ± 0.18	0.4 ± 0.01	ns	ns	$p < 0.01$	ns
	Sod1	0.16 ± 0.01	0.15 ± 0.01	0.17 ± 0.03	0.15 ± 0.04	ns	ns	ns	ns
	Sod2	0.16 ± 0.02	0.15 ± 0.01	0.19 ± 0.01	0.14 ± 0.03	ns	$p < 0.05$	ns	ns
	Scarb1	0.01 ± 0.001	0.02 ± 0.01	0.02 ± 0.02	0.06 ± 0.02	ns	$p < 0.05$	ns	$p < 0.05$
	Abca1	0.02 ± 0.01	0.06 ± 0.03	0.12 ± 0.10	0.1 ± 0.04	ns	ns	ns	ns
	Mct3	6 ± 3.22	8.15 ± 1.05	7.09 ± 3.38	1.5 ± 0.43	ns	$p < 0.05$	ns	$p < 0.05$
	Gnat1	< 0.001	< 0.001	0.003 ± 0.01	< 0.001	ns	ns	ns	ns

Supplementary Table S2

Supplementary Table S3. Phospholipid composition of the retina/eyecup samples from WT and *Pon1*$^{-/-}$ mice at the age of 8 weeks (8w) and 1 year (1y), and from mice exposed to light (page 93 and 94).

Phospholipid (PL) analysis was performed by LC-MS. Content of PL, phosphatidylcholines (PC), phosphatidylethanolamines (PE), sphingomyelins (SM) and lysophosphatidylcholines (LPC), ceramides/hexosylceramides (Cer/HexCer), phosphatidylglycerols (PG) and phosphotungstic acids (PA) was calculated as nmol/ mg of retina and eyecup protein. Total phospholipids represent sum of molecular species of a given class. The median and ranges are given from N=10 for WT (8w), N=10 for *Pon1*$^{-/-}$ (8w), N=5 for WT (1y), N=6 for *Pon1*$^{-/-}$ (1y), N=10 for WT (LD), N=10 for *Pon1*$^{-/-}$ (LD). Total concentration is shown for PC, SM, LPC, PE, Cer/HexCer, PG, PA lipids. Man-Whitney U test was applied since data were not normally distributed. After Bonferroni correction for 37 tests a p-value of 0.00135 corresponds to a significance level of 0.05. Bold letters indicate statistically significant levels. An assignment of PL species includes number of carbon atoms and double bonds in both acyl chains (for example, PC 34:1 consist of 34 carbon atoms and one double bond and can correspond to the following species PC 16:0/18:1 or PC 18:0/16:1, etc.). Sphingomyelin assignment comprises number of carbon atoms and double bonds in both sphingoid base and in N-linked fatty acid.

PLs	Median (min;max) [nmol/mg]						Mann-Whitney Test, p values						
	WT 8w	*Pon1*$^{-/-}$ 8w	WT 1y	*Pon1*$^{-/-}$ 1y	WT LD	*Pon1*$^{-/-}$ LD	WT 8w vs *Pon1*$^{-/-}$ 8w	WT 8w vs WT 1y	*Pon1*$^{-/-}$ 8w vs *Pon1*$^{-/-}$ 1y	WT 1y vs *Pon1*$^{-/-}$ 1y	WT 8w vs WT LD	*Pon1*$^{-/-}$ 8w vs *Pon1*$^{-/-}$ LD	WT LD vs *Pon1*$^{-/-}$ LD
Total PC	143.5(92;170.5)	120.5(54.1;140.3)	89.1(65.5;147.9)	109.2(39.4;147.7)	140.5(58.3;173.7)	151.9(121.7;235.6)	0.0233	0.0275	0.4477	0.8551	0.8206	0.0025	0.2265
Total SM	20(7.2;26.8)	17(7.2;23.7)	16.6(11.1;22.9)	18.6(6.1;28.9)	17.7(6.7;23.8)	19.7(13.5;30.3)	0.1736	0.5403	0.7449	1.0000	0.2899	0.1736	0.3643
Total LPC	5.2(2.1;5.9)	2.5(1.2;4.1)	1.9(1.5;6.8)	3.1(1.3;5.3)	5(2.2;6.5)	3.7(3;8.6)	**0.0013**	0.0864	0.7449	1.0000	0.9397	0.0025	0.0588
Total PE	26.5(16.2;29.8)	21.9(11.4;24.6)	16.4(11.6;22.1)	19.1(6.9;22.6)	29.4(19;51)	27.2(18;37.8)	0.0126	0.0071	0.0652	1.0000	0.0821	0.0343	0.4497
Total Cer/HexCer	5.6(2.7;7.6)	6.1(2.6;9.4)	6.9(4.5;7.3)	6.7(2.5;8.6)	6.3(1.8;10.7)	6(3.9;10.1)	0.5453	0.3272	0.7449	0.8551	0.3258	0.8206	0.8798
Total PG	1.2(0.2;1.9)	0.9(0.3;1.5)	0.5(0.2;1.7)	0.7(0.3;1.4)	1.3(0.7;1.9)	0.6(0.3;3)	0.2530	0.2703	0.6407	0.7540	0.5340	0.2885	0.0506
Total PA	2.8(2.3;3.1)	2.9(2.5;3.2)	2.8(2.6;3)	2.8(2.4;3.2)	0.9(0.6;1.1)	1.3(0.9;1.6)	0.3258	1,0000	0.5876	0.8551	**0.0004**	**0.0002**	0.0025
PC 32:0	27.3(15.5;31.5)	23.3(10.9;27.7)	15.4(12.4;21.2)	18.7(7;24.2)	25.6(10.6;30.5)	28.6(21.4;43.8)	0.0696	0.0048	0.0509	0.8551	0.5453	0.0102	0.1988
PC 32:1	2.7(2.1;3.5)	2.1(1.1;2.6)	1.4(1.2;2.2)	1.5(0.6;2.4)	2.5(0.9;3.5)	2.4(1.3;4)	0.0102	0.0048	0.1585	1.0000	0.7624	0.2899	0.7055
PC 34:0	6.4(3.7;8)	5.9(3;7.6)	5.2(3.2;6.1)	4.8(1.7;6.5)	6.6(3.2;8.8)	8.3(4.1;11.7)	0.2568	0.0864	0.1931	0.8551	0.7624	0.0082	0.0696
PC 34:1	27.8(18.8;33.4)	23.4(10.9;28.9)	16.8(13.3;27.3)	21(7.6;29.2)	28.1(11.1;34.3)	34.1(21.9;48.9)	0.0156	0.0143	0.5876	1.0000	1,0000	0.0032	0.0494
PC 34:2	4.7(3;5.9)	4.2(1.7;4.6)	3(2.1;5.6)	3.5(1.8;5.8)	4.8(1.6;6.6)	5.3(3.3;9.8)	0.0963	0.1416	0.329	0.8551	0.7055	0.0156	0.3258
PC 36:1	14.1(8;16.2)	11.1(5.3;13.3)	8.5(6;14.3)	10.5(3.7;14.8)	13.4(6.2;17.2)	14.9(9.7;23.7)	0.0191	0.0373	0.5876	0.8551	0.7624	0.0052	0.2568
PC 36:2	5.6(4.3;7.2)	4.7(2.2;5.8)	3.6(2.9;6.5)	4.8(1.6;6.4)	6(2.7;7.4)	7(5.1;11)	0.0233	0.0275	0.9136	0.8551	0.8206	**0.0015**	0.1306
PC 36:3	1.5(1;2)	1.3(0.4;1.7)	1.1(0.7;1.7)	1(0.4;1.8)	1.6(0.7;2.4)	1.7(0.7;4.8)	0.0696	0.0500	0.3855	0.8551	0.8798	0.0821	0.4057
PC 36:4	6.4(4.1;7.2)	5.4(2.6;6.3)	4.1(2.5;8.1)	4.7(1.8;7.9)	6(2.5;8.5)	5.6(3.7;10.8)	0.0587	0.1775	0.5876	0.7150	0.8205	0.2568	0.9397
PC 38:4	7.9(4.7;10.4)	6.6(2.8;8.3)	5.2(3.6;10.2)	7(2.1;9.4)	7.5(2.2;10.3)	6.8(5.9;13.3)	0.0126	0.0864	0.8283	0.8551	0.2899	0.4057	0.7055
PC 38:5	2.5(1.6;2.8)	2.4(0.9;2.9)	1.3(1;3.3)	1.7(0.9;3.3)	1.9(0.3;4.9)	2.7(0.8;5.2)	0.4497	0.0864	0.2328	1.0000	0.2265	0.3258	0.1509
PC 38:6	12.1(7.6;15.1)	9.5(4;12.3)	8(5.1;13.2)	8.6(3.4;11.3)	12.5(6.1;15.2)	12.6(9.1;19.4)	0.0126	0.0500	0.3855	0.8551	0.8798	0.0233	0.9397
PC 40:5	1.7(0.7;2.3)	1.3(0.8;1.9)	1.1(0.8;2.2)	0.9(0.3;1.6)	2(0.7;3.3)	2.5(0.4;4.1)	0.0233	0.1779	0.1037	0.3613	0.3643	0.2899	0.6501
PC 40:6	17.7(12.2;20.4)	13.7(5.7;15.6)	11.4(7.7;19.4)	13.7(4.6;17.8)	15.1(6.8;20.8)	17.2(10.2;26.5)	0.0041	0.0500	0.8283	0.8551	0.2568	0.0052	0.2265
PC 40:7	1.4(1.2;2.4)	1.1(0.5;1.5)	0.8(0.8;1.6)	1.1(0.4;1.3)	1.2(0.3;1.9)	0.9(0.5;1.8)	0.0082	0.0373	0.5505	0.8551	0.2899	0.6501	0.2568
PC 44:12	4.9(3.7;8.3)	3.9(1.4;5.7)	2.3(1.9;5.1)	3.4(1.1;4.5)	4.8(2.4;6.2)	4(2.6;13.6)	0.0156	0.0143	0.3855	0.8551	0.2899	0.4057	0.7624

Supplementary Table S3 (part A)

PLs	Median (min;max) [nmol/mg]						Mann-Whitney Test, p values						
	WT 8w	*Pon1*$^{-/-}$ 8w	WT 1y	*Pon1*$^{-/-}$ 1y	WT LD	*Pon1*$^{-/-}$ LD	WT 8w vs *Pon1*$^{-/-}$ 8w	WT 8w vs WT 1y	*Pon1*$^{-/-}$ 8w vs *Pon1*$^{-/-}$ 1y	WT 1y vs *Pon1*$^{-/-}$ 1y	WT 8w vs WT LD	*Pon1*$^{-/-}$ 8w vs *Pon1*$^{-/-}$ LD	WT LD vs *Pon1*$^{-/-}$ LD
SM34:1	5.8(2.3;7.6)	5.2(2.4;7.2)	5.5(3.5;6.9)	5.5(2.2;8.5)	6.4(2.8;9.5)	7.4(4.9;11.5)	0.1736	0.7133	0.8283	1.0000	0.0821	0.0191	0.5453
SM36:1	4.7(1.9;6.4)	3.9(1.9;5.5)	3.4(2.1;5)	4.1(1.1;5.8)	4.6(1.6;6.1)	4.8(3;8.6)	0.1988	0.1779	0.7449	0.8551	0.8206	0.0821	0.5453
SM38:1	2.4(0.8;3.3)	2.2(0.7;2.9)	2.4(1.1;2.9)	2.4(0.7;3.8)	1.9(0.4;2.4)	2.3(1.4;3.2)	0.1988	0.5403	0.5876	0.8551	0.0233	0.5453	0.1509
SM40:1	2.2(0.8;3.2)	2(0.8;2.9)	1.7(1.3;2.8)	2.5(0.6;3.7)	1.6(0.6;2.4)	1.7(1.2;3)	0.1988	0.4624	0.4477	0.5839	0.0102	0.5453	0.5967
SM42:1	2.1(0.6;2.7)	1.7(0.5;2.6)	1.7(1.1;2.2)	1.9(0.7;3.2)	1.1(0.5;1.9)	1.4(0.8;2.8)	0.1306	0.1779	0.8283	0.8551	0.0032	0.3258	0.1509
SM42:2	2.2(0.8;3.4)	1.8(0.7;2.7)	1.7(1.2;2.9)	1.8(0.8;3.3)	1.7(0.6;2.3)	1.6(0.7;3.5)	0.2568	0.6242	1.0000	0.8551	0.0156	0.8798	0.9397
SM42:3	0.4(0.1;0.5)	0.3(0.1;0.4)	0.3(0.2;0.6)	0.2(0.1;0.5)	0.3(0.2;0.5)	0.4(0.2;0.7)	0.0588	0.4624	0.8283	0.5839	0.1124	0.0413	0.0821
LPC 18:0	0.8(0.6;0.8)	0.7(0.4;0.9)	0.7(0.4;1.1)	0.9(0.4;1.1)	1.2(0.5;1.4)	1.2(0.6;1.9)	0.1306	0.2703	0.2328	0.5839	0.0025	0.0065	0.7055
LPC 18:1	1.7(0.6;2)	0.7(0.4;1.2)	0.6(0.5;2)	0.9(0.4;1.7)	1.3(0.5;2)	0.8(0.4;2.4)	0.0019	0.0864	0.7449	1.0000	0.1736	0.2568	0.0284
LPC 22:6	2.8(0.9;3.1)	1.2(0.4;2)	0.7(0.5;3.8)	1.3(0.4;2.5)	2.6(1.3;3.2)	1.7(1.4;4.8)	**0.0013**	0.0662	0.7449	1.0000	1.0000	0.0052	0.0494
PE 34:1	0.8(0.6;0.9)	0.7(0.4;0.9)	0.6(0.4;0.6)	0.6(0.3;0.9)	1.2(0.7;1.4)	1.1(0.9;1.4)	0.2899	0.0022	0.2781	0.7150	**0.0012**	**0.0002**	0.4963
PE 36:0	0.3(0.2;0.4)	0.3(0.2;0.4)	0.2(0.2;0.3)	0.2(0.2;0.3)	0.6(0.6;0.8)	0.6(0.6;0.7)	0.8798	0.0500	0.3290	0.7150	**0.0002**	**0.0002**	0.6501
PE 36:2	0.9(0.8;1.2)	0.9(0.7;1.1)	0.7(0.6;1.1)	0.8(0.4;1.1)	1.2(0.9;1.5)	1(0.8;1.2)	0.1509	0.1416	0.4477	0.7150	0.0065	0.0588	0.0284
PE 36:4	0.6(0.4;0.8)	0.6(0.4;0.8)	0.5(0.4;0.7)	0.5(0.3;0.7)	0.9(0.7;1.1)	0.9(0.7;1.2)	0.6501	0.1779	0.4477	1.0000	**0.0005**	**0.0004**	0.9397
PE 38:4	3.3(1.8;3.7)	2.6(1.5;3.1)	2(1.5;3)	2.7(0.9;3.1)	3.7(1.5;5.5)	3.6(1.6;5.4)	0.0191	0.0373	0.9136	0.4652	0.3643	0.0025	0.7055
PE 38:6	5(2.8;6.3)	4.2(2;5.1)	2.7(1.8;4.1)	3.4(1.3;4.1)	6(3.8;11.4)	5.2(3.9;7.5)	0.0082	0.0048	0.0170	1.0000	0.0343	0.0284	0.2265
PE 40:6	12.2(7.6;13.8)	10.3(5.1;11.4)	8.6(5.3;10.1)	9(2.7;11)	15.3(9.1;25.6)	13.7(5.8;20.3)	0.0126	0.0071	0.0652	1.0000	0.0156	0.0233	0.4057
PE 44:12	2.9(1.9;3.8)	2.3(1.1;2.7)	1.4(1.2;2.3)	1.7(0.5;2.3)	1.2(0.9;3.8)	1.1(0.9;2)	0.0126	0.0048	0.0827	0.8551	0.0025	**0.0007**	0.4497

Supplementary Table S3 (part B)

3.3.2 Revealing the role of PON1 in RPE cell cultures *in vitro*

Unpublished data

Contributors

Jadwiga Oczos[1] and Christian Grimm[1]

[1] Lab for Retinal Cell Biology, Department of Ophthalmology, University of Zurich, Zurich, Switzerland

Personal contribution

Isolation, culture and experiments on mouse RPE cells, culture and experiments on ARPE19 cell line, light microscopy, RNA preparation and analysis of gene expression

PURPOSE

We detected high levels of PON1 transcripts in the RPE, a cellular layer strongly affected in AMD. To further characterize function of PON1 in the RPE and its contribution to AMD, we established primary mouse RPE cultures *in vitro.*

METHODS

Isolation and culture of mouse RPE (mRPE) cells

RPE cell cultures were established from mouse at 6-8 weeks of age. Intact eye balls were isolated and placed in ice cold PBS, pH 7.4 (PAA Laboratories GmbH, Pasching, Austria). Each eye ball was opened by a round cut below the ora serata, and the cornea, lens and vitreous were removed. Remaining tissue (choroid, RPE, and retina) was incubated in 1 mM PBS-EDTA buffer, pH 7.4 (0.5 M EDTA, pH 8.0; Gibco, Paisley, UK) for 20 min at 37°C to let the retina dissociate from the RPE. After gentle removal of the retina, the remaining eye cup underwent protease treatment for 23 min at 37°C (1U papain (Roche Diagnostics GmbH, Mannheim, Germany) per 1 ml of dissociation buffer (1 mM PBS-EDTA containing 3 mM L-cystein (Sigma-Aldrich, St. Louis, MO, USA) and 1 mg/ml BSA (PAA Laboratories GmbH)). Protease digestion was stopped by the addition of culturing media containing 10% FBS (DMEM/Ham's F-12 (Sigma-Aldrich) containing 2.5 mM L-glutamine, 15 mM HEPES, 0.5 mM sodium pyruvate, 1.05 mM calcium chloride, and 1.2 g/L sodium

bicarbonate, additionally supplemented with 2% FBS-Gold (PAA Laboratories GmbH), 1% penicillin-streptomycin (PAA Laboratories GmbH), 500 µl/L insulin-transferrin-selenium (Gibco), and 10 ml/L non-essential amino acids (PAA Laboratories GmbH)) and RPE cells were immediately released by gentle pipetting. Culturing medium containing RPE cells was centrifuged (300 rcf, 3 min). The resulting pellet of RPE cells was resuspended in 50 µl of fresh culturing medium. Cells were seeded in a drop in culture dishes of various size (TPP, Trasadingen, Switzerland) and cultivated at 37°C in a humidified atmosphere of 95% air and 5% CO_2. After 2 days 1 ml of medium was added. Culturing medium was changed every 3 to 4 days. For passaging, mRPE cultures were incubated in trypsin-EDTA solution (PAA Laboratories GmbH) for 5 min at 37°C, and released by gentle pipetting.

Culture of human ARPE19 cell line

Human ARPE19 cells at passage 19 were purchased from the American Type Culture Collection (ATCC, Manassas, VA, USA; product ATCC-CRL-2302), and handled according to the provider's instructions. Cells were cultivated in culturing medium DMEM/Ham's F-12 (Sigma-Aldrich) containing 2.5 mM L-glutamine, 15 mM HEPES, 0.5 mM sodium pyruvate, 1.05 mM calcium chloride, and 1.2 g/L sodium bicarbonate, additionally supplemented with 10% FBS-Gold (PAA Laboratories GmbH) and 1% penicillin-streptomycin (PAA Laboratories GmbH) at 37°C in 5% CO_2 in air. Passaging of ARPE19 cultures was performed by incubation in trypsin-EDTA solution (PAA Laboratories GmbH) for 7 min at 37°C.

Light microscopy

Living mRPE and ARPE19 cells in culture dishes were observed using an inverted microscope (Axiovert 25, Zeiss, Feldbach, Switzerland).

Restoration of *PON1* expression in ARPE19 cells

ARPE19 cells at passage 24-26 were seeded in 12-well culture dishes (TPP) at a density of 10^5/well (24h incubation time) or 7×10^4/well (48h incubation time) in culturing medium. Various compounds (Table 5) were added in an attempt to restore *PON1* expression in ARPE19 cells. Light microscopy served to monitor eventual toxic effects of each chemical. After 24h or 48h incubation time cells were washed and lysed with RLT buffer (Qiagen, Hilden, Germany) and RNA was extracted for analysis of gene expression (see below).

For a long-term culture ARPE19 cells were seeded in 12-well culture dishes (TPP) at a density of 10^5/well. Cells were maintained for 60 days in culturing medium containing reduced amount of FBS (2%). Medium was exchanged every 3

to 4 days. At day 60 DMEM/Ham's F-12 was replaced by the culturing medium additionally containing compounds listed in table 5, and cells were further cultured for 24h prior to the lysis and RNA extraction.

Compound	Solvent	Final concentration
Gallic acid	culturing medium absolute ethanol	10 μM, 20 μM, 50 μM
Resveratrol	absolute ethanol	10 μM, 20 μM
Quercetin	DMSO	50 μM
Aspirin (400 mg acetylsalicylacid pro tablet)	absolute ethanol	0.25 mM, 0.5 mM, 1 mM of acetylsalicylacid
All-*trans* retinoic acid	DMSO chloroform	20 μM, 50 μM, 100 μM
22(R)-hydroxycholesterol	DMSO	20 μM, 50 μM, 100 μM
Human HDL crude	——	25 μg/ml, 50 μg/ml
Human HDL dialyzed	——	25 μg/ml, 50 μg/ml

Table 5. List of compounds used to attempt to restore expression of *PON1* in ARPE19 cells.
Gallic acid, resveratrol, quercetin, all-*trans* retinoic acid, and 22(R)-hydroxycholesterol were purchased from Sigma-Aldrich; aspirin was from Bayer Schweiz (Zürich, Switzerland). Human HDL was prepared by sequential ultracentrifugation from normolipidemic human plasma (blood bank of Kantonsspital Schaffhausen, Switzerland) at the Institute of Clinical Chemistry, UniversitätsSpital Zürich, Switzerland, according to the protocol described by Tong et al., 1998.

RNA preparation and analysis of gene expression

Total RNA was prepared with an RNA isolation kit including a DNase treatment to digest residual genomic DNA. For primary mRPE cells the RNeasy Micro kit (Qiagen) and for ARPE19 cultures the RNeasy Mini kit (Qiagen) were used. cDNA was synthesized by means of random hexamer primers (High-Capacity cDNA Reverse Transcription Kit; Applied Biosystems, Foster City, CA, USA) or oligo(dT) and M-MLV reverse transcriptase (Promega, Madison, WI, USA) for primary mRPE and ARPE19 cultures, respectively.

Gene expression was analyzed either by agarose gel electrophoresis of the PCR products or by semi-quantitative real-time PCR. Conventional PCR reaction consisted of an initial denaturation step (95°C, 5 minutes), 35 amplification cycles (denaturation: 95°C, 45 seconds; annealing: specific temperatures for each primer pair listed in table 4, 30 seconds; extension: 72°C, 30 seconds), and a final extension step (72°C, 10 minutes). Real-time PCR was performed using specific primer pairs (Table 6), a polymerase ready mix (LightCycler 480 SYBR Green I Master Mix;

Roche Diagnostics, Basel, Switzerland), and a thermocycler (LightCycler480, Roche Diagnostics). Signals were normalized to β-actin and relative gene expression was calculated using the ΔΔCt method.

For ARPE19 line experiments human liver cDNA served as a positive control.

Gene	Forward 5' → 3'	Reverse 5' → 3'	AT (°C)	Product (bp)
Pon1	GAGCCAGCAGTGTCAGAGTT	GACGAGGAGTCTGGATGGTT	60	137
Pon2	CAGAGGCTCTTCGTGTACCA	ATGTTCTGAATGCGGAGGAC	60	88
Pon3	TTGACCGTTGATCCAGCCAC	GAAGCACAGAGCCGTTGTTC	62	175
Mct3	GGCTCAACCCTAAATCCAGA	CTTCGGAGTTTCCTCACCAG	58	75
Rpe65	ATGACTGAGAAGAGGATTGTC	CTGCTTTCAGTGGAGGGATC	60	366
Rlbp1	CCTTTCCAGTCGGGACAAGTATG	GGGTTTCCTCATTTTCCAGCAG	60	140
Rdh5	GGCTACTGTGTCTCCAAGTT	CTGGTCACCTTCGTTAGTTC	62	278
Pde6a	GGCTGAGATCCTGCAAGGAG	ATCTGGATGCCGCACTTCAC	62	114
Pde6c	GGCCATATTGAAGGAGGACT	GCATTTAACCAACTCGTGCT	62	100
Gfap	CCACCAAACTGGCTGATGTCTAC	TTCTCTCCAAATCCACACGAGC	62	240
Actb	CAACGGCTCCGGCATGTGC	CTCTTGCTCTGGGCCTCG	62	153
PON1	GACTGGCACTCTTCAGGAAC	GGCAGTATCTCCAAGTCTTCA	62	139
PON2	CGAGAGGCTTCTGGCACTCA	GTGCAAAGCTGTGGAGTCCTG	62	182
PON3	TCTCAGCAGACCAGAAGTATG	CAGGTTATCCACTAAGGTGC	62	131
RPE65	ACAAGGCTGACACAGGCAAG	CAAGCCAAGTCCATACGCAT	62	194
ACTB	CCTGGCACCCAGCACAAT	GGGCCGGACTCGTCATAC	62	144

Table 6. Primers and conditions for conventional and for real-time PCR.
Human genes are written in uppercase letters. In mouse genes only first letter is uppercase and the rest is lowercase. AT, annealing temperature.

RESULTS

Characterization of the primary mRPE cultures

Isolation procedures and culture conditions are known to alter the morphological and functional features of the primary cells. In order to study RPE cell behaviour under the conditions resembling an *in vivo* situation, there is a need to evaluate and adopt isolation and culture protocols to obtain *in vitro* RPE cultures that retain the native RPE structure and characteristics.

Morphology of primary mRPE cultures was evaluated by light microscopy. Figure 14A illustrates a typical appearance of a cell culture 8 days after the isolation. RPE cells formed a monolayer of highly pigmented, polygonal cells. Proliferating cells, which were found only on the outskirts of the culture (cells seeded in a drop), displayed a decrease in the pigment density and an elongated form. After the first passage numerous RPE cells were less pigmented and lost their

polygonal shape. Cells were dividing more dynamically and mitotic doublets were present throughout the culture (Fig. 14B). After the second passage fibroblast-like morphology became more striking (Fig. 14C). Although many dividing cells were observed, the number of living cells suggested reduced proliferation after passage 2. Cultures obtained from two mouse eyes gave on average 6.4×10^4 RPE cells at passage 1, 1.5×10^5 cells at passage 2, and only 6.2×10^4 cells at passage 3, indicating approximately 2.4-fold increase in proliferation after passage 1 and comparable decrease in proliferation after passage 2. Number of RPE cells directly after isolation could not be assessed because of the high content of the RPE sheets and fragments of other cells (e.g. photoreceptor outer segments) in the extract.

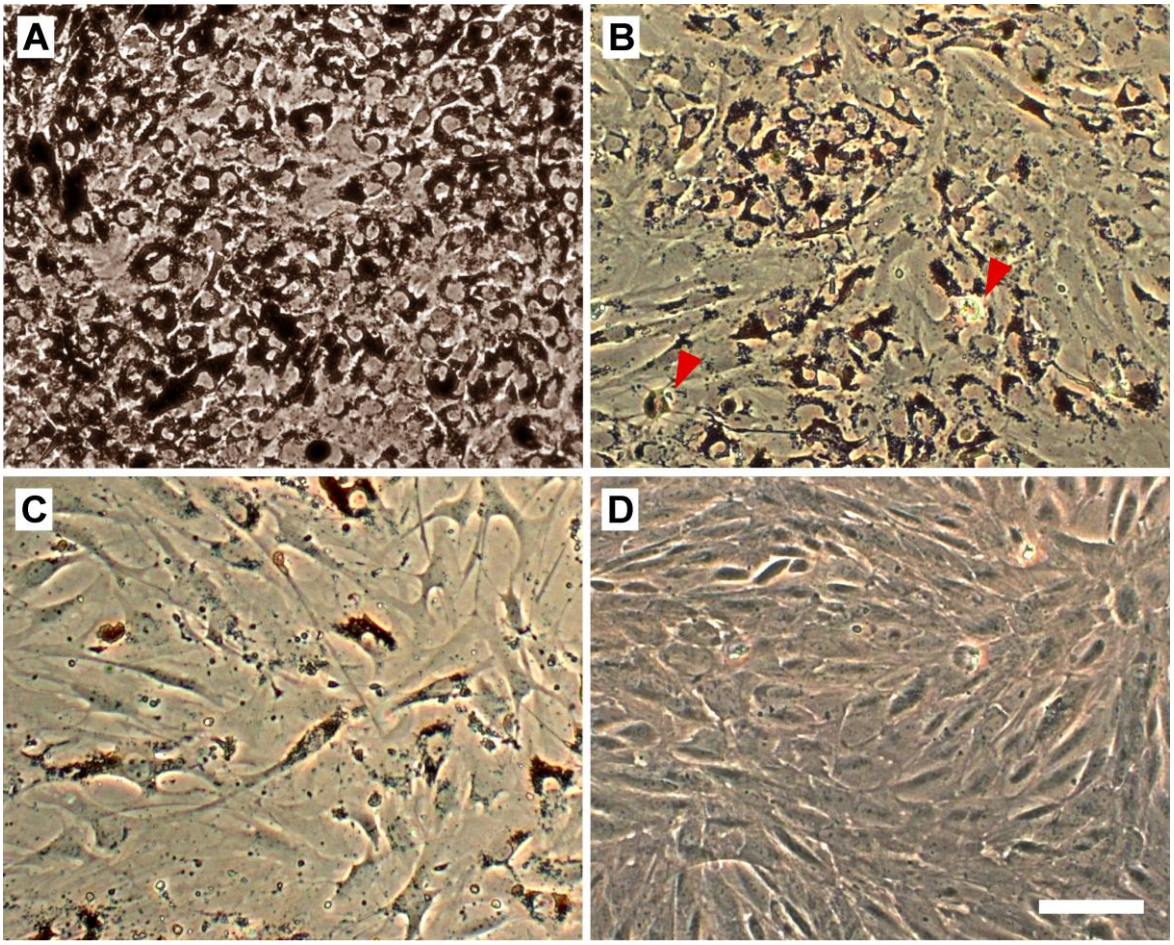

Figure 14. Morphology of primary mRPE cultures
(A) 8 days after isolation of mRPE, cells formed a monolayer of highly pigmented, regularly shaped cells. **(B)** After passage one, highly pigmented polygonal cells were grouped in islands surrounded by less pigmented elongated cells. Dividing cells were present throughout the culture (red arrowheads). **(C)** After passage two, the majority of cells lost pigmentation and displayed fibroblast-like morphology. **(D)** Confluent culture of undifferentiated ARPE19 cells at passage 24. Scale bar = 50 μm.

An important step in characterisation of the primary RPE cultures is monitoring of the expression of specific RPE markers. Monocarboxylate transporter 3 (MCT3) is known to be expressed in the basolateral membrane of the RPE and to be unique to this monolayer among the other retinal cells (Philp et al., 1998; Yoon et al., 1997). In the cultured RPE cells the level of MCT3 mRNA depends on the degree of cell differentiation (Philp et al., 2003). Our RPE extracts (fresh mRPE) showed high expression of *Mct3* (Fig. 15A), which was massively down-regulated after one day in culture and completely lost after 8 days in culture (Fig. 15A, C). Although it has been reported that RPE cells cultured for 60 days are highly differentiated and therefore express *Mct3* (Philp et al., 2003), we could not detect any *Mct3* mRNA in such cultures (Fig. 15C). Nevertheless, all RPE cultures that were not passaged formed a monolayer of highly pigmented, polygonal cells, indicative for RPE.

One of the main functions of the RPE *in vivo* is recycling of the chromophore 11-*cis*-retinal. Expression of the various enzymes and binding proteins involved in this process by cultured RPE cells can be indicative of their state of differentiation (Pfeffer, 1991). We did not detect any transcripts encoding the isomerase RPE65 or CRALBP (*Rlbp1*) in RPE cells after 8 days and 4 weeks in culture, even though they were present in freshly isolated RPE (Fig. 15A). In contrast, RPE-specific retinol dehydrogenase (RDH5) mRNA was found in all analysed RPE samples.

To test whether the RPE extracts and cultures were contaminated with adjacent photoreceptor cells we tested mRNA expression of a rod and cone cGMP-specific 3',5'-cyclic phosphodiesterase subunit (*Pde6a* and *Pde6c*, respectively; Fig. 15A). Presence of those transcripts in freshly isolated RPE, but not in cultured RPE cells suggests that RPE extracts contained some photoreceptor cells (or cellular debris), which did not survive in culture. Additionally, we checked expression of *Gfap* (glial fibrillary acidic protein), a marker for Müller cells (Fig. 15A). Presence of *Gfap* mRNA in one freshly isolated RPE sample indicated its contamination with glial cells, and suggested that *Rlbp1* transcripts detected in this sample originated both from the RPE and Müller cells. It is important to notice differences in contamination with rods, cones and glial cells between RPE isolations.

We tried to modify the basic composition of culturing media according to several reports in order to obtain differentiated RPE monolayers expressing RPE markers. Reduction of serum to 1%, supplementation with all-*trans*-retinoic acid (Pfeffer, 1991) or with mouse retinal extracts (Hu, 2000; Pfeffer et al., 1986) did not improve characteristics of primary mRPE cultures (data not shown).

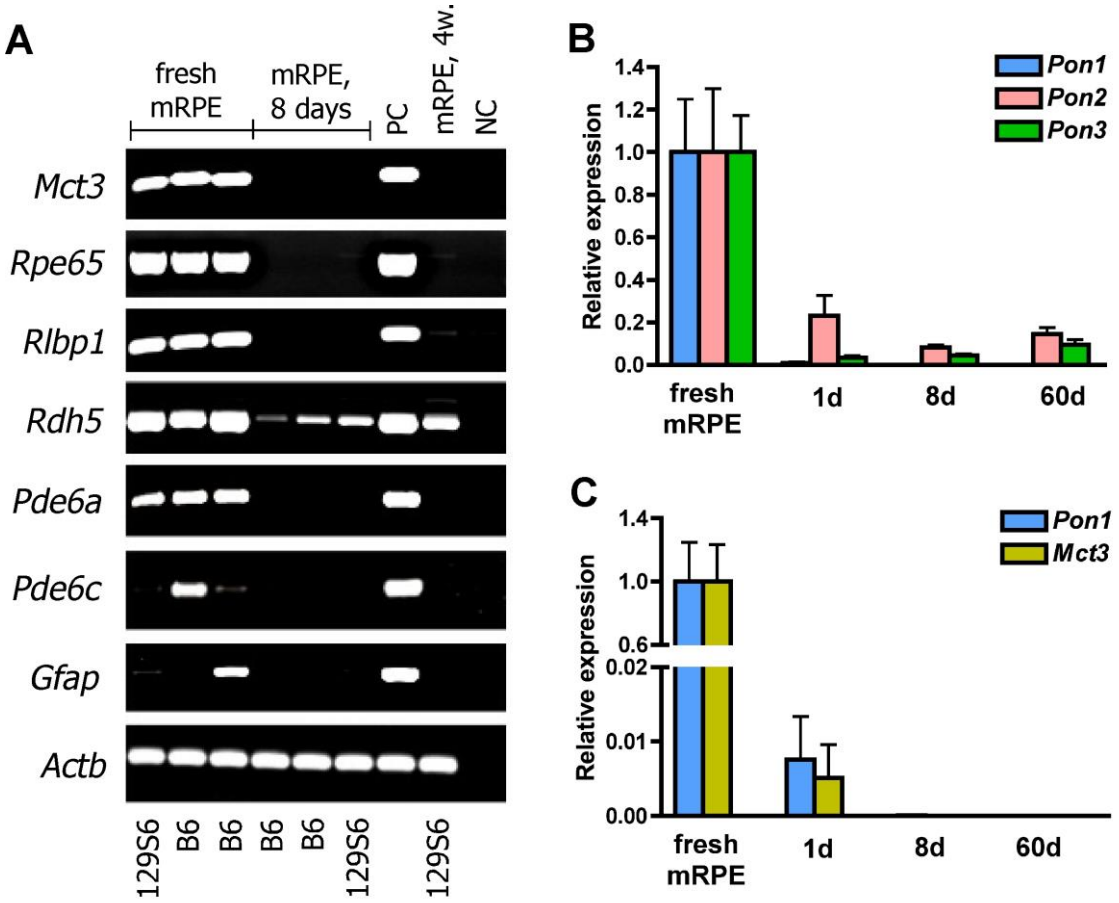

Figure 15. Expression of RPE markers and paraoxonases in primary mRPE cultures.
(A) RNA was prepared from freshly isolated mouse RPE and primary mRPE cells cultured for 8 days or 4 weeks (mRPE, 4w.), which were obtained from 129S6/SvEvTac (129S6) or C57Bl/6 (B6) wild type mice. Expression of various genes was analysed by agarose gel electrophoresis of PCR products amplified from cDNA with the use of specific primer pairs (Table 6). All tested RPE-specific genes were expressed in fresh RPE, but only *Rdh5* was detected in primary mRPE cultures. Fresh RPE showed variable contamination with photoreceptors (*Pde6a*, *Pde6c* as marker) or Müller cells (*Gfap* as marker), whereas mRPE cultures were free of contamination. Eye cup or retinal cDNA were used as a positive control (PC) for RPE-specific genes and contamination controls, respectively. *β-actin* (*Actb*) served as a control for RNA integrity. NC, negative control; *Mct3*, monocarboxylate transporter 3; *Rpe65*, retinal pigment epithelium 65kDa protein; *Rlbp1*, cellular retinaldehyde binding protein; *Rdh5*, retinol dehydrogenase 5; *Pde6a*, rod cGMP-specific 3',5'-cyclic phosphodiesterase subunit alpha; *Pde6c*, cone cGMP-specific 3',5'-cyclic phosphodiesterase subunit alpha; *Gfap*, glial fibrillary acidic protein.
(B, C) Expression of paraoxonases and *Mct3* gene was determined by semi-quantitative real-time PCR in fresh mRPE and primary mRPE cells cultured for 1 day (1d), 8 days (8d), or 60 days (60d), which were obtained from 129S6 wild type mice. Shown are mean values ± SD of N = 3. Values were normalized to *β-actin*, and levels in fresh mRPE were set to 1. *Pon1* was rapidly down-regulated in culture and followed the expression pattern of *Mct3*. PON2 and PON3 mRNA levels were lower in one and eight day old cultures, compared to fresh RPE, but prolonged cultivation caused slight increase in their abundance.

Expression of paraoxonases in primary mRPE cultures

The main aim of establishing primary mouse RPE cultures was to set up cultures either expressing PON1 (wild type 129S6 mice) or lacking PON1 protein (*Pon1*$^{-/-}$ mice), to test their behaviour upon oxidative stress (H_2O_2, oxLDL), and thus reveal if and how PON1 is involved in a potential response to such conditions. Therefore in the first place we characterized expression of *Pon1* gene in mRPE cultures obtained from wild type animals. As shown in figure 15B, RPE cells in culture were rapidly losing *Pon1* mRNA expression, and one day after isolation contained only about 1% of the transcripts present in fresh RPE. After 8 days in culture no *Pon1* mRNA could be detected. Interestingly, decay of *Pon1* expression in RPE cultures was strikingly similar to the down-regulation of *Mct3* (Fig. 15C). Additionally, we found decreased levels of *Pon2* and *Pon3* mRNA in 1- and 8-day old cultures, compared to the freshly isolated RPE. But, in contrast to *Pon1*, the *Pon2* and *Pon3* transcripts were present in RPE cells cultured for 60 days at slightly increased levels compared to the 8-day old cultures. Application of modified media did not lead to up-regulation of *Pon1* expression in primary mRPE cultures.

Noticeably, the ARPE19 cells expressed *PON2* mRNA at levels comparable with human liver, whereas neither *PON1* nor *PON3* transcripts could be detected (data not shown).

Restoration of *PON1* expression in ARPE19 cells

The observed complete loss of *PON1* mRNA in primary mRPE cultures would disable the execution of our planed experiments on *Pon1*$^{+/+}$ and *Pon1*$^{-/-}$ RPE cells. Therefore, we conducted extensive trials to restore *PON1* expression in cultured cells by applying molecules previously reported to up-regulate *PON1* expression *in vitro*. Because of the limited supply in primary mouse RPE cells, we performed all experiments on the ARPE19 cell line, which also does not express *PON1* (data not shown). Importantly, primary mRPE and ARPE19 cells display a similar expression pattern of the nuclear receptors involved in regulation of the *PON1* gene (Dwyer et al., 2011). We supplemented culture medium with various concentrations of resveratrol, quercetin and aspirin that are known to induce *PON1* expression via interaction with aryl hydrocarbon receptor (AhR) (Gouedard et al., 2004a, b; Jaichander et al., 2008); with gallic acid, an activator of PPARγ nuclear receptor (Khateeb et al., 2010); and with 22(R)-hydroxycholesterol, which up-regulates *PON1* expression via liver X receptor (LXR) (Gouedard et al., 2003). Although all-*trans* retinoic acid (ATRA) has not been reported to regulate expression of *PON1* gene, we tested its influence on *PON1* transcript level in ARPE19 culture. We hypothesized that presence of ATRA could improve differentiation state and

polarity of the cells and therefore affect expression of *PON1*. Additionally, we tested if presence of human HDL in medium restored *PON1* expression.

We measured *PON1* gene expression both in undifferentiated and in 60 days old ARPE19 cells cultured in presence of the above substances, but we could not detect any *PON1* transcripts in any of the analyzed cultures (data not shown).

DISCUSSION

Our initial experiments demonstrated that primary mRPE cells were rapidly losing *Pon1* expression in culture. Since this phenomenon was accompanied by the loss of *Mct3*, *Rpe65* and *Rlbp1* expression, we concluded that expression of *Pon1*, in contrast to *Pon2* and *Pon3*, is dependent on the state of differentiation and polarization of RPE cells. Such assumption was confirmed by the detection of *Pon1* mRNA in highly polarized mouse RPE cultures by our collaborators (personal communication with Rosario Fernández Godino, Ocular Genomics Institute, Harvard Medical School, Boston, MA, USA). Additional supplementation of the culturing medium with substances known to promote differentiation of RPE cells (Pfeffer, 1991) neither improved characteristics of cultures established in our laboratory, nor induced *Pon1* expression. Another possible modification of the culture procedure would be an application of culture dishes with Transwell filters that were successfully used by several groups to establish a polarized RPE cell culture (Sonoda et al., 2009).

The *in vitro* cultures of polarized primary mRPE cells on Transwell filters would serve to answer several questions. Analysis of the apical and basal culture medium by western blot or by paraoxonase activity assays would reveal whether PON1 is retained in the RPE cell membranes, or whether it is secreted basally or apically. Survival of *Pon1*$^{-/-}$ and *Pon1*$^{+/+}$ RPE cells and production of MDA upon treatment with oxLDL could be examined to test a protective function of RPE-derived PON1 against lipid peroxides (Aviram et al., 1998; Besler et al., 2011; Kim et al., 2012; Yin et al., 2012). Study of the lipid efflux from *Pon1*$^{-/-}$ and *Pon1*$^{+/+}$ RPE cells would help to establish the function of PON1 in this process (Duncan et al., 2009; Ishida et al., 2006).

Alternatively, the experiments proposed above might be performed in the ARPE19 cell line expressing the human *PON1* gene from an expression vector. However, since originally described ARPE19 cultures displayed pronounced heterogeneity resulting in a low transepithelial resistance (Dunn et al., 1996), their application for more complex studies, such as polarized secretion of proteins, might be limited.

IV. CONCLUDING DISCUSSION

In the final discussion I will not focus on specific aspects of each project, since they were discussed in detail in the previous sections of this dissertation, but rather try to present a general picture on the role of PON1 in the retina and in AMD that emerged from current analyses and previous reports.

Our case-control study showed for the first time association between the upstream regulatory region of *PON1* and neovascular AMD. We found four SNPs (rs705379, rs705381, rs854573, rs757158) and two 7-SNP haplotypes (TGGCCTC and CGATGCT) significantly associated with the disease. Inclusion of haplotype analysis increased power of the association and provided insight into the *cis*-interaction between the analyzed loci (Liu et al., 2008). Nevertheless, our study did not clarify the involvement of *PON1* genotypes at the early or intermediate stage of the disease, or in geographic atrophy. Since genetic association may change with the form of AMD (Adams et al., 2012), additional association studies between the *PON1* gene and early, intermediate, or nonexudative AMD would complement our analysis.

In a functional assay *in vitro* we showed that protective and risk *PON1* 5'UTR haplotypes affect gene expression differently. The TGG haplotype, which appeared to be protective against AMD in association study, yielded the lowest level of luciferase activity in both ARPE19 and Caco-2 cells. Also protective alleles -107T and -162G (our association study) decreased *PON1* expression (present and previous studies (Brophy et al., 2001a; Brophy et al., 2001b; Leviev and James, 2000; Suehiro et al., 2000)). Thus, it may be difficult to understand, how lower levels of an anti-oxidant and anti-inflammatory PON1 protein can be associated with a decreased risk for AMD. One possible explanation is that the -107T and -162G alleles are in linkage disequilibrium with the p.55M coding variant (Aviram et al., 1998; Leviev and James, 2000) that was shown to affect PON1 activity towards lipid peroxides, with the MM genotype being more effective than the LL genotype (Mackness et al., 1998). As a consequence, lower levels of PON1 may be linked to its higher activity against lipid peroxides and therefore confer protection against AMD by decreasing serum oxLDL levels (Ikeda et al., 2001). Another important notion is that in a pathological situation PON1 serum content and its paraoxonase and arylesterase activity show inverse trend. For example, in CAD higher serum PON1 levels are accompanied by decreased enzymatic activities (Besler et al., 2011). Similar scenario might happen in AMD, since affected individuals display lower serum PON1 activity in comparison to controls (Ates et al., 2009; Baskol et al., 2006).

PON1 enzymatic activity in human tissue, which is relevant for its protective function against AMD, depends on several factors: (i) among genetic factors *PON1* polymorphisms within upstream regulatory region influence PON1 activity by regulating gene expression (the more molecules of protein synthesized, the more acting molecules and the higher measurable enzymatic activity), *PON1* coding polymorphisms affect conformation of the protein and therefore catalytic activity of PON1; (ii) among environmental factors smoking (Isik et al., 2007; Solak et al., 2005), age (Marchegiani et al., 2008), and disease status (e.g. CAD, AMD (Deakin and James, 2004; Ng et al., 2005)) reduce PON1 enzymatic activity in serum. The interaction between all these factors is not fully understood. It is not clear yet, how PON1 levels and activity in serum and/or ocular tissue affect the onset and progression of AMD. Alternatively, how PON1 function is affected by the disease. Further studies are required to better understand this interaction.

Our analyses of *Pon1*$^{+/+}$ and *Pon1*$^{-/-}$ retina/eyecup revealed a specific function for PON1 in modulating the composition of retinal phospholipids, in particular, in increasing the lysophosphatidylcholines (LPC) content. Since LPC stimulate cholesterol efflux from macrophages (Hara et al., 1997; Rosenblat et al., 2006; Rosenblat et al., 2005), PON1-mediated release of LPC might control this process in the retina or RPE as well. Further studies on primary RPE cultures would help to understand the potential role of PON1 in the lipid efflux from RPE. Strikingly, besides the decreased levels of LPC, retinas of *Pon1*$^{-/-}$ mice seemed not to be affected by the absence of PON1 under any tested conditions, suggesting that this protein is not essential for normal development, function, defense against light damage and aging of the mouse retina and RPE.

In mouse models of atherosclerosis PON1 was protective against the formation of atherosclerotic plaque (Rozenberg et al., 2003; Shih et al., 1998; Shih et al., 2000; Tward et al., 2002). However, lack of PON1 together with advanced age were insufficient to promote formation of atherosclerotic lesions in mice (Rozenberg et al., 2003), implicating that PON1 does not act as a "switch" from a healthy to a pathological condition, but rather as a modulatory factor that slows down progression of a pathology. Considering parallels in etiology of atherosclerosis and AMD, I would expect a similar protective role of PON1 in the formation of drusen in the eye. This protective role might become prominent in mice already bearing some drusen-like lipid deposits, e.g. in aged transgenic *ApoE* mice on a high fat diet (Malek et al., 2005). Drusenogenesis in mice progresses differently than in human (Mishima and Hasebe, 1978; Ramkumar et al., 2010), therefore no mouse model can truly mimic AMD. Nevertheless, because of the limitation in the availability of human ocular tissue for analyses and the lack of other, more convincing model organism to study AMD, the mouse would still be my

model organism of choice to further investigate a potential protective role of PON1 in drusenogenesis.

Taken together, findings presented in this thesis advance our understanding of the function of PON1 in the eye and its contribution to AMD. Association found between *PON1* gene and neovascular AMD confirms involvement of PON1 at the end stage of the disease, which might be related to altered levels of PON1 protein in serum and ocular tissue. Our studies on *Pon1*$^{-/-}$ mice together with previous reports suggest that PON1 may be involved in AMD as a modulatory protein and that interplay with additional factors could influence its role in disease development and/or progression.

V. REFERENCES

Abecasis, G.R., Yashar, B.M., Zhao, Y., Ghiasvand, N.M., Zareparsi, S., Branham, K.E., Reddick, A.C., Trager, E.H., Yoshida, S., Bahling, J., Filippova, E., Elner, S., Johnson, M.W., Vine, A.K., Sieving, P.A., Jacobson, S.G., Richards, J.E., Swaroop, A., 2004. Age-related macular degeneration: a high-resolution genome scan for susceptibility loci in a population enriched for late-stage disease. Am J Hum Genet 74, 482-494.

Ablonczy, Z., Higbee, D., Anderson, D.M., Dahrouj, M., Grey, A.C., Gutierrez, D., Koutalos, Y., Schey, K.L., Hanneken, A., Crouch, R.K., 2013. Lack of correlation between the spatial distribution of A2E and lipofuscin fluorescence in the human retinal pigment epithelium. Invest Ophthalmol Vis Sci 54, 5535-5542.

Adams, M.K., Simpson, J.A., Richardson, A.J., Guymer, R.H., Williamson, E., Cantsilieris, S., English, D.R., Aung, K.Z., Makeyeva, G.A., Giles, G.G., Hopper, J., Robman, L.D., Baird, P.N., 2012. Can genetic associations change with age? CFH and age-related macular degeneration. Hum Mol Genet 21, 5229-5236.

Adelman, R., Saul, R.L., Ames, B.N., 1988. Oxidative damage to DNA: relation to species metabolic rate and life span. Proc Natl Acad Sci U S A 85, 2706-2708.

Aharoni, S., Aviram, M., Fuhrman, B., 2013. Paraoxonase 1 (PON1) reduces macrophage inflammatory responses. Atherosclerosis 228, 353-361.

Ahmed, Z., Babaei, S., Maguire, G.F., Draganov, D., Kuksis, A., La Du, B.N., Connelly, P.W., 2003. Paraoxonase-1 reduces monocyte chemotaxis and adhesion to endothelial cells due to oxidation of palmitoyl, linoleoyl glycerophosphorylcholine. Cardiovasc Res 57, 225-231.

Aldridge, W.N., 1953. Serum esterases. II. An enzyme hydrolysing diethyl p-nitrophenyl phosphate (E600) and its identity with the A-esterase of mammalian sera. Biochem J 53, 117-124.

Altenhofer, S., Witte, I., Teiber, J.F., Wilgenbus, P., Pautz, A., Li, H., Daiber, A., Witan, H., Clement, A.M., Forstermann, U., Horke, S., 2010. One enzyme, two functions: PON2 prevents mitochondrial superoxide formation and apoptosis independent from its lactonase activity. J Biol Chem 285, 24398-24403.

Ambati, J., Anand, A., Fernandez, S., Sakurai, E., Lynn, B.C., Kuziel, W.A., Rollins, B.J., Ambati, B.K., 2003. An animal model of age-related macular degeneration in senescent Ccl-2- or Ccr-2-deficient mice. Nat Med 9, 1390-1397.

Ambati, J., Atkinson, J.P., Gelfand, B.D., 2013. Immunology of age-related macular degeneration. Nat Rev Immunol 13, 438-451.

Anderson, J.L., Adams, C.D., Antman, E.M., Bridges, C.R., Califf, R.M., Casey, D.E., Jr., Chavey, W.E., 2nd, Fesmire, F.M., Hochman, J.S., Levin, T.N., Lincoff, A.M., Peterson, E.D., Theroux, P., Wenger, N.K., Wright, R.S., Smith, S.C., Jr., Jacobs, A.K., Halperin, J.L., Hunt, S.A., Krumholz, H.M., Kushner, F.G., Lytle, B.W., Nishimura, R., Ornato, J.P., Page, R.L., Riegel, B., 2007. ACC/AHA 2007 guidelines for the management of patients with unstable angina/non ST-elevation myocardial infarction: a report of the American College of Cardiology/American Heart Association Task Force on Practice Guidelines (Writing Committee to Revise the 2002 Guidelines for the Management of Patients With Unstable Angina/Non ST-Elevation Myocardial Infarction): developed in collaboration with the American College of Emergency Physicians, the Society for Cardiovascular Angiography and Interventions, and the Society of Thoracic Surgeons: endorsed by the American Association of Cardiovascular and Pulmonary

Rehabilitation and the Society for Academic Emergency Medicine. Circulation 116, e148-304.

Ates, O., Azizi, S., Alp, H.H., Kiziltunc, A., Beydemir, S., Cinici, E., Kocer, I., Baykal, O., 2009. Decreased serum paraoxonase 1 activity and increased serum homocysteine and malondialdehyde levels in age-related macular degeneration. Tohoku J Exp Med 217, 17-22.

Aviram, M., Rosenblat, M., Billecke, S., Erogul, J., Sorenson, R., Bisgaier, C.L., Newton, R.S., La Du, B., 1999. Human serum paraoxonase (PON 1) is inactivated by oxidized low density lipoprotein and preserved by antioxidants. Free Radic Biol Med 26, 892-904.

Aviram, M., Rosenblat, M., Bisgaier, C.L., Newton, R.S., Primo-Parmo, S.L., La Du, B.N., 1998. Paraoxonase inhibits high-density lipoprotein oxidation and preserves its functions. A possible peroxidative role for paraoxonase. J Clin Invest 101, 1581-1590.

Baird, P.N., Chu, D., Guida, E., Vu, H.T., Guymer, R., 2004. Association of the M55L and Q192R paraoxonase gene polymorphisms with age-related macular degeneration. Am J Ophthalmol 138, 665-666.

Barral, S., Francis, P.J., Schultz, D.W., Schain, M.B., Haynes, C., Majewski, J., Ott, J., Acott, T., Weleber, R.G., Klein, M.L., 2006. Expanded genome scan in extended families with age-related macular degeneration. Invest Ophthalmol Vis Sci 47, 5453-5459.

Baskol, G., Karakucuk, S., Oner, A.O., Baskol, M., Kocer, D., Mirza, E., Saraymen, R., Ustdal, M., 2006. Serum paraoxonase 1 activity and lipid peroxidation levels in patients with age-related macular degeneration. Ophthalmologica 220, 12-16.

Beatty, S., Koh, H., Phil, M., Henson, D., Boulton, M., 2000. The role of oxidative stress in the pathogenesis of age-related macular degeneration. Surv Ophthalmol 45, 115-134.

Besler, C., Heinrich, K., Rohrer, L., Doerries, C., Riwanto, M., Shih, D.M., Chroni, A., Yonekawa, K., Stein, S., Schaefer, N., Mueller, M., Akhmedov, A., Daniil, G., Manes, C., Templin, C., Wyss, C., Maier, W., Tanner, F.C., Matter, C.M., Corti, R., Furlong, C., Lusis, A.J., von Eckardstein, A., Fogelman, A.M., Luscher, T.F., Landmesser, U., 2011. Mechanisms underlying adverse effects of HDL on eNOS-activating pathways in patients with coronary artery disease. J Clin Invest 121, 2693-2708.

Billecke, S., Draganov, D., Counsell, R., Stetson, P., Watson, C., Hsu, C., La Du, B.N., 2000. Human serum paraoxonase (PON1) isozymes Q and R hydrolyze lactones and cyclic carbonate esters. Drug Metab Dispos 28, 1335-1342.

Bligh, E.G., Dyer, W.J., 1959. A rapid method of total lipid extraction and purification. Can J Biochem Physiol 37, 911-917.

Booij, J.C., Baas, D.C., Beisekeeva, J., Gorgels, T.G., Bergen, A.A., 2010. The dynamic nature of Bruch's membrane. Prog Retin Eye Res 29, 1-18.

Bora, P.S., Hu, Z., Tezel, T.H., Sohn, J.H., Kang, S.G., Cruz, J.M., Bora, N.S., Garen, A., Kaplan, H.J., 2003. Immunotherapy for choroidal neovascularization in a laser-induced mouse model simulating exudative (wet) macular degeneration. Proc Natl Acad Sci U S A 100, 2679-2684.

Bosch, E., Horwitz, J., Bok, D., 1993. Phagocytosis of outer segments by retinal pigment epithelium: phagosome-lysosome interaction. J Histochem Cytochem 41, 253-263.

Boulton, M., Dayhaw-Barker, P., 2001. The role of the retinal pigment epithelium: topographical variation and ageing changes. Eye (Lond) 15, 384-389.

Brion, M., Sanchez-Salorio, M., Corton, M., de la Fuente, M., Pazos, B., Othman, M., Swaroop, A., Abecasis, G., Sobrino, B., Carracedo, A., 2011. Genetic association study of age-related macular degeneration in the Spanish population. Acta Ophthalmol 89, e12-22.

Brophy, V.H., Hastings, M.D., Clendenning, J.B., Richter, R.J., Jarvik, G.P., Furlong, C.E., 2001a. Polymorphisms in the human paraoxonase (PON1) promoter. Pharmacogenetics 11, 77-84.

Brophy, V.H., Jampsa, R.L., Clendenning, J.B., McKinstry, L.A., Jarvik, G.P., Furlong, C.E., 2001b. Effects of 5' regulatory-region polymorphisms on paraoxonase-gene (PON1) expression. Am J Hum Genet 68, 1428-1436.

Brophy, V.H., Jarvik, G.P., Richter, R.J., Rozek, L.S., Schellenberg, G.D., Furlong, C.E., 2000. Analysis of paraoxonase (PON1) L55M status requires both genotype and phenotype. Pharmacogenetics 10, 453-460.

Cachafeiro, M., Bemelmans, A.P., Samardzija, M., Afanasieva, T., Pournaras, J.A., Grimm, C., Kostic, C., Philippe, S., Wenzel, A., Arsenijevic, Y., 2013. Hyperactivation of retina by light in mice leads to photoreceptor cell death mediated by VEGF and retinal pigment epithelium permeability. Cell Death Dis 4, e781.

Carpenter, A.E., Jones, T.R., Lamprecht, M.R., Clarke, C., Kang, I.H., Friman, O., Guertin, D.A., Chang, J.H., Lindquist, R.A., Moffat, J., Golland, P., Sabatini, D.M., 2006. CellProfiler: image analysis software for identifying and quantifying cell phenotypes. Genome Biol 7, R100.

Carter-Dawson, L.D., LaVail, M.M., 1979. Rods and cones in the mouse retina. I. Structural analysis using light and electron microscopy. J Comp Neurol 188, 245-262.

Chang, B., Mandal, M.N., Chavali, V.R., Hawes, N.L., Khan, N.W., Hurd, R.E., Smith, R.S., Davisson, M.L., Kopplin, L., Klein, B.E., Klein, R., Iyengar, S.K., Heckenlively, J.R., Ayyagari, R., 2008. Age-related retinal degeneration (arrd2) in a novel mouse model due to a nonsense mutation in the Mdm1 gene. Hum Mol Genet 17, 3929-3941.

Chen, W., Stambolian, D., Edwards, A.O., Branham, K.E., Othman, M., Jakobsdottir, J., Tosakulwong, N., Pericak-Vance, M.A., Campochiaro, P.A., Klein, M.L., Tan, P.L., Conley, Y.P., Kanda, A., Kopplin, L., Li, Y., Augustaitis, K.J., Karoukis, A.J., Scott, W.K., Agarwal, A., Kovach, J.L., Schwartz, S.G., Postel, E.A., Brooks, M., Baratz, K.H., Brown, W.L., Brucker, A.J., Orlin, A., Brown, G., Ho, A., Regillo, C., Donoso, L., Tian, L., Kaderli, B., Hadley, D., Hagstrom, S.A., Peachey, N.S., Klein, R., Klein, B.E., Gotoh, N., Yamashiro, K., Ferris Iii, F., Fagerness, J.A., Reynolds, R., Farrer, L.A., Kim, I.K., Miller, J.W., Corton, M., Carracedo, A., Sanchez-Salorio, M., Pugh, E.W., Doheny, K.F., Brion, M., Deangelis, M.M., Weeks, D.E., Zack, D.J., Chew, E.Y., Heckenlively, J.R., Yoshimura, N., Iyengar, S.K., Francis, P.J., Katsanis, N., Seddon, J.M., Haines, J.L., Gorin, M.B., Abecasis, G.R., Swaroop, A., 2010. Genetic variants near TIMP3 and high-density lipoprotein-associated loci influence susceptibility to age-related macular degeneration. Proc Natl Acad Sci U S A 107, 7401-7406.

Coffey, P.J., Gias, C., McDermott, C.J., Lundh, P., Pickering, M.C., Sethi, C., Bird, A., Fitzke, F.W., Maass, A., Chen, L.L., Holder, G.E., Luthert, P.J., Salt, T.E., Moss, S.E., Greenwood, J., 2007. Complement factor H deficiency in aged mice causes retinal abnormalities and visual dysfunction. Proc Natl Acad Sci U S A 104, 16651-16656.

Combadiere, C., Feumi, C., Raoul, W., Keller, N., Rodero, M., Pezard, A., Lavalette, S., Houssier, M., Jonet, L., Picard, E., Debre, P., Sirinyan, M., Deterre, P., Ferroukhi, T., Cohen, S.Y., Chauvaud, D., Jeanny, J.C., Chemtob, S., Behar-Cohen, F., Sennlaub, F., 2007. CX3CR1-dependent subretinal microglia cell accumulation is associated with cardinal features of age-related macular degeneration. J Clin Invest 117, 2920-2928.

Combadiere, C., Raoul, W., Guillonneau, X., Sennlaub, F., 2013. Comment on "Ccl2, Cx3cr1 and Ccl2/Cx3cr1 chemokine deficiencies are not sufficient to cause age-related retinal degeneration" by Luhmann et al. (Exp. Eye Res. 2013; 107: 80.doi: 10.1016). Exp Eye Res 111, 134-135.

Costa, L.G., Cole, T.B., Jarvik, G.P., Furlong, C.E., 2003. Functional genomic of the paraoxonase (PON1) polymorphisms: effects on pesticide sensitivity, cardiovascular disease, and drug metabolism. Annu Rev Med 54, 371-392.

Crabb, J.W., Miyagi, M., Gu, X., Shadrach, K., West, K.A., Sakaguchi, H., Kamei, M., Hasan, A., Yan, L., Rayborn, M.E., Salomon, R.G., Hollyfield, J.G., 2002. Drusen proteome analysis: an approach to the etiology of age-related macular degeneration. Proc Natl Acad Sci U S A 99, 14682-14687.

Curcio, C.A., Johnson, M., Huang, J.D., Rudolf, M., 2010. Apolipoprotein B-containing lipoproteins in retinal aging and age-related macular degeneration. J Lipid Res 51, 451-467.

Curcio, C.A., Johnson, M., Rudolf, M., Huang, J.D., 2011. The oil spill in ageing Bruch membrane. Br J Ophthalmol 95, 1638-1645.

Curcio, C.A., Presley, J.B., Malek, G., Medeiros, N.E., Avery, D.V., Kruth, H.S., 2005. Esterified and unesterified cholesterol in drusen and basal deposits of eyes with age-related maculopathy. Exp Eye Res 81, 731-741.

Curcio, C.A., Saunders, P.L., Younger, P.W., Malek, G., 2000. Peripapillary chorioretinal atrophy: Bruch's membrane changes and photoreceptor loss. Ophthalmology 107, 334-343.

Curcio, C.A., Sloan, K.R., Kalina, R.E., Hendrickson, A.E., 1990. Human photoreceptor topography. J Comp Neurol 292, 497-523.

Deakin, S., Leviev, I., Brulhart-Meynet, M.C., James, R.W., 2003. Paraoxonase-1 promoter haplotypes and serum paraoxonase: a predominant role for polymorphic position - 107, implicating the Sp1 transcription factor. Biochem J 372, 643-649.

Deakin, S.P., James, R.W., 2004. Genetic and environmental factors modulating serum concentrations and activities of the antioxidant enzyme paraoxonase-1. Clin Sci (Lond) 107, 435-447.

Di Liegro, C.M., Schiera, G., Di Liegro, I., 2014. Regulation of mRNA transport, localization and translation in the nervous system of mammals (Review). Int J Mol Med 33, 747-762.

Doyle, S.L., Campbell, M., Ozaki, E., Salomon, R.G., Mori, A., Kenna, P.F., Farrar, G.J., Kiang, A.S., Humphries, M.M., Lavelle, E.C., O'Neill, L.A., Hollyfield, J.G., Humphries, P., 2012. NLRP3 has a protective role in age-related macular degeneration through the induction of IL-18 by drusen components. Nat Med 18, 791-798.

Draganov, D.I., La Du, B.N., 2004. Pharmacogenetics of paraoxonases: a brief review. Naunyn Schmiedebergs Arch Pharmacol 369, 78-88.

Draganov, D.I., Stetson, P.L., Watson, C.E., Billecke, S.S., La Du, B.N., 2000. Rabbit serum paraoxonase 3 (PON3) is a high density lipoprotein-associated lactonase and protects low density lipoprotein against oxidation. J Biol Chem 275, 33435-33442.

Draganov, D.I., Teiber, J.F., Speelman, A., Osawa, Y., Sunahara, R., La Du, B.N., 2005. Human paraoxonases (PON1, PON2, and PON3) are lactonases with overlapping and distinct substrate specificities. J Lipid Res 46, 1239-1247.

Duncan, K.G., Hosseini, K., Bailey, K.R., Yang, H., Lowe, R.J., Matthes, M.T., Kane, J.P., LaVail, M.M., Schwartz, D.M., Duncan, J.L., 2009. Expression of reverse cholesterol transport proteins ATP-binding cassette A1 (ABCA1) and scavenger receptor BI (SR-BI) in the retina and retinal pigment epithelium. Br J Ophthalmol 93, 1116-1120.

Dunn, K.C., Aotaki-Keen, A.E., Putkey, F.R., Hjelmeland, L.M., 1996. ARPE-19, a human retinal pigment epithelial cell line with differentiated properties. Exp Eye Res 62, 155-169.

Dwyer, M.A., Kazmin, D., Hu, P., McDonnell, D.P., Malek, G., 2011. Research resource: nuclear receptor atlas of human retinal pigment epithelial cells: potential relevance to age-related macular degeneration. Mol Endocrinol 25, 360-372.

Edwards, A.O., Ritter, R., 3rd, Abel, K.J., Manning, A., Panhuysen, C., Farrer, L.A., 2005. Complement factor H polymorphism and age-related macular degeneration. Science 308, 421-424.

Erdos, E.G., Debay, C.R., Westerman, M.P., 1959. Activation and inhibition of the arylesterase of human serum. Nature 184, 430-431.

Esfandiary, H., Chakravarthy, U., Patterson, C., Young, I., Hughes, A.E., 2005. Association study of detoxification genes in age related macular degeneration. Br J Ophthalmol 89, 470-474.

Fagerness, J.A., Maller, J.B., Neale, B.M., Reynolds, R.C., Daly, M.J., Seddon, J.M., 2009. Variation near complement factor I is associated with risk of advanced AMD. Eur J Hum Genet 17, 100-104.

Fisher, S.A., Abecasis, G.R., Yashar, B.M., Zareparsi, S., Swaroop, A., Iyengar, S.K., Klein, B.E., Klein, R., Lee, K.E., Majewski, J., Schultz, D.W., Klein, M.L., Seddon, J.M., Santangelo, S.L., Weeks, D.E., Conley, Y.P., Mah, T.S., Schmidt, S., Haines, J.L., Pericak-Vance, M.A., Gorin, M.B., Schulz, H.L., Pardi, F., Lewis, C.M., Weber, B.H., 2005. Meta-analysis of genome scans of age-related macular degeneration. Hum Mol Genet 14, 2257-2264.

Fliesler, S.J., Anderson, R.E., 1983. Chemistry and metabolism of lipids in the vertebrate retina. Prog Lipid Res 22, 79-131.

Friedman, E., 2004. Update of the vascular model of AMD. Br J Ophthalmol 88, 161-163.

Furlong, C.E., Richter, R.J., Seidel, S.L., Motulsky, A.G., 1988. Role of genetic polymorphism of human plasma paraoxonase/arylesterase in hydrolysis of the insecticide metabolites chlorpyrifos oxon and paraoxon. Am J Hum Genet 43, 230-238.

Garin, M.C., Kalix, B., Morabia, A., James, R.W., 2005. Small, dense lipoprotein particles and reduced paraoxonase-1 in patients with the metabolic syndrome. J Clin Endocrinol Metab 90, 2264-2269.

Geldmacher-von Mallinckrodt, M., Lindorft, H. H., Petenyi, M., Flugel, M., Fischer, T., Hiller, T, 1973. Genetisch determinierter Polymorphismus de menschlichen Serum-Paroxonase (E.C.3.1.1.2). Humangenetik 17, 331-335.

Giusto, N.M., Pasquare, S.J., Salvador, G.A., Castagnet, P.I., Roque, M.E., Ilincheta de Boschero, M.G., 2000. Lipid metabolism in vertebrate retinal rod outer segments. Prog Lipid Res 39, 315-391.

Glenn, J.V., Mahaffy, H., Wu, K., Smith, G., Nagai, R., Simpson, D.A., Boulton, M.E., Stitt, A.W., 2009. Advanced glycation end product (AGE) accumulation on Bruch's membrane: links to age-related RPE dysfunction. Invest Ophthalmol Vis Sci 50, 441-451.

Gold, B., Merriam, J.E., Zernant, J., Hancox, L.S., Taiber, A.J., Gehrs, K., Cramer, K., Neel, J., Bergeron, J., Barile, G.R., Smith, R.T., Hageman, G.S., Dean, M., Allikmets, R., 2006. Variation in factor B (BF) and complement component 2 (C2) genes is associated with age-related macular degeneration. Nat Genet 38, 458-462.

Gouedard, C., Barouki, R., Morel, Y., 2004a. Dietary polyphenols increase paraoxonase 1 gene expression by an aryl hydrocarbon receptor-dependent mechanism. Mol Cell Biol 24, 5209-5222.

Gouedard, C., Barouki, R., Morel, Y., 2004b. Induction of the paraoxonase-1 gene expression by resveratrol. Arterioscler Thromb Vasc Biol 24, 2378-2383.

Gouedard, C., Koum-Besson, N., Barouki, R., Morel, Y., 2003. Opposite regulation of the human paraoxonase-1 gene PON-1 by fenofibrate and statins. Mol Pharmacol 63, 945-956.

Grimm, C., Reme, C.E., 2013. Light damage as a model of retinal degeneration. Methods Mol Biol 935, 87-97.

Guymer, R.H., Chong, E.W., 2006. Modifiable risk factors for age-related macular degeneration. Med J Aust 184, 455-458.

Hafezi, F., Grimm, C., Simmen, B.C., Wenzel, A., Reme, C.E., 2000. Molecular ophthalmology: an update on animal models for retinal degenerations and dystrophies. Br J Ophthalmol 84, 922-927.

Hafezi, F., Marti, A., Munz, K., Reme, C.E., 1997. Light-induced apoptosis: differential timing in the retina and pigment epithelium. Exp Eye Res 64, 963-970.

Haimi, P., Uphoff, A., Hermansson, M., Somerharju, P., 2006. Software tools for analysis of mass spectrometric lipidome data. Anal Chem 78, 8324-8331.

Hammond, C.J., Webster, A.R., Snieder, H., Bird, A.C., Gilbert, C.E., Spector, T.D., 2002. Genetic influence on early age-related maculopathy: a twin study. Ophthalmology 109, 730-736.

Handa, J.T., 2012. How does the macula protect itself from oxidative stress? Mol Aspects Med 33, 418-435.

Handa, J.T., Verzijl, N., Matsunaga, H., Aotaki-Keen, A., Lutty, G.A., te Koppele, J.M., Miyata, T., Hjelmeland, L.M., 1999. Increase in the advanced glycation end product pentosidine in Bruch's membrane with age. Invest Ophthalmol Vis Sci 40, 775-779.

Hara, S., Shike, T., Takasu, N., Mizui, T., 1997. Lysophosphatidylcholine promotes cholesterol efflux from mouse macrophage foam cells. Arterioscler Thromb Vasc Biol 17, 1258-1266.

Harel, M., Aharoni, A., Gaidukov, L., Brumshtein, B., Khersonsky, O., Meged, R., Dvir, H., Ravelli, R.B., McCarthy, A., Toker, L., Silman, I., Sussman, J.L., Tawfik, D.S., 2004. Structure and evolution of the serum paraoxonase family of detoxifying and anti-atherosclerotic enzymes. Nat Struct Mol Biol 11, 412-419.

Hassett, C., Richter, R.J., Humbert, R., Chapline, C., Crabb, J.W., Omiecinski, C.J., Furlong, C.E., 1991. Characterization of cDNA clones encoding rabbit and human serum paraoxonase: the mature protein retains its signal sequence. Biochemistry 30, 10141-10149.

Hollyfield, J.G., Perez, V.L., Salomon, R.G., 2010. A hapten generated from an oxidation fragment of docosahexaenoic acid is sufficient to initiate age-related macular degeneration. Mol Neurobiol 41, 290-298.

Horke, S., Witte, I., Wilgenbus, P., Kruger, M., Strand, D., Forstermann, U., 2007. Paraoxonase-2 reduces oxidative stress in vascular cells and decreases endoplasmic reticulum stress-induced caspase activation. Circulation 115, 2055-2064.

Hu, J.B., D., 2000. A cell culture medium that supports the differentiation of human retinal pigment epithelium into functionally polarized monolayers. Molecular Vision 7, 14-19.

Humbert, R., Adler, D.A., Disteche, C.M., Hassett, C., Omiecinski, C.J., Furlong, C.E., 1993. The molecular basis of the human serum paraoxonase activity polymorphism. Nat Genet 3, 73-76.

Ikeda, T., Obayashi, H., Hasegawa, G., Nakamura, N., Yoshikawa, T., Imamura, Y., Koizumi, K., Kinoshita, S., 2001. Paraoxonase gene polymorphisms and plasma oxidized low-density lipoprotein level as possible risk factors for exudative age-related macular degeneration. Am J Ophthalmol 132, 191-195.

Imamura, Y., Noda, S., Hashizume, K., Shinoda, K., Yamaguchi, M., Uchiyama, S., Shimizu, T., Mizushima, Y., Shirasawa, T., Tsubota, K., 2006. Drusen, choroidal neovascularization, and retinal pigment epithelium dysfunction in SOD1-deficient mice: a model of age-related macular degeneration. Proc Natl Acad Sci U S A 103, 11282-11287.

Ishida, B.Y., Duncan, K.G., Bailey, K.R., Kane, J.P., Schwartz, D.M., 2006. High density lipoprotein mediated lipid efflux from retinal pigment epithelial cells in culture. Br J Ophthalmol 90, 616-620.

Isik, B., Ceylan, A., Isik, R., 2007. Oxidative stress in smokers and non-smokers. Inhal Toxicol 19, 767-769.

Iyengar, S.K., Song, D., Klein, B.E., Klein, R., Schick, J.H., Humphrey, J., Millard, C., Liptak, R., Russo, K., Jun, G., Lee, K.E., Fijal, B., Elston, R.C., 2004. Dissection of genomewide-scan data in extended families reveals a major locus and oligogenic susceptibility for age-related macular degeneration. Am J Hum Genet 74, 20-39.

Jager, R.D., Mieler, W.F., Miller, J.W., 2008. Age-related macular degeneration. N Engl J Med 358, 2606-2617.

Jaichander, P., Selvarajan, K., Garelnabi, M., Parthasarathy, S., 2008. Induction of paraoxonase 1 and apolipoprotein A-I gene expression by aspirin. J Lipid Res 49, 2142-2148.

Jakubowski, H., Ambrosius, W.T., Pratt, J.H., 2001. Genetic determinants of homocysteine thiolactonase activity in humans: implications for atherosclerosis. FEBS Lett 491, 35-39.

James, R.W., Brulhart-Meynet, M.C., Singh, A.K., Riederer, B., Seidler, U., Out, R., Van Berkel, T.J., Deakin, S., 2010. The scavenger receptor class B, type I is a primary determinant of paraoxonase-1 association with high-density lipoproteins. Arterioscler Thromb Vasc Biol 30, 2121-2127.

James, R.W., Deakin, S.P., 2004. The importance of high-density lipoproteins for paraoxonase-1 secretion, stability, and activity. Free Radic Biol Med 37, 1986-1994.

James, R.W., Leviev, I., Ruiz, J., Passa, P., Froguel, P., Garin, M.C., 2000. Promoter polymorphism T(-107)C of the paraoxonase PON1 gene is a risk factor for coronary heart disease in type 2 diabetic patients. Diabetes 49, 1390-1393.

Jarvik, G.P., Hatsukami, T.S., Carlson, C., Richter, R.J., Jampsa, R., Brophy, V.H., Margolin, S., Rieder, M., Nickerson, D., Schellenberg, G.D., Heagerty, P.J., Furlong, C.E., 2003. Paraoxonase activity, but not haplotype utilizing the linkage disequilibrium structure, predicts vascular disease. Arterioscler Thromb Vasc Biol 23, 1465-1471.

Jarvik, G.P., Rozek, L.S., Brophy, V.H., Hatsukami, T.S., Richter, R.J., Schellenberg, G.D., Furlong, C.E., 2000. Paraoxonase (PON1) phenotype is a better predictor of vascular disease than is PON1(192) or PON1(55) genotype. Arterioscler Thromb Vasc Biol 20, 2441-2447.

Johnson, L.V., Ozaki, S., Staples, M.K., Erickson, P.A., Anderson, D.H., 2000. A potential role for immune complex pathogenesis in drusen formation. Exp Eye Res 70, 441-449.

Joly, S., Francke, M., Ulbricht, E., Beck, S., Seeliger, M., Hirrlinger, P., Hirrlinger, J., Lang, K.S., Zinkernagel, M., Odermatt, B., Samardzija, M., Reichenbach, A., Grimm, C., Reme, C.E., 2009. Cooperative phagocytes: resident microglia and bone marrow immigrants remove dead photoreceptors in retinal lesions. Am J Pathol 174, 2310-2323.

Joly, S., Lange, C., Thiersch, M., Samardzija, M., Grimm, C., 2008. Leukemia inhibitory factor extends the lifespan of injured photoreceptors in vivo. J Neurosci 28, 13765-13774.

Justilien, V., Pang, J.J., Renganathan, K., Zhan, X., Crabb, J.W., Kim, S.R., Sparrow, J.R., Hauswirth, W.W., Lewin, A.S., 2007. SOD2 knockdown mouse model of early AMD. Invest Ophthalmol Vis Sci 48, 4407-4420.

Keeler, C.E., 1924. The Inheritance of a Retinal Abnormality in White Mice. Proc Natl Acad Sci U S A 10, 329-333.

Khandhadia, S., Lotery, A., 2010. Oxidation and age-related macular degeneration: insights from molecular biology. Expert Rev Mol Med 12, e34.

Khateeb, J., Gantman, A., Kreitenberg, A.J., Aviram, M., Fuhrman, B., 2010. Paraoxonase 1 (PON1) expression in hepatocytes is upregulated by pomegranate polyphenols: a role for PPAR-gamma pathway. Atherosclerosis 208, 119-125.

Khersonsky, O., Tawfik, D.S., 2005. Structure-reactivity studies of serum paraoxonase PON1 suggest that its native activity is lactonase. Biochemistry 44, 6371-6382.

Khersonsky, O., Tawfik, D.S., 2006. The histidine 115-histidine 134 dyad mediates the lactonase activity of mammalian serum paraoxonases. J Biol Chem 281, 7649-7656.

Kim, J.H., Lee, S.J., Kim, K.W., Yu, Y.S., 2012. Oxidized low density lipoprotein-induced senescence of retinal pigment epithelial cells is followed by outer blood-retinal barrier dysfunction. Int J Biochem Cell Biol 44, 808-814.

Kinnunen, K., Petrovski, G., Moe, M.C., Berta, A., Kaarniranta, K., 2012. Molecular mechanisms of retinal pigment epithelium damage and development of age-related macular degeneration. Acta Ophthalmol 90, 299-309.

Kiser, P.D., Golczak, M., Maeda, A., Palczewski, K., 2012. Key enzymes of the retinoid (visual) cycle in vertebrate retina. Biochim Biophys Acta 1821, 137-151.

Klaver, C.C., Wolfs, R.C., Assink, J.J., van Duijn, C.M., Hofman, A., de Jong, P.T., 1998. Genetic risk of age-related maculopathy. Population-based familial aggregation study. Arch Ophthalmol 116, 1646-1651.

Klein, M.L., Schultz, D.W., Edwards, A., Matise, T.C., Rust, K., Berselli, C.B., Trzupek, K., Weleber, R.G., Ott, J., Wirtz, M.K., Acott, T.S., 1998. Age-related macular degeneration. Clinical features in a large family and linkage to chromosome 1q. Arch Ophthalmol 116, 1082-1088.

Klein, R., Klein, B.E., Jensen, S.C., Meuer, S.M., 1997. The five-year incidence and progression of age-related maculopathy: the Beaver Dam Eye Study. Ophthalmology 104, 7-21.

Klein, R.J., Zeiss, C., Chew, E.Y., Tsai, J.Y., Sackler, R.S., Haynes, C., Henning, A.K., SanGiovanni, J.P., Mane, S.M., Mayne, S.T., Bracken, M.B., Ferris, F.L., Ott, J., Barnstable, C., Hoh, J., 2005. Complement factor H polymorphism in age-related macular degeneration. Science 308, 385-389.

Kleinman, M.E., Yamada, K., Takeda, A., Chandrasekaran, V., Nozaki, M., Baffi, J.Z., Albuquerque, R.J., Yamasaki, S., Itaya, M., Pan, Y., Appukuttan, B., Gibbs, D., Yang, Z., Kariko, K., Ambati, B.K., Wilgus, T.A., DiPietro, L.A., Sakurai, E., Zhang, K., Smith, J.R., Taylor, E.W., Ambati, J., 2008. Sequence- and target-independent angiogenesis suppression by siRNA via TLR3. Nature 452, 591-597.

Kolb, H., 2003. How the Retina Works, American Scientist, pp. 28-35.

La Du, B.N., Aviram, M., Billecke, S., Navab, M., Primo-Parmo, S., Sorenson, R.C., Standiford, T.J., 1999. On the physiological role(s) of the paraoxonases. Chem Biol Interact 119-120, 379-388.

Leviev, I., James, R.W., 2000. Promoter polymorphisms of human paraoxonase PON1 gene and serum paraoxonase activities and concentrations. Arterioscler Thromb Vasc Biol 20, 516-521.

Li, C.M., Chung, B.H., Presley, J.B., Malek, G., Zhang, X., Dashti, N., Li, L., Chen, J., Bradley, K., Kruth, H.S., Curcio, C.A., 2005. Lipoprotein-like particles and cholesteryl esters in human Bruch's membrane: initial characterization. Invest Ophthalmol Vis Sci 46, 2576-2586.

Liu, N., Zhang, K., Zhao, H., 2008. Haplotype-association analysis. Adv Genet 60, 335-405.

Luhmann, U.F., Carvalho, L.S., Robbie, S.J., Bainbridge, J.W., Ali, R.R., 2013a. Reply to comment on "Ccl2, Cx3cr1 and Ccl2/Cx3cr1 chemokine deficiencies are not sufficient to cause age-related retinal degeneration" by Luhmann et al. (Exp. Eye Res. 107, February 2013, 80-87). Exp Eye Res 111, 136.

Luhmann, U.F., Carvalho, L.S., Robbie, S.J., Cowing, J.A., Duran, Y., Munro, P.M., Bainbridge, J.W., Ali, R.R., 2013b. Ccl2, Cx3cr1 and Ccl2/Cx3cr1 chemokine deficiencies are not sufficient to cause age-related retinal degeneration. Exp Eye Res 107, 80-87.

Mackness, B., Davies, G.K., Turkie, W., Lee, E., Roberts, D.H., Hill, E., Roberts, C., Durrington, P.N., Mackness, M.I., 2001. Paraoxonase status in coronary heart disease: are activity and concentration more important than genotype? Arterioscler Thromb Vasc Biol 21, 1451-1457.

Mackness, B., Durrington, P.N., Abuashia, B., Boulton, A.J., Mackness, M.I., 2000a. Low paraoxonase activity in type II diabetes mellitus complicated by retinopathy. Clin Sci (Lond) 98, 355-363.

Mackness, B., Mackness, M.I., Arrol, S., Turkie, W., Durrington, P.N., 1998. Effect of the human serum paraoxonase 55 and 192 genetic polymorphisms on the protection by high density lipoprotein against low density lipoprotein oxidative modification. FEBS Lett 423, 57-60.

MacKness, B., Mackness, M.I., Durrington, P.N., Arrol, S., Evans, A.E., McMaster, D., Ferrieres, J., Ruidavets, J.B., Williams, N.R., Howard, A.N., 2000b. Paraoxonase activity in two healthy populations with differing rates of coronary heart disease. Eur J Clin Invest 30, 4-10.

Mackness, M.I., 1989. 'A'-esterases. Enzymes looking for a role? Biochem Pharmacol 38, 385-390.

Mackness, M.I., Arrol, S., Abbott, C., Durrington, P.N., 1993. Protection of low-density lipoprotein against oxidative modification by high-density lipoprotein associated paraoxonase. Atherosclerosis 104, 129-135.

Mackness, M.I., Arrol, S., Durrington, P.N., 1991. Paraoxonase prevents accumulation of lipoperoxides in low-density lipoprotein. FEBS Lett 286, 152-154.

Mackness, M.I., Durrington, P.N., 1995. HDL, its enzymes and its potential to influence lipid peroxidation. Atherosclerosis 115, 243-253.

Majewski, J., Schultz, D.W., Weleber, R.G., Schain, M.B., Edwards, A.O., Matise, T.C., Acott, T.S., Ott, J., Klein, M.L., 2003. Age-related macular degeneration--a genome scan in extended families. Am J Hum Genet 73, 540-550.

Majji, A.B., Cao, J., Chang, K.Y., Hayashi, A., Aggarwal, S., Grebe, R.R., De Juan, E., Jr., 2000. Age-related retinal pigment epithelium and Bruch's membrane degeneration in senescence-accelerated mouse. Invest Ophthalmol Vis Sci 41, 3936-3942.

Malek, G., Johnson, L.V., Mace, B.E., Saloupis, P., Schmechel, D.E., Rickman, D.W., Toth, C.A., Sullivan, P.M., Bowes Rickman, C., 2005. Apolipoprotein E allele-dependent pathogenesis: a model for age-related retinal degeneration. Proc Natl Acad Sci U S A 102, 11900-11905.

Maller, J.B., Fagerness, J.A., Reynolds, R.C., Neale, B.M., Daly, M.J., Seddon, J.M., 2007. Variation in complement factor 3 is associated with risk of age-related macular degeneration. Nat Genet 39, 1200-1201.

Marchegiani, F., Marra, M., Olivieri, F., Cardelli, M., James, R.W., Boemi, M., Franceschi, C., 2008. Paraoxonase 1: genetics and activities during aging. Rejuvenation Res 11, 113-127.

Marsillach, J., Mackness, B., Mackness, M., Riu, F., Beltran, R., Joven, J., Camps, J., 2008. Immunohistochemical analysis of paraoxonases-1, 2, and 3 expression in normal mouse tissues. Free Radic Biol Med 45, 146-157.

Masland, R.H., Martin, P.R., 2007. The unsolved mystery of vision. Curr Biol 17, R577-582.

Mastorikou, M., Mackness, B., Liu, Y., Mackness, M., 2008. Glycation of paraoxonase-1 inhibits its activity and impairs the ability of high-density lipoprotein to metabolize membrane lipid hydroperoxides. Diabet Med 25, 1049-1055.

Mata, N.L., Tzekov, R.T., Liu, X., Weng, J., Birch, D.G., Travis, G.H., 2001. Delayed dark-adaptation and lipofuscin accumulation in abcr+/- mice: implications for involvement of ABCR in age-related macular degeneration. Invest Ophthalmol Vis Sci 42, 1685-1690.

Mishima, H., Hasebe, H., 1978. Some observations in the fine structure of age changes of the mouse retinal pigment epithelium. Albrecht Von Graefes Arch Klin Exp Ophthalmol 209, 1-9.

Mullins, R.F., Russell, S.R., Anderson, D.H., Hageman, G.S., 2000. Drusen associated with aging and age-related macular degeneration contain proteins common to extracellular deposits associated with atherosclerosis, elastosis, amyloidosis, and dense deposit disease. FASEB J 14, 835-846.

Neale, B.M., Fagerness, J., Reynolds, R., Sobrin, L., Parker, M., Raychaudhuri, S., Tan, P.L., Oh, E.C., Merriam, J.E., Souied, E., Bernstein, P.S., Li, B., Frederick, J.M., Zhang, K., Brantley, M.A., Jr., Lee, A.Y., Zack, D.J., Campochiaro, B., Campochiaro, P., Ripke, S., Smith, R.T., Barile, G.R., Katsanis, N., Allikmets, R., Daly, M.J., Seddon, J.M., 2010. Genome-wide association study of advanced age-related macular degeneration identifies a role of the hepatic lipase gene (LIPC). Proc Natl Acad Sci U S A 107, 7395-7400.

Newman, A.M., Gallo, N.B., Hancox, L.S., Miller, N.J., Radeke, C.M., Maloney, M.A., Cooper, J.B., Hageman, G.S., Anderson, D.H., Johnson, L.V., Radeke, M.J., 2012. Systems-level analysis of age-related macular degeneration reveals global biomarkers and phenotype-specific functional networks. Genome Med 4, 16.

Ng, C.J., Shih, D.M., Hama, S.Y., Villa, N., Navab, M., Reddy, S.T., 2005. The paraoxonase gene family and atherosclerosis. Free Radic Biol Med 38, 153-163.

Oczos, J., Grimm, C., Barthelmes, D., Sutter, F., Menghini, M., Kloeckener-Gruissem, B., Berger, W., 2013. Regulatory regions of the paraoxonase 1 (PON1) gene are associated with neovascular age-related macular degeneration (AMD). Age (Dordr) 35, 1651-1662.

Oda, M.N., Bielicki, J.K., Ho, T.T., Berger, T., Rubin, E.M., Forte, T.M., 2002. Paraoxonase 1 overexpression in mice and its effect on high-density lipoproteins. Biochem Biophys Res Commun 290, 921-927.

Palczewski, K., 2012. Chemistry and biology of vision. J Biol Chem 287, 1612-1619.

Pauer, G.J., Sturgill, G.M., Peachey, N.S., Hagstrom, S.A., 2010. Protective effect of paraoxonase 1 gene variant Gln192Arg in age-related macular degeneration. Am J Ophthalmol 149, 513-522.

Pfeffer, B.A., 1991. Improved methodology for cell culture of human and monkey retinal pigment epithelium. Progress in Retinal Research 10, 251-291.

Pfeffer, B.A., Clark, V.M., Flannery, J.G., Bok, D., 1986. Membrane receptors for retinol-binding protein in cultured human retinal pigment epithelium. Invest Ophthalmol Vis Sci 27, 1031-1040.

Philp, N.J., Wang, D., Yoon, H., Hjelmeland, L.M., 2003. Polarized expression of monocarboxylate transporters in human retinal pigment epithelium and ARPE-19 cells. Invest Ophthalmol Vis Sci 44, 1716-1721.

Philp, N.J., Yoon, H., Grollman, E.F., 1998. Monocarboxylate transporter MCT1 is located in the apical membrane and MCT3 in the basal membrane of rat RPE. Am J Physiol 274, R1824-1828.

Playfer, J.R., Eze, L.C., Bullen, M.F., Evans, D.A., 1976. Genetic polymorphism and interethnic variability of plasma paroxonase activity. J Med Genet 13, 337-342.

Prasad, S., Galetta, S.L., 2011. Anatomy and physiology of the afferent visual system. Handb Clin Neurol 102, 3-19.

Primo-Parmo, S.L., Sorenson, R.C., Teiber, J., La Du, B.N., 1996. The human serum paraoxonase/arylesterase gene (PON1) is one member of a multigene family. Genomics 33, 498-507.

Ramkumar, H.L., Zhang, J., Chan, C.C., 2010. Retinal ultrastructure of murine models of dry age-related macular degeneration (AMD). Prog Retin Eye Res 29, 169-190.

Ramrattan, R.S., van der Schaft, T.L., Mooy, C.M., de Bruijn, W.C., Mulder, P.G., de Jong, P.T., 1994. Morphometric analysis of Bruch's membrane, the choriocapillaris, and the choroid in aging. Invest Ophthalmol Vis Sci 35, 2857-2864.

Reme, C.E., Grimm, C., Hafezi, F., Wenzel, A., Williams, T.P., 2000. Apoptosis in the Retina: The Silent Death of Vision. News Physiol Sci 15, 120-124.

Richter, R.J., Furlong, C.E., 1999. Determination of paraoxonase (PON1) status requires more than genotyping. Pharmacogenetics 9, 745-753.

Rizzolo, L.J., Peng, S., Luo, Y., Xiao, W., 2011. Integration of tight junctions and claudins with the barrier functions of the retinal pigment epithelium. Prog Retin Eye Res 30, 296-323.

Rosenblat, M., Draganov, D., Watson, C.E., Bisgaier, C.L., La Du, B.N., Aviram, M., 2003. Mouse macrophage paraoxonase 2 activity is increased whereas cellular paraoxonase 3 activity is decreased under oxidative stress. Arterioscler Thromb Vasc Biol 23, 468-474.

Rosenblat, M., Gaidukov, L., Khersonsky, O., Vaya, J., Oren, R., Tawfik, D.S., Aviram, M., 2006. The catalytic histidine dyad of high density lipoprotein-associated serum paraoxonase-1 (PON1) is essential for PON1-mediated inhibition of low density lipoprotein oxidation and stimulation of macrophage cholesterol efflux. J Biol Chem 281, 7657-7665.

Rosenblat, M., Vaya, J., Shih, D., Aviram, M., 2005. Paraoxonase 1 (PON1) enhances HDL-mediated macrophage cholesterol efflux via the ABCA1 transporter in association with increased HDL binding to the cells: a possible role for lysophosphatidylcholine. Atherosclerosis 179, 69-77.

Rosenblat, M., Volkova, N., Ward, J., Aviram, M., 2011. Paraoxonase 1 (PON1) inhibits monocyte-to-macrophage differentiation. Atherosclerosis 219, 49-56.

Rozenberg, O., Shih, D.M., Aviram, M., 2003. Human serum paraoxonase 1 decreases macrophage cholesterol biosynthesis: possible role for its phospholipase-A2-like

activity and lysophosphatidylcholine formation. Arterioscler Thromb Vasc Biol 23, 461-467.

Samardzija, M., Wenzel, A., Aufenberg, S., Thiersch, M., Reme, C., Grimm, C., 2006. Differential role of Jak-STAT signaling in retinal degenerations. FASEB J 20, 2411-2413.

Seddon, J.M., Ajani, U.A., Mitchell, B.D., 1997. Familial aggregation of age-related maculopathy. Am J Ophthalmol 123, 199-206.

Seddon, J.M., Santangelo, S.L., Book, K., Chong, S., Cote, J., 2003. A genomewide scan for age-related macular degeneration provides evidence for linkage to several chromosomal regions. Am J Hum Genet 73, 780-790.

Seddon, J.M., Yu, Y., Miller, E.C., Reynolds, R., Tan, P.L., Gowrisankar, S., Goldstein, J.I., Triebwasser, M., Anderson, H.E., Zerbib, J., Kavanagh, D., Souied, E., Katsanis, N., Daly, M.J., Atkinson, J.P., Raychaudhuri, S., 2013. Rare variants in CFI, C3 and C9 are associated with high risk of advanced age-related macular degeneration. Nat Genet.

Seeliger, M.W., Grimm, C., Stahlberg, F., Friedburg, C., Jaissle, G., Zrenner, E., Guo, H., Reme, C.E., Humphries, P., Hofmann, F., Biel, M., Fariss, R.N., Redmond, T.M., Wenzel, A., 2001. New views on RPE65 deficiency: the rod system is the source of vision in a mouse model of Leber congenital amaurosis. Nat Genet 29, 70-74.

Shamir, R., Hartman, C., Karry, R., Pavlotzky, E., Eliakim, R., Lachter, J., Suissa, A., Aviram, M., 2005. Paraoxonases (PONs) 1, 2, and 3 are expressed in human and mouse gastrointestinal tract and in Caco-2 cell line: selective secretion of PON1 and PON2. Free Radic Biol Med 39, 336-344.

Shih, D.M., Gu, L., Xia, Y.R., Navab, M., Li, W.F., Hama, S., Castellani, L.W., Furlong, C.E., Costa, L.G., Fogelman, A.M., Lusis, A.J., 1998. Mice lacking serum paraoxonase are susceptible to organophosphate toxicity and atherosclerosis. Nature 394, 284-287.

Shih, D.M., Xia, Y.R., Wang, X.P., Miller, E., Castellani, L.W., Subbanagounder, G., Cheroutre, H., Faull, K.F., Berliner, J.A., Witztum, J.L., Lusis, A.J., 2000. Combined serum paraoxonase knockout/apolipoprotein E knockout mice exhibit increased lipoprotein oxidation and atherosclerosis. J Biol Chem 275, 17527-17535.

Smith, W., Assink, J., Klein, R., Mitchell, P., Klaver, C.C., Klein, B.E., Hofman, A., Jensen, S., Wang, J.J., de Jong, P.T., 2001. Risk factors for age-related macular degeneration: Pooled findings from three continents. Ophthalmology 108, 697-704.

Snodderly, D.M., 1995. Evidence for protection against age-related macular degeneration by carotenoids and antioxidant vitamins. Am J Clin Nutr 62, 1448S-1461S.

Solak, Z.A., Kabaroglu, C., Cok, G., Parildar, Z., Bayindir, U., Ozmen, D., Bayindir, O., 2005. Effect of different levels of cigarette smoking on lipid peroxidation, glutathione enzymes and paraoxonase 1 activity in healthy people. Clin Exp Med 5, 99-105.

Sonoda, S., Spee, C., Barron, E., Ryan, S.J., Kannan, R., Hinton, D.R., 2009. A protocol for the culture and differentiation of highly polarized human retinal pigment epithelial cells. Nat Protoc 4, 662-673.

Sorenson, R.C., Primo-Parmo, S.L., Camper, S.A., La Du, B.N., 1995. The genetic mapping and gene structure of mouse paraoxonase/arylesterase. Genomics 30, 431-438.

Sparrow, J.R., Boulton, M., 2005. RPE lipofuscin and its role in retinal pathobiology. Exp Eye Res 80, 595-606.

Sparrow, J.R., Nakanishi, K., Parish, C.A., 2000. The lipofuscin fluorophore A2E mediates blue light-induced damage to retinal pigmented epithelial cells. Invest Ophthalmol Vis Sci 41, 1981-1989.

Sparrow, J.R., Zhou, J., Cai, B., 2003. DNA is a target of the photodynamic effects elicited in A2E-laden RPE by blue-light illumination. Invest Ophthalmol Vis Sci 44, 2245-2251.

Spencer, K.L., Hauser, M.A., Olson, L.M., Schmidt, S., Scott, W.K., Gallins, P., Agarwal, A., Postel, E.A., Pericak-Vance, M.A., Haines, J.L., 2007. Protective effect of complement factor B and complement component 2 variants in age-related macular degeneration. Hum Mol Genet 16, 1986-1992.

Strauss, O., 2005. The retinal pigment epithelium in visual function. Physiol Rev 85, 845-881.

Suehiro, T., Nakamura, T., Inoue, M., Shiinoki, T., Ikeda, Y., Kumon, Y., Shindo, M., Tanaka, H., Hashimoto, K., 2000. A polymorphism upstream from the human paraoxonase (PON1) gene and its association with PON1 expression. Atherosclerosis 150, 295-298.

Swaroop, A., Branham, K.E., Chen, W., Abecasis, G., 2007. Genetic susceptibility to age-related macular degeneration: a paradigm for dissecting complex disease traits. Hum Mol Genet 16 Spec No. 2, R174-182.

Tabas, I., Williams, K.J., Boren, J., 2007. Subendothelial lipoprotein retention as the initiating process in atherosclerosis: update and therapeutic implications. Circulation 116, 1832-1844.

Takeda, T., Hosokawa, M., Higuchi, K., Hosono, M., Akiguchi, I., Katoh, H., 1994. A novel murine model of aging, Senescence-Accelerated Mouse (SAM). Arch Gerontol Geriatr 19, 185-192.

Tanimoto, N., Muehlfriedel, R.L., Fischer, M.D., Fahl, E., Humphries, P., Biel, M., Seeliger, M.W., 2009. Vision tests in the mouse: Functional phenotyping with electroretinography. Front Biosci (Landmark Ed) 14, 2730-2737.

Tarallo, V., Hirano, Y., Gelfand, B.D., Dridi, S., Kerur, N., Kim, Y., Cho, W.G., Kaneko, H., Fowler, B.J., Bogdanovich, S., Albuquerque, R.J., Hauswirth, W.W., Chiodo, V.A., Kugel, J.F., Goodrich, J.A., Ponicsan, S.L., Chaudhuri, G., Murphy, M.P., Dunaief, J.L., Ambati, B.K., Ogura, Y., Yoo, J.W., Lee, D.K., Provost, P., Hinton, D.R., Nunez, G., Baffi, J.Z., Kleinman, M.E., Ambati, J., 2012. DICER1 loss and Alu RNA induce age-related macular degeneration via the NLRP3 inflammasome and MyD88. Cell 149, 847-859.

Teiber, J.F., Billecke, S.S., La Du, B.N., Draganov, D.I., 2007. Estrogen esters as substrates for human paraoxonases. Arch Biochem Biophys 461, 24-29.

Thumann, G., Bartz-Schmidt, K.U., Kociok, N., Kayatz, P., Heimann, K., Schraermeyer, U., 1999. Retinal damage by light in the golden hamster: an ultrastructural study in the retinal pigment epithelium and Bruch's membrane. J Photochem Photobiol B 49, 104-111.

Tomas, M., Senti, M., Garcia-Faria, F., Vila, J., Torrents, A., Covas, M., Marrugat, J., 2000. Effect of simvastatin therapy on paraoxonase activity and related lipoproteins in familial hypercholesterolemic patients. Arterioscler Thromb Vasc Biol 20, 2113-2119.

Tong, H., Knapp, H.R., VanRollins, M., 1998. A low temperature flotation method to rapidly isolate lipoproteins from plasma. J Lipid Res 39, 1696-1704.

Tuo, J., Bojanowski, C.M., Zhou, M., Shen, D., Ross, R.J., Rosenberg, K.I., Cameron, D.J., Yin, C., Kowalak, J.A., Zhuang, Z., Zhang, K., Chan, C.C., 2007. Murine ccl2/cx3cr1 deficiency results in retinal lesions mimicking human age-related macular degeneration. Invest Ophthalmol Vis Sci 48, 3827-3836.

Tward, A., Xia, Y.R., Wang, X.P., Shi, Y.S., Park, C., Castellani, L.W., Lusis, A.J., Shih, D.M., 2002. Decreased atherosclerotic lesion formation in human serum paraoxonase transgenic mice. Circulation 106, 484-490.

van de Ven, J.P., Nilsson, S.C., Tan, P.L., Buitendijk, G.H., Ristau, T., Mohlin, F.C., Nabuurs, S.B., Schoenmaker-Koller, F.E., Smailhodzic, D., Campochiaro, P.A., Zack, D.J., Duvvari, M.R., Bakker, B., Paun, C.C., Boon, C.J., Uitterlinden, A.G., Liakopoulos, S., Klevering, B.J., Fauser, S., Daha, M.R., Katsanis, N., Klaver, C.C., Blom, A.M., Hoyng, C.B., den Hollander, A.I., 2013. A functional variant in the CFI gene confers a high risk of age-related macular degeneration. Nat Genet 45, 813-817.

Vasireddy, V., Jablonski, M.M., Khan, N.W., Wang, X.F., Sahu, P., Sparrow, J.R., Ayyagari, R., 2009. Elovl4 5-bp deletion knock-in mouse model for Stargardt-like macular degeneration demonstrates accumulation of ELOVL4 and lipofuscin. Exp Eye Res 89, 905-912.

von Lintig, J., 2012. Metabolism of carotenoids and retinoids related to vision. J Biol Chem 287, 1627-1634.

Wang, L., Clark, M.E., Crossman, D.K., Kojima, K., Messinger, J.D., Mobley, J.A., Curcio, C.A., 2010. Abundant lipid and protein components of drusen. PLoS One 5, e10329.

Watson, A.D., Berliner, J.A., Hama, S.Y., La Du, B.N., Faull, K.F., Fogelman, A.M., Navab, M., 1995. Protective effect of high density lipoprotein associated paraoxonase. Inhibition of the biological activity of minimally oxidized low density lipoprotein. J Clin Invest 96, 2882-2891.

Weeks, D.E., Conley, Y.P., Tsai, H.J., Mah, T.S., Schmidt, S., Postel, E.A., Agarwal, A., Haines, J.L., Pericak-Vance, M.A., Rosenfeld, P.J., Paul, T.O., Eller, A.W., Morse, L.S., Dailey, J.P., Ferrell, R.E., Gorin, M.B., 2004. Age-related maculopathy: a genomewide scan with continued evidence of susceptibility loci within the 1q31, 10q26, and 17q25 regions. Am J Hum Genet 75, 174-189.

Weismann, D., Hartvigsen, K., Lauer, N., Bennett, K.L., Scholl, H.P., Charbel Issa, P., Cano, M., Brandstatter, H., Tsimikas, S., Skerka, C., Superti-Furga, G., Handa, J.T., Zipfel, P.F., Witztum, J.L., Binder, C.J., 2011. Complement factor H binds malondialdehyde epitopes and protects from oxidative stress. Nature 478, 76-81.

Weng, J., Mata, N.L., Azarian, S.M., Tzekov, R.T., Birch, D.G., Travis, G.H., 1999. Insights into the function of Rim protein in photoreceptors and etiology of Stargardt's disease from the phenotype in abcr knockout mice. Cell 98, 13-23.

Wenzel, A., Grimm, C., Samardzija, M., Reme, C.E., 2005. Molecular mechanisms of light-induced photoreceptor apoptosis and neuroprotection for retinal degeneration. Prog Retin Eye Res 24, 275-306.

West, X.Z., Malinin, N.L., Merkulova, A.A., Tischenko, M., Kerr, B.A., Borden, E.C., Podrez, E.A., Salomon, R.G., Byzova, T.V., 2010. Oxidative stress induces angiogenesis by activating TLR2 with novel endogenous ligands. Nature 467, 972-976.

Wheeler, J.G., Keavney, B.D., Watkins, H., Collins, R., Danesh, J., 2004. Four paraoxonase gene polymorphisms in 11212 cases of coronary heart disease and 12786 controls: meta-analysis of 43 studies. Lancet 363, 689-695.

Wing, G.L., Blanchard, G.C., Weiter, J.J., 1978. The topography and age relationship of lipofuscin concentration in the retinal pigment epithelium. Invest Ophthalmol Vis Sci 17, 601-607.

Yamada, Y., Ishibashi, K., Bhutto, I.A., Tian, J., Lutty, G.A., Handa, J.T., 2006. The expression of advanced glycation endproduct receptors in rpe cells associated with basal deposits in human maculas. Exp Eye Res 82, 840-848.

Yang, Z., Stratton, C., Francis, P.J., Kleinman, M.E., Tan, P.L., Gibbs, D., Tong, Z., Chen, H., Constantine, R., Yang, X., Chen, Y., Zeng, J., Davey, L., Ma, X., Hau, V.S., Wang, C., Harmon, J., Buehler, J., Pearson, E., Patel, S., Kaminoh, Y., Watkins, S., Luo, L., Zabriskie, N.A., Bernstein, P.S., Cho, W., Schwager, A., Hinton, D.R., Klein, M.L., Hamon, S.C., Simmons,

E., Yu, B., Campochiaro, B., Sunness, J.S., Campochiaro, P., Jorde, L., Parmigiani, G., Zack, D.J., Katsanis, N., Ambati, J., Zhang, K., 2008. Toll-like receptor 3 and geographic atrophy in age-related macular degeneration. N Engl J Med 359, 1456-1463.

Yates, J.R., Sepp, T., Matharu, B.K., Khan, J.C., Thurlby, D.A., Shahid, H., Clayton, D.G., Hayward, C., Morgan, J., Wright, A.F., Armbrecht, A.M., Dhillon, B., Deary, I.J., Redmond, E., Bird, A.C., Moore, A.T., 2007. Complement C3 variant and the risk of age-related macular degeneration. N Engl J Med 357, 553-561.

Yin, L., Shi, Y., Liu, X., Zhang, H., Gong, Y., Gu, Q., Wu, X., Xu, X., 2012. A rat model for studying the biological effects of circulating LDL in the choriocapillaris-BrM-RPE complex. Am J Pathol 180, 541-549.

Yoon, H., Fanelli, A., Grollman, E.F., Philp, N.J., 1997. Identification of a unique monocarboxylate transporter (MCT3) in retinal pigment epithelium. Biochem Biophys Res Commun 234, 90-94.

Yuan, X., Gu, X., Crabb, J.S., Yue, X., Shadrach, K., Hollyfield, J.G., Crabb, J.W., 2010. Quantitative proteomics: comparison of the macular Bruch membrane/choroid complex from age-related macular degeneration and normal eyes. Mol Cell Proteomics 9, 1031-1046.

Zamiri, P., Sugita, S., Streilein, J.W., 2007. Immunosuppressive properties of the pigmented epithelial cells and the subretinal space. Chem Immunol Allergy 92, 86-93.

Zhao, Z., Chen, Y., Wang, J., Sternberg, P., Freeman, M.L., Grossniklaus, H.E., Cai, J., 2011. Age-related retinopathy in NRF2-deficient mice. PLoS One 6, e19456.

Zhou, J., Jang, Y.P., Kim, S.R., Sparrow, J.R., 2006. Complement activation by photooxidation products of A2E, a lipofuscin constituent of the retinal pigment epithelium. Proc Natl Acad Sci U S A 103, 16182-16187.

ABBREVIATIONS

A2E	Bis-retinoid N-retinylidene-N-retinylethanolamine
ABCA	ATP-binding cassette transporter, sub-family A
ACS	Acute coronary syndrome
AGE	Advanced glycation end product
AhR	Aryl hydrocarbon receptor
AMD	Age-related macular degeneration
ApoE	Apolipoprotein E
ARPE19	Retinal pigment epithelium-derived cell line
BRB	Blood-retinal barrier
BrM	Bruch's membrane
Caco-2	Colon carcinoma-derived cell line
CAD	Coronary artery disease
CC	Choriocapillaris
Ccl2	Chemokine (C-C motif) ligand 2
Ccr2	Chemokine (C-C motif) receptor 2
CEP	Carboxyethyl pyrrole
CEPT	Cholesterylester transfer protein
CFH	Complement factor H
CFI	Complement factor I
cGMP	Cyclic guanosine monophosphate
CH	Choroid
CNV	Choroidal neovascularization
CRALBP	Cellular retinaldehyde binding protein
CRBP	Cellular retinol-binding protein
Cx3cr1	Chemokine (C-X3-C motif) receptor 1
DAMP	Damage-associated molecular patterns
DMEM	Dulbecco's Modified Eagle Medium
DMSO	Dimethyl sulfoxide
EDTA	Ethylenediaminetetraacetic acid
ELOVL4	Elongation of very long chain fatty acids protein 4
ER	Endoplasmic reticulum
ERG	Electroretinogram

FBS	Fetal bovine serum
GA	Geographic atrophy
GCL	Ganglion cell layer
GDP	Guanosine diphosphate
GFAP	Glial fibrillary acidic protein
GTP	Guanosine triphosphate
GWAS	Genome-wide association scans
HDL	High-density lipoprotein
HEK293	Human embryonic kidney-derived cell line
INL	Inner nuclear layer
INL	Inner plexiform layer
IRBP	Interphotoreceptor retinoid-binding protein
LCA	Leber congenital amaurosis
LD	Light damage
LDL	Low-density lipoprotein
LIPC	Hepatic lipase
LPC	Lysophosphatidylcholine
LPL	Lipoprotein lipase
LRAT	Lecithin:retinol acyltransferase
LXR	Liver X receptor
MAF	Minor allele frequency
MCT3	Monocarboxylate transporter 3
MDA	Malondialdehyde
mRNA	Messenger ribonucleic acid
NLRP3	NLR family, pyrin domain containing 3
Nrf2	Nuclear factor-like 2
ONL	Outer nuclear layer
OPL	Outer plexiform layer
OR	Odds ratio
oxLDL	Oxidized low-density lipoprotein
PBS	Phosphate buffer saline
PDE	Phosphodiesterase
Pde6a	Rod cGMP-specific 3',5'-cyclic phosphodiesterase subunit alpha
Pde6c	Cone cGMP-specific 3',5'-cyclic phosphodiesterase subunit alpha
PEDF	Pigment epithelial derived factor

PIS	Photoreceptor inner segments
PON	Paraoxonase
POS	Photoreceptor outer segments
PPARγ	Peroxisome proliferator-activated receptor gamma
PRR	Pattern recognition receptors
PUFA	Polyunsaturated fatty acid
RAL	All-*trans*-retinal
RBP	Retinol-binding protein
RDH	Retinol dehydrogenase
REs	Retinyl esters
ROL	All-*trans*-retinol
ROS	Rod outer segments
ROS	Reactive oxygen species
RP	Retinitis pigmentosa
RPE	Retinal pigment epithelium
RPE65	Retinal pigment epithelium 65kDa protein
SAM	Senescence-Accelerated Mouse
SD	Standard deviation
siRNA	Small interference ribonucleic acid
SNP	Single nucleotide polymorphism
Sod	Superoxide dismutase
TIMP3	Tissue metalloproteinase inhibitor 3
TLR	Toll-like receptor
UTR	Untranslated region
UUR	Upstream untranscribed region
VEGF	Vascular endothelial growth factor

CURRICULUM VITEA

Family name: **OCZOS**
First name: **Jadwiga**
Date of birth: **August 29, 1983**
Nationality: **Polish**
Address: **Rautistrasse 319**
8048 Zurich
Switzerland
E-mail: **jad.oczos@gmail.com**
Tel.: **+41 77 480 15 03**

EDUCATION

08.2010 – present **PhD in Molecular Biology;** Faculty of Science, University of Zurich, Zurich, Switzerland;

PhD Research Project: *The role of paraoxonase-1 in retinal physiology and age-related macular degeneration*

10.2002 – 06.2007 **MSc in Biochemistry;** Faculty of Biochemistry, Biophysics, and Biotechnology, Jagiellonian University, Krakow, Poland;

MSc Research Project: *Application of resonance energy transfer phenomenon for investigation of interaction between dopamine receptor and G protein*

03-09.2006 **Research Project** at the Max Planck Institute of Biochemistry, Martinsried, Germany; Project title: *Solving the structure of CAP350 protein*

PROFESSIONAL EXPERIENCE

05.2009 – 05.2010 **Research assistant**; Division of Cell Biophysics, Jagiellonian University, Krakow, Poland; Project title: *Interaction of fluorescent dyes with chromatin in mammalian cells*

10.2007 – 12.2008 Music teacher and accompanist; Private primary school "Scherzo", Krakow, Poland

SCHOLARSHIPS and AWARDS

- Young Scientist Travel Award, The Fifth International Conference on Paraoxonases, The Ohio State University, Columbus, USA **(2012)**
- Socrates/ Erasmus Scholarship Abroad Program at the Ludwig-Maximilians University, Munich, Germany **(2006)**
- Jagiellonian University Scientific Scholarship **(2004, 2006)**

TEACHING ACTIVITIES

- Course: Molecular Human Genetics, Institute of Medical Molecular Genetics, University of Zurich; autumn semester 2012
- Course: Systems Neurobiology, Lab for Retinal Cell Biology, Dept. Ophthalmology, University of Zurich; spring semester 2012 and 2013

PUBLICATIONS

- **Oczos J**, Sutter I, Kloeckener-Gruissem B, Berger W, Hornemann T, von Eckardstein A, Grimm C. **(2014)** *Lack of paraoxonase-1 alters phospholipid composition but not morphology and function of the mouse retina.* (Manuscript submitted in IOVS).
- **Oczos J**, Grimm C, Barthelmes D, Sutter F, Menghini M, Kloeckener-Gruissem B, Berger W. **(2012)** *Regulatory regions of the paraoxonase-1 (PON1) gene are associated with neovascular age-related macular degeneration (AMD).* Age 35(5):1651-62.
- Zhao H, **Oczos J**, Janowski P, Trembecka D, Dobrucki J, Darzynkiewicz Z, Wlodkowic D. **(2010)** *Rationale for the real-time and dynamic cell death assays using propidium iodide.* Cytometry A 77(4): 399-405.

POSTER PRESENTATIONS

- **Oczos J**, Kloeckener-Gruissem B, Berger W, Grimm C. **(2013)** *Paraoxonase-1 (PON1) in retinal physiology and pathophysiology.* Annual meeting of The Association for Research in Vision and Ophthalmology (ARVO), Seattle, USA
- **Oczos J**, Kloeckener-Gruissem B, Berger W, Grimm C. **(2013)** *Characterization of paraoxonase-1 (PON1) in the mouse retina.* 12th Day of Clinical Research, University Hospital, Zurich, Switzerland.
- **Oczos J**, Grimm C, Barthelmes D, Sutter F, Menghini M, Kloeckener-Gruissem B, Berger W. **(2012)** *SNPs within the upstream regulatory region of PON1 gene modulate gene expression and are associated with neovascular AMD.* The Fifth International Conference on Paraoxonases, Columbus, USA
- **Oczos J**, Kloeckener-Gruissem B, Grimm C, Berger W. **(2011)** *Assessment of PON1 as a susceptibility locus for a neovascular AMD.* 7th Symposium of the Zurich Center for Integrative Human Physiology, Zurich, Switzerland.
- Sutter I, Grimm C, **Oczos J**, Rentsch K. **(2011)** *Quantification of long-chain fatty acids with GC-MS and application of the method in retina samples of PON1 knockout mice.* 7th Symposium of the Zurich Center for Integrative Human Physiology, Zurich, Switzerland.

ORAL PRESENTATIONS

- *Searching for a physiological link between paraoxonase-1 and age-related macular degeneration*. Swiss Eye Research Meeting, Biel, Switzerland **(2014)**
- *Paraoxonase-1 SNPs upstream of the protein-coding region are associated with neovascular AMD*. Swiss Eye Research Meeting, Biel, Switzerland **(2012)**

COURSES

- Project management for research; FS2013
- Next generation sequencing – practical course; HS2012
- Bioinformatics I (BCH401); HS2011
- Introductory course in laboratory animal science (LTK1); FS2011

ACKNOWLEDGEMENTS

I would like to acknowledge all those who have contributed to this work, assisted and supported me during my PhD.

First, I would like to thank members of my PhD committee, Prof. Wolfgang Berger, Prof. Christian Grimm, Dr. Barbara Kloeckener-Gruissem, Prof. Arnold von Eckardstein and Dr. Volker Enzmann for their valuable advice during committee meetings and for reviewing my thesis.

I am particularly grateful to my PhD supervisors, Prof. Christian Grimm, Prof. Wolfgang Berger and Dr. Barbara Kloeckener-Gruissem who gave me the opportunity to work on this diverse, complex and very interesting project. Thank you for guiding me through the everyday PhD life, teaching me critical, independent thinking and showing me different working styles.

I would also like to thank all my colleagues from the Institute of Medical Molecular Genetics (IMMG) and the Lab for Retinal Cell Biology (LRCB). Special thank you goes to Barbara Kloeckener-Gruissem, who introduced me to most of the laboratory methods in IMMG, always had time for extensive discussions and helped me to improve my presentation skills. I am also grateful to Marijana Samardzija, Severin Heynen and Christian Caprara who introduced me to the technical work in the LRCB. I thank all the other current and former members of both groups (Divya Ail, Romain da Costa, Britta Seebauer, Sajad Hamid, Maya Barben, Christian Schori, Katrin Klee, Brigitt Kast, Cornelia Imsand, Christel Beck, Andera Gubler, Daniel Prata, John Neidhardt, István Magyar, Samuel Koller, Amit Tiwari, Silke Feil, Michel Bielecki, Sonja Zimmer, Jordi Maggi, Pooja Gangras, Cavit Agca, Isabelle Meneau, Ghislaine Traber, Philipp Geiger, Lucas Mohn, Jurian Zürcher, Lea Sollfrank, Esther Glaus, Mariana Wittmer) for sharing their experience in the lab, and for all the chillout moments: having tea, having drinks, having discussions, snowboarding, hiking, lab retreats. Being in two labs was demanding from intellectual, but especially from interpersonal point of view. You managed to “share” me gently. Thanks!

I would also like to acknowledge our collaborators from the Institute of Clinical Chemistry and the Cardiovascular Center who essentially contributed to the *PON1 project*. Especially I thank Iryna Sutter for performing the retinal lipidome analysis and for inspiring discussions, as well as Damir Perisa and Reda Hasballa for their involvement in experiments with HDL and LDL.

I am very grateful to the group of Prof. Olaf Strauss from the University of Regensburg for teaching me the method of isolating and culturing primary RPE cells.

I would like to thank all my “Zürich-friends”, especially Christoph, and all my friends from previous times for motivating me and basically for being on my side during the good times and the tough times of the PhD.

Finally, I would like to thank my dear family for their continuous support.
Kochana Rodzinko, dziękuję Wam za stałą obecność, zainteresowanie i wsparcie pomimo odległości. Bez Was nie byłabym tym, kim jestem. Dziękuję!